~~[illegible]~~ Copy 520

[redacted]

NASA TM X-354

NASA TM X-354

GPO PRICE $ _____

CFSTI PRICE(S) $ _____

Hard copy (HC) 4.00

Microfiche (MF) 1.00

ff 653 July 65

TECHNICAL MEMORANDUM

X-354

Declassified by authority of NASA
Classification Change Notices No. 43
Dated ** 12/29/65

INVESTIGATION OF THE SUBSONIC AND SUPERSONIC RELEASE CHARACTERISTICS OF AN EXTERNALLY CARRIED FUEL TANK FROM A 1/40-SCALE MODEL OF A BOMBER AIRPLANE

By William F. Hinson

Langley Research Center
Langley Field, Va.

DECLASSIFIED
ATS 480

AUTHORITY
DROBKA TO LEBOW
MEMO DATED 12/13/6

[redacted]

Declassified by authority of NASA
Classification Change Notices No. 43
Dated ** 12/29/65

[redacted]

[redacted]

FACILITY FORM 602

N66 19727 (ACCESSION NUMBER)	(THRU)
142 (PAGES)	1 (CODE)
TMX 354 (NASA CR OR TMX OR AD NUMBER)	01 (CATEGORY)

NATIONAL AERONAUTICS AND SPACE ADMINISTRATION

WASHINGTON January 1961

DECL[redacted]AI[redacted]FIED

AUTHORITY DROBKA TO LEBOW MEMO DATED 12/13/6

NATIONAL AERONAUTICS AND SPACE ADMINISTRATION

TECHNICAL MEMORANDUM X-354

INVESTIGATION OF THE SUBSONIC AND SUPERSONIC RELEASE CHARACTERISTICS OF AN EXTERNALLY CARRIED FUEL TANK FROM A 1/40-SCALE MODEL OF A BOMBER AIRPLANE*

By William F. Hinson

DECLASSIFIED ATS 430

SUMMARY

19727

An investigation has been conducted to determine the release characteristics and flight behavior of a dynamically scaled, externally carried fuel tank when released at subsonic and supersonic free-stream Mach numbers of 0.69 to 0.92, 1.39, 1.59, 1.80, and 1.98. The fuel-tank models were released from a 1/40-scale model of a supersonic bomber-airplane configuration at simulated altitudes of sea level and 2,500, 26,000, and 36,000 feet. Three different arrangements of tail fins were used on a fuel tank with a fineness ratio of 11.37 to stabilize it in free flight. These arrangements were (1) cruciform tail fins, (2) three tail fins mounted 120° apart, and (3) two tail fins mounted 30° downward of the horizontal. Two canard surfaces located forward of the center-of-gravity station and symmetrical about the center line were used to aid in more positive tank release characteristics. The following canard-surface deflections were used: 2°, 0°, -2°, -4°, -6°, -15°, and -20°.

The results indicate that satisfactory releases can be obtained with the proper combination of canard-surface deflection and tail fins. The canard surfaces appeared to be ineffective when set at large negative deflections with the airplane model at a large positive angle of attack to the free stream. Decreasing the canard-surface deflection for a fixed wing angle of attack resulted in an increase in time to obtain a fixed pitch angle. As the wing angle of attack was increased with a constant canard-surface deflection, the time to obtain a fixed pitch angle was increased. Lateral translation did not appear to cause any unsatisfactory releases.

auchr

*Title, Unclassified.

[redacted]

Declassified by authority of NASA
Classification Change Notices No. 43
Dated ** 12/9/65

[redacted]

INTRODUCTION

Most current military aircraft are required to jettison or launch stores of various types: fuel tanks, bombs, rockets, missiles, and so forth. High operational speeds lead to special problems in predicting and analyzing the behavior of these stores immediately after release. The interacting flow fields of store and airplane perturb the free motion of the store; these induced motions may cause the released store to strike the carrying aircraft.

To extend the range and mission capability of a current supersonic bomber airplane, a two-component, externally carried pod was developed. The pod consists of a bomb which is attached to the airplane fuselage by a pylon and a fuel tank which is fitted over the lower part of the bomb so that the bomb is semisubmerged in the fuel-tank body. The fuel tank is released prior to the release of the bomb. Therefore, the problem of concern in this investigation is the release of the fuel tank in such a manner as not to strike the bomb or carrying aircraft.

L
9
1
5

The investigation was made in the preflight jet of the NASA Wallops Station with 1/40-scale models of the pod and the bomber-airplane configurations. Tests were made at subsonic and supersonic free-stream Mach numbers of 0.69 to 0.92, 1.39, 1.59, 1.80, and 1.98 at simulated altitudes of sea level and 2,500, 26,000, and 36,000 feet; however, tests were not conducted at all altitudes for each Mach number.

The Reynolds number per foot for the dynamically scaled fuel-tank models was approximately 7×10^6 to 14×10^6.

SYMBOLS

d	maximum fuel-tank diameter, 1.47 in.
h	simulated altitude, ft
I_Y	moment of inertia in pitch plane, lb-in.^{2}
L	characteristic length
M	free-stream Mach number
p	free-stream static pressure, lb/sq ft
t	time, milliseconds

[redacted]

W	weight, lb
x	horizontal coordinate of fuel-tank displacement with origin at center-of-gravity position at initial release, positive downstream, in.
z	vertical coordinate of fuel-tank displacement with origin at center-of-gravity position at initial release, positive downward, in.
α	angle of attack, deg
β	angle of sideslip, deg
δ	canard-surface deflection, deg
λ	scale factor, $\frac{L_M}{L_P}$
θ	fuel-tank pitch angle with respect to the horizontal, deg

L
9
1
5

Subscripts:

M	model
P	prototype

MODELS AND APPARATUS

Fuel Tank

The basic fuel-tank body and its ordinates are shown in figure 1. Fuel-tank-model weights, altitudes, moments of inertia, and test data are given in table I.

Photographs and sketches of the 1/40-scale fuel tank (approximately 2,181 pounds empty weight, full scale) are shown in figures 2 to 5. Canard fins (one on either side of the fuel-tank body) were mounted on the forward portion of the fuel-tank body for the purpose of producing a negative pitching moment after release. The canard-surface deflection could be varied and was preset before each test. In the photographs and sketches of the fuel tank, the top view shows the cavity into which the bomb is recessed when the pod is installed.

Figure 2 shows the fuel tank with the cruciform tail fins while figure 3 shows the three tail fins mounted 120° apart (triadic tail

fins). When the triadic configuration is installed on the airplane model, the upper fin is very close to the airplane fuselage. In some tests the triadic tail-fin configuration was modified in that the upper fin was removed before the test. This configuration was called dyadic. Figures 4 and 5 show detailed sketches of the fuel-tank and tail-fin configurations.

Release Mechanism

The fuel-tank model was attached to the bomb by a spring-loaded pin as shown in figure 6. When the pin was in the depressed position, it fitted into a hole in the bottom of the bomb. A drilled hole in the pin permitted the insertion of a pull rod which secured the fuel-tank model in place. Four small set screws, two on either side of the fuel-tank model, were used for proper alinement with the airstream. The pull rod was actuated by an air cylinder through a cable and pulley arrangement as shown in figure 7. An electric solenoid actuated the air cylinder, thereby permitting the fuel tank to be dropped.

Figure 8 shows a closeup view of the airplane model with the pod attached as mounted in the preflight jet.

Airplane Model

Figure 9 shows a sketch of the 1/40-scale bomber. The model consists of a 60° delta wing, a fuselage designed by the area rule, pylon-mounted engine nacelles, and a vertical stabilizer. As stated previously, the two-component pod is carried externally. In this investigation, the bomb was a permanent installation on the airplane model and housed part of the fuel-tank release mechanism. The prototype bomb, in release condition, incorporates triadic tail fins of which one is mounted on the extreme bottom portion of the tail cone; this lower fin is retracted when the prototype fuel tank is installed. In this investigation, the lower fin was removed from the bomb to simulate a retracted fin. Therefore, to prepare for the various tests, it was necessary only to fit the fuel tank over the bomb. The wing angle of attack was set before each test by an angle-of-attack adapter plate which was also used to attach the airplane model to the beam-support mechanism. The complete setup in the preflight jet is shown in figure 10.

Photographic Records

High-speed microflash photographs were made of the fuel-tank release. Lighting was supplied by a series of flashbulbs which were

electronically timed to overlap. The film was exposed through narrow radial slits in a rotating disk placed in front of the camera lens. Motion pictures (2,500 frames per second) were also made during the tests.

TESTS

Dynamic Similarity

The "heavy-model method," as described in reference 1, was used for dynamic similarity. The method requires that the nondimensional radii of gyration, Mach numbers, and air properties at test and full-scale conditions be equal and that the model and prototype be geometrically similar. The model weight and moment of inertia are given by the following expressions:

$$W_M = (\lambda)^2 \frac{p_M}{p_P} W_P \tag{1}$$

$$I_{Y,M} = (\lambda)^4 \frac{p_M}{p_P} I_{Y,P} \tag{2}$$

In this method, the aerodynamically produced accelerations are independent of the scale.

Test Methods

A canard-surface deflection of -15° was used with cruciform tail fins except for one test in which a 2° deflection was used. In tests with the triadic and dyadic tail fins, the canard surface was set at deflections of 0°, -2°, -4°, -6°, and -20°. In all tests, the canard-surface deflection was set before the fuel-tank model was attached to the airplane model.

The wing angle of attack was also set before each test by the use of a vertical angle-of-attack adapter plate. This plate was the connecting link between the airplane model and the vertical strut of the support mechanism. The airplane model with the fuel tank attached was held out of the tunnel airstream until the stream was brought to design conditions; then the complete configuration was inserted in the stream. Simultaneously with the firing of the flashbulbs, the solenoid air valve

was actuated and it, in turn, released the fuel tank. During the time the fuel-tank model was traversing the airstream, two 8-inch by 10-inch cameras were taking side and bottom exposures of the fuel-tank motions. The photograph obtained with the side camera was a scaled-time trajectory of the fuel tank. The bottom camera photograph shows lateral translation. The airplane model was removed from the tunnel airstream before tunnel shutdown. The insertion and removal of the airplane model were performed during tunnel operation to prevent the starting and stopping aerodynamic loads of the tunnel from being imposed on the airplane model.

DATA REDUCTION

The pitch oscillations and trajectories were measured directly from the microflash multiple-exposure photographs. The trajectory measurements were nondimensionalized by using as the characteristic length the maximum diameter of the fuel-tank body. Zero time was taken at the instant of the pull-rod release.

A summary of the estimated maximum probable errors for the tests and fuel tank is presented in the following table:

x/d	±0.004
z/d	±0.004
θ, deg	±0.5
p, lb/sq in.	±0.02
M	±0.02
W_p simulated prototype weight based on tunnel dynamic pressure, lb	+0.0009 -0.0032
h simulated altitude based on tunnel dynamic pressure, ft	±0.02

RESULTS AND DISCUSSION

A motion-picture film supplement has been prepared and is available on loan. A request card form and a description of the films will be found at the back of this paper, on the page immediately preceding the abstract page.

The results are presented herein in the form of microflash photographs, pitch-oscillation plots, and trajectory plots. Because of the erratic motions of the fuel tank in some tests, data measurements were not attempted; however, the photographs are presented. Results obtained with the cruciform tail fins, triadic tail fins, and dyadic tail fins

are presented. When data are available, comparison plots are presented to show trends or effects with M, α, and δ.

Satisfactory tests are defined as those releases in which the fuel-tank model did not come in contact with the airplane model after release and followed a downward trajectory.

Cruciform Tail Fins

The basic data of the cruciform tail-fin configuration are presented in figure 11 (tests 1 to 11).

Subsonic Mach numbers.- In figure 11 it is shown that at $\alpha = 11^{\circ}13'$ and $\delta = -15^{\circ}$ (test 1) the fuel tank experienced a positive pitching moment and came in contact with the airplane model. A satisfactory test was obtained by decreasing α to $5^{\circ}31'$ (test 2). Apparently in test 1 the canard surface was ineffective in producing a sufficiently large negative pitching moment to overcome the initial aerodynamic loading on the fuel-tank body. Test 3 shows a satisfactory release with $\delta = 2^{\circ}$ and $\alpha = 3^{\circ}16'$.

M = 1.39.- One release was made with $\delta = -15^{\circ}$, $\alpha = 3^{\circ}42'$ (test 4) and was satisfactory.

M = 1.59.- With $\delta = -15^{\circ}$ and $\alpha = 5^{\circ}56'$ and $3^{\circ}16'$ (tests 5 and 7), the fuel tank rolled after release and a tail fin struck the airplane model. In test 6 (a repeat of test 5) no roll occurred and the release was satisfactory. The roll in both tests 5 and 7 was attributed to improper alinement of the fuel tank in the tunnel airstream. Test 8 was a satisfactory release with $\delta = -15^{\circ}$ and $\alpha = 4^{\circ}30'$.

M = 1.98.- Satisfactory releases were obtained with wing angles of attack of $3^{\circ}16'$ and $5^{\circ}06'$ with $\delta = -15^{\circ}$ (tests 9 and 10). When the wing angle of attack was increased to $6^{\circ}37'$ (test 11) and an altitude of 36,000 feet was simulated, the fuel tank experienced a positive pitching moment and came in contact with the airplane model. Thus the canard surfaces appeared to be ineffective, as in test 1.

Figures 12(a) and (b) are comparison plots of satisfactory tests showing the effect of change in wing angle of attack with constant canard-surface deflection at M = 1.59 and 1.98. In both plots it is apparent that as the wing angle of attack is increased the time to obtain a fixed pitch angle is increased. The trajectories are almost identical for approximately 6 fuel-tank diameters below the airplane model.

Three Tail Fins (Triadic)

The microflash photographs and plotted data of the triadic configuration are presented in figure 13 (tests 12 to 34).

Subsonic Mach numbers.- In tests 12 to 23, canard-surface deflections of 0°, -2°, -4°, and -6° were used at an approximate simulated altitude of sea level, a deflection of -6° was used at a simulated altitude of 2,500 feet, and a deflection of -20° was used at a simulated altitude of 26,000 feet. Satisfactory results were obtained except for two tests (tests 13 and 20). In test 13 ($M = 0.69$, $\delta = -4^{\circ}$, and $\alpha = 5^{\circ}11'$), the fuel tank rolled after release. In a repeat test (test 15) the fuel tank did not roll and release was satisfactory. Apparently in test 13 the fuel tank was improperly alined with the airstream, as in tests 5 and 7. In test 20 ($M = 0.91$, $\delta = -20^{\circ}$, $\alpha = 11^{\circ}13'$), the fuel tank experienced a positive pitching moment which caused the nose to strike the airplane model. The canard surfaces appeared to be ineffective, as in tests 1 and 11.

$M = 1.39$.- A satisfactory release was obtained with $\delta = -6^{\circ}$ and $\alpha = 4^{\circ}30'$ (test 24).

$M = 1.59$.- In tests 25 to 31 canard-surface deflections of 0°, -6°, and -20° were used with various wing angles of attack. All tests were unsatisfactory from a release standpoint except test 27. For test 27, $\delta = -6^{\circ}$ was used in combination with $\alpha = 5^{\circ}56'$. The initial induced-interference effects on this arrangement appeared less severe than those for the other cases at the same Mach number. It appears that at $M = 1.59$ the interference effects are unfavorable when the fuel tank is attached to the airplane model. These interference effects induce loads on the tank which result in large initial pitching moments at release. Force data obtained in the Langley Unitary Plan wind tunnel indicate that the initial pitching moment changes approximately 200 percent from negative to positive at $M = 1.59$ to $M = 1.98$ when the fuel tank is installed on the airplane model, and with $\alpha = 3^{\circ}$. With $\alpha = 8.5^{\circ}$ and the fuel tank attached to the airplane model the initial positive pitching moment increases approximately 400 percent from $M = 1.59$ to $M = 1.98$. Therefore it appears that the negative canard-surface deflections used in this investigation were too large. No comparison plots were made at $M = 1.59$; however, the basic data are presented.

$M = 1.98$.- Canard-surface deflections of -6° ($\alpha = 3^{\circ}16'$; test 33) and -20° ($\alpha = 5^{\circ}06'$ and $6^{\circ}37'$; tests 32 and 34) were tested. All these tests were considered satisfactory.

A comparison plot showing the effect of change in wing angle of attack with constant canard-surface deflection at subsonic speeds is

shown in figure 14(a). Figure 14(b) shows the effect of changing the canard-surface deflection with constant wing angle of attack at $M = 1.98$. In both plots the time to reach a fixed pitch angle is increased.

Two Tail Fins (Dyadic)

The upper tail fin of the triadic-tail-fin configuration was removed in an attempt to prevent the tail section of the fuel tank from striking the airplane model. The basic data of the dyadic configuration are presented in figure 15 (tests 35 to 52).

Subsonic Mach numbers.- One test (test 35) was made at $M = 0.92$, $\alpha = 3^{\circ}36'$, $\delta = -2^{\circ}$, and $\beta = 1^{\circ}$; this test was considered satisfactory.

$M = 1.39$.- Canard-surface deflections of -2° ($\alpha = 3^{\circ}21'$, $3^{\circ}40'$, and $4^{\circ}56'$; tests 36, 37, and 39, respectively) and -20° ($\alpha = 4^{\circ}56'$ and $6^{\circ}30'$; tests 38 and 40, respectively) were used. With $\delta = -2^{\circ}$ (test 36), the tail cone came in contact with the airplane model. Test 37, with $\delta = -2^{\circ}$, was satisfactory. Apparently in test 36 the negative pitching moment was decreased as a result of the increase in fuel-tank angle of attack. In tests 38 and 40, α was increased while δ was held at -20° with satisfactory results.

$M = 1.59$.- Canard-surface deflections of -2° ($\alpha = 6^{\circ}07'$, $3^{\circ}20'$, and $4^{\circ}03'$; tests 42, 43, and 44) and -20° ($\alpha = 3^{\circ}16'$; test 41) were used. In test 42 the fuel-tank tail cone hit the airplane model. However, with the increased α in tests 43 and 44, satisfactory results were obtained. Apparently, the initial negative pitching moment was decreased by the increase in wing angle of attack. Test 41 is a repeat of test 31 with the upper fin removed. However, in test 41 the tail cone hit the airplane model as did the upper tail fin in test 31. Apparently the initial negative pitching moment was too large even though the upper fin was removed in test 41.

$M = 1.80$.- Canard-surface deflections of -2° ($\alpha = 3^{\circ}26'$ and $4^{\circ}09'$; tests 45 and 46, respectively) and -20° ($\alpha = 4^{\circ}09'$ and $6^{\circ}35'$; tests 47 and 48, respectively) were used. Satisfactory results were obtained in all tests.

$M = 1.98$.- Canard-surface deflections of -2° ($\alpha = 3^{\circ}16'$ and $4^{\circ}03'$; tests 49 and 50) and -20° ($\alpha = 3^{\circ}16'$ and $5^{\circ}03'$; tests 51 and 52, respectively) were used. In test 50 with $\delta = -2^{\circ}$ and $\alpha = 4^{\circ}03'$ the fuel tank experienced a positive pitching moment after release and came in contact with the airplane model. Apparently the -2° canard-surface deflection was not sufficient to overcome the upward aerodynamic loading on the fuel-tank body. All other tests were considered satisfactory.

Comparison plots of the effect of changing the canard-surface deflection while keeping the wing angle of attack constant are shown in figure 16(a). Figures 16(b), (c), and (d) show the effect of keeping the canard-surface deflection constant while varying the wing angle of attack. As stated previously, the time to obtain a particular pitch angle is increased as the wing angle of attack is increased or as the canard-surface deflection is increased.

Lateral Translation

Sideslip angles of 0° and 1° were used in the test program. (See table I.) In general, lateral translation near time zero did not appear to be excessive.

CONCLUSIONS

An investigation has been conducted to determine the release characteristics and flight behavior of a dynamically scaled fuel tank which is carried externally on a supersonic bomber airplane. Releases were made at subsonic and supersonic free-stream Mach numbers of 0.69 to 0.92, 1.39, 1.59, 1.80, and 1.98. The three fuel-tank model tail-fin configurations tested were (1) cruciform tail fins, (2) triadic tail fins, and (3) dyadic tail fins. Canard fins were mounted on the forward portion of the fuel-tank body for the purpose of producing a pitching moment after release. Canard-surface deflections of 2° and -15° were used with the cruciform tail fins and deflections of 0°, -2°, -4°, -6°, and -20° were used with the triadic and dyadic tail fins. The following conclusions are indicated:

1. Satisfactory releases can be obtained with the proper canard-surface deflections and tail-fin combination.

2. At large wing angles of attack, the canard surfaces appear ineffective in producing negative pitching moments sufficient to overcome the upward aerodynamic loading on the fuel-tank body.

3. As the wing angle of attack is increased with constant canard-surface deflection, the time required to obtain a fixed pitch angle is increased.

4. As the canard-surface deflection is decreased from negative toward positive, with constant wing angle of attack, the time to obtain a fixed pitch angle is increased.

5. In general, lateral deviation did not appear excessive enough to cause the fuel tank to strike the airplane model.

Langley Research Center,
National Aeronautics and Space Administration,
Langley Field, Va., July 28, 1960.

REFERENCE

1. Sandahl, Carl A., and Faget, Maxime A.: Similitude Relations for Free-Model Wind-Tunnel Studies of Store-Dropping Problems. NACA TN 3907, 1957.

[redacted]

TABLE I.- SUMMARY OF TEST DATA

Test	M	α	δ, deg	β, deg	h, ft	W, lb	$I_{Y,M}$, lb-in.^{2}	Number of tail fins	Remarks	Figure
1	0.91	11°13'	-15	0	25,400	3.81	63.813	4	Model experienced positive pitching moment and struck airplane model	11(a)
2	.91	5°30'	-15	0	25,500	3.76	63.239	4	Satisfactory	11(b)
3	.89	3°16'	2	0	1,300	1.426	23.938	4	Satisfactory	11(c)
4	1.39	3°42'	-15	0	25,350	3.73	62.514	4	Satisfactory	11(d)
5	1.59	5°56'	-15	0	25,600	3.77	62.846	4	Model rolled, tail fin struck airplane model	11(e)
6	1.59	5°56'	-15	0	25,600	3.77	63.302	4	Repeat of test 5, satisfactory	11(e)
7	1.59	3°16'	-15	0	25,650	3.78	64.309	4	Model rolled immediately after release, causing tail fins to strike airplane model	11(f)
8	1.59	4°30'	-15	0	25,650	3.78	63.934	4	Satisfactory	11(g)
9	1.98	3°16'	-15	0	25,700	3.79	64.067	4	Satisfactory	11(h)
10	1.98	5°06'	-15	0	25,700	3.79	63.703	4	Satisfactory	11(i)
11	1.98	6°37'	-15	0	36,000	6.07	100.799	4	Model experienced positive pitching moment and struck airplane model	11(j)
12	.69	5°11'	-6	0	0	1.360	22.566	3	Satisfactory	13(a)
13	.69	5°11'	-4	0	2,200	1.495	25.179	3	Model rolled immediately after release	13(b)
14	.70	5°11'	-2	0	100	1.370	22.880	3	Satisfactory	13(c)
15	.72	5°11'	-4	0	100	1.370	22.880	3	Repeat of test 19, satisfactory	13(d)
16	.80	6°45'	-20	0	26,200	3.880	66.180	3	Satisfactory	13(e)
17	.90	9°20'	-20	1	26,150	3.87	65.594	3	Satisfactory	13(f)
18	.90	3°36'	-2	0	0	1.360	22.892	3	Satisfactory	13(g)
19	.91	3°36'	0	0	0	1.360	22.892	3	Satisfactory	13(h)
20	.91	11°13'	-20	0	25,950	3.83	64.161	3	Model experienced positive pitching moment and struck airplane model	13(i)
21	.91	3°16'	-6	0	2,450	1.495	25.116	3	Satisfactory	13(j)
22	.91	3°16'	-6	1	2,450	1.495	25.116	3	Satisfactory	13(j)
23	.92	5°30'	-20	0	25,650	3.78	64.431	3	Satisfactory	13(k)
24	1.39	4°30'	-6	0	26,000	3.84	65.163	3	Satisfactory	13(l)
25	1.59	5°56'	-20	0	25,650	3.780	64.764	3	Model upper tail fin struck airplane model	13(m)
26	1.59	6°30'	-20	0	26,000	3.836	65.032	3	Model upper tail fin struck airplane model	13(n)

TABLE I.- SUMMARY OF TEST DATA - Concluded

Test	M	α	δ, deg	β, deg	h, ft	W, lb	$I_{Y,M}$, lb-in.^{2}	Number of tail fins	Remarks	Figure
27	1.59	5°56'	-6	0	25,950	3.830	65.389	3	Satisfactory	13(o)
28	1.59	4°30'	-6	0	25,950	3.820	64.671	3	Model upper tail fin struck airplane model	13(p)
29	1.59	4°03'	0	0	25,850	3.810	65.161	3	Model upper tail fin struck airplane model	13(q)
30	1.59	6°07'	0	0	25,600	3.770	64.288	3	Model rolled and struck airplane model	13(r)
31	1.59	3°16'	-20	0	25,650	3.780	64.087	3	Model upper tail fin struck airplane model	13(s)
32	1.98	5°06'	-20	0	25,900	3.820	64.898	3	Satisfactory	13(t)
33	1.98	3°16'	-6	0	25,400	3.740	62.548	3	Satisfactory	13(u)
34	1.98	6°37'	-20	0	35,600	5.96	100.974	3	Satisfactory	13(v)
35	.92	3°36'	-2	1	0	1.360	22.892	2	Satisfactory	15(a)
36	1.39	3°21'	-2	0	26,250	3.915	65.730	2	Model tail cone struck airplane model	15(b)
37	1.39	3°40'	-2	0	26,150	3.890	65.633	2	Satisfactory	15(c)
38	1.39	4°56'	-20	0	25,400	3.745	63.977	2	Satisfactory	15(d)
39	1.39	4°56'	-2	1	26,000	3.835	64.876	2	Satisfactory	15(e)
40	1.39	6°30'	-20	1	25,850	3.815	64.677	2	Satisfactory	15(f)
41	1.59	3°16'	-20	0	26,150	3.860	65.958	2	Repeat of test 37, without upper tail fin. Model tail cone struck airplane model	15(g)
42	1.59	6°07'	-2	1	26,000	3.835	65.321	2	Satisfactory	15(h)
43	1.59	3°20'	-2	0	26,050	3.850	65.695	2	Model tail cone struck airplane model	15(i)
44	1.59	4°03'	-2	0	27,000	4.035	67.388	2	Satisfactory	15(j)
45	1.80	3°26'	-2	0	25,700	3.785	64.659	2	Satisfactory	15(k)
46	1.80	4°09'	-2	1	25,750	3.800	64.128	2	Satisfactory	15(l)
47	1.80	4°09'	-20	0	25,800	3.805	65.206	2	Satisfactory	15(m)
48	1.80	6°35'	-20	1	25,800	3.820	65.329	2	Satisfactory	15(n)
49	1.98	3°16'	-2	1	25,800	3.820	65.110	2	Satisfactory	15(o)
50	1.98	4°03'	-2	1	26,350	3.900	65.902	2	Model experienced positive pitching moment and struck airplane model	15(p)
51	1.98	3°16'	-20	0	25,450	3.750	64.259	2	Satisfactory	15(q)
52	1.98	5°03'	-20	1	26,075	3.860	65.301	2	Satisfactory	15(r)

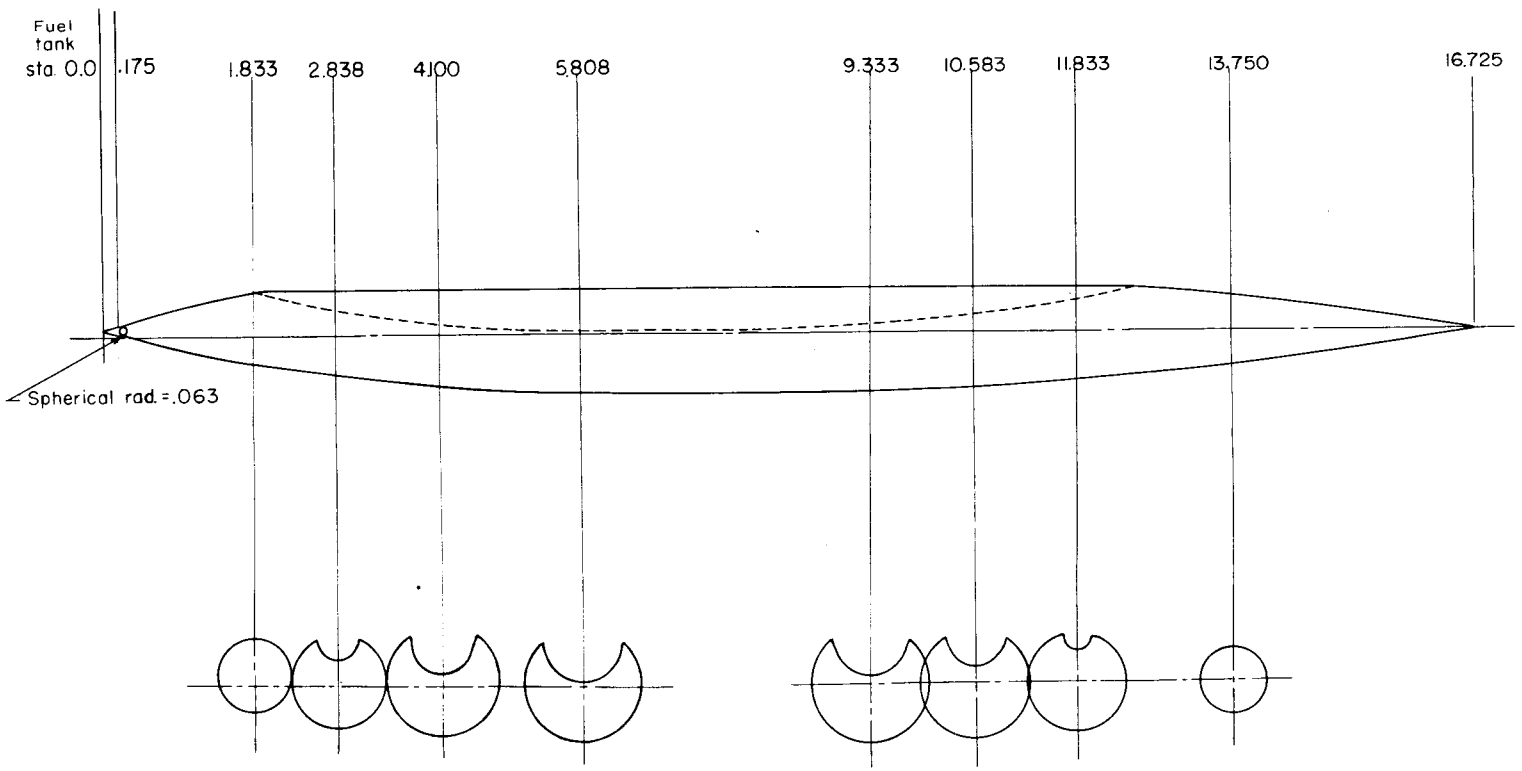

(a) Sketch. Dimensions are in inches.

Figure 1.- Details of the basic fuel-tank body.

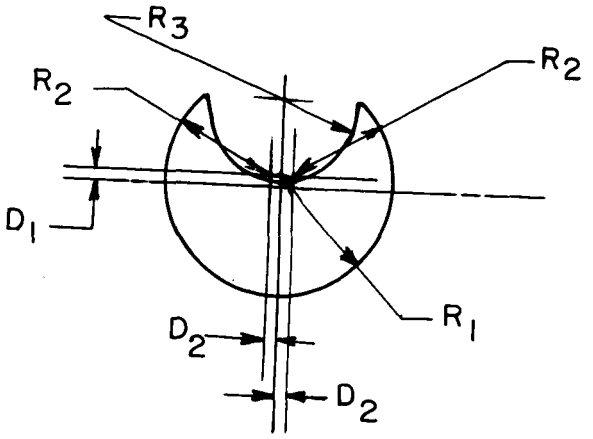

Station, in.	D_1, in.	D_2, in.	R_1, in.	R_2, in.	R_3, in.
0.000	0.077	0.000	0.000	0.000	0.000
.175	.077	.000	.000	.000	.000
.655	.077	.000	.175	.175	.000
1.280	.077	.000	.321	.321	.000
1.784	.077	.000	.321	.321	.000
1.833	.077	.000	.433	.433	.012
2.838	.060	.080	.578	.498	.232
3.470	.047	.081	.641	.560	.338
4.100	.035	.096	.690	.594	.418
4.718	.022	.075	.723	.648	.472
5.808	.000	.000	.738	.738	.510
7.615	.000	.000	.738	.738	.510
7.984	.000	.006	.738	.732	.507
8.583	.000	.028	.734	.706	.491
9.333	.000	.058	.720	.662	.450
9.958	.000	.077	.700	.623	.399
10.583	.000	.084	.672	.588	.332
11.208	.000	.076	.637	.561	.250
11.833	.000	.053	.595	.542	.151
12.645	.000	.000	.528	.528	.000
13.125	.000	.000	.483	.483	.000
13.750	.000	.000	.417	.417	.000
14.375	.000	.000	.343	.343	.000
15.000	.000	.000	.262	.262	.000
15.625	.000	.000	.174	.174	.000
16.250	.000	.000	.078	.078	.000
16.725	.000	.000	.000	.000	.000

(b) Coordinates.

Figure 1.- Concluded.

L-915

[redacted]

[redacted]

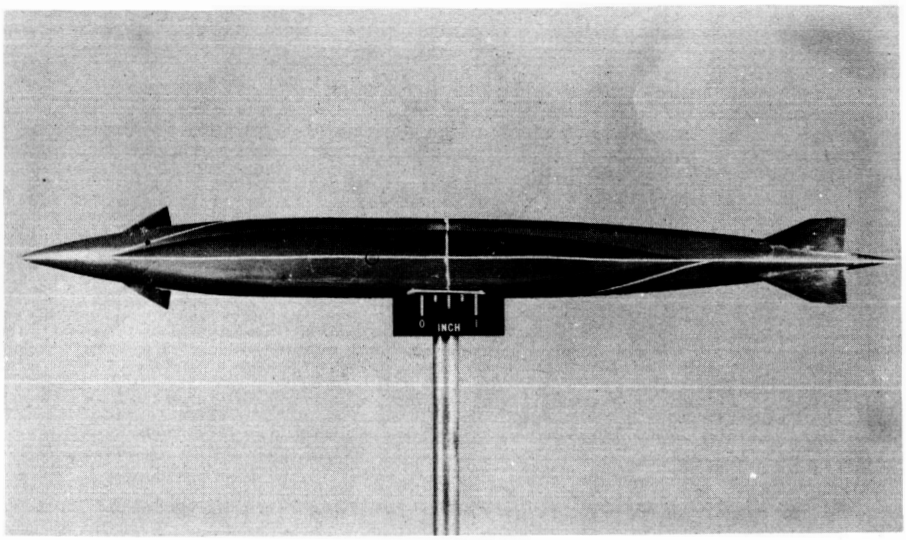

L-59-2024

Top view

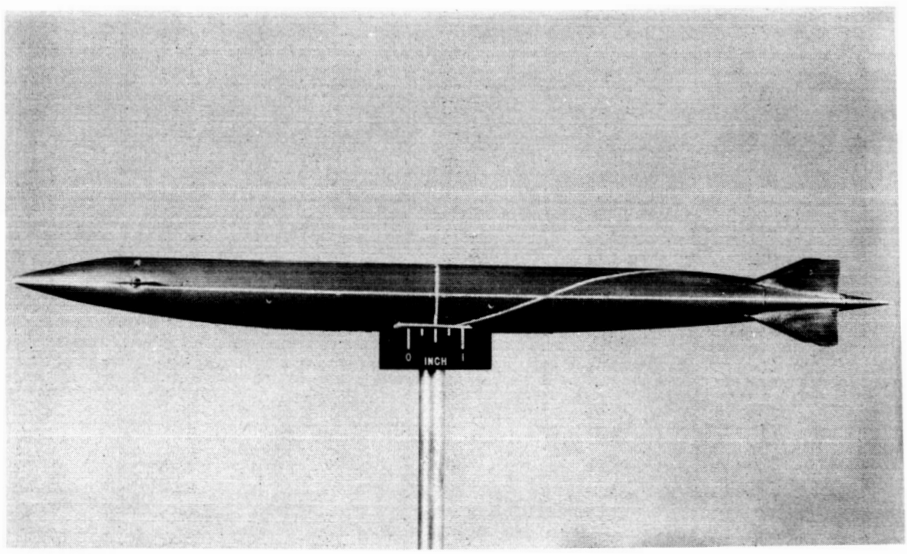

Side view

L-59-2025

Figure 2.- Photographs of the fuel-tank model with cruciform tail fins.

L-915

[redacted]

DECLASSIFIED

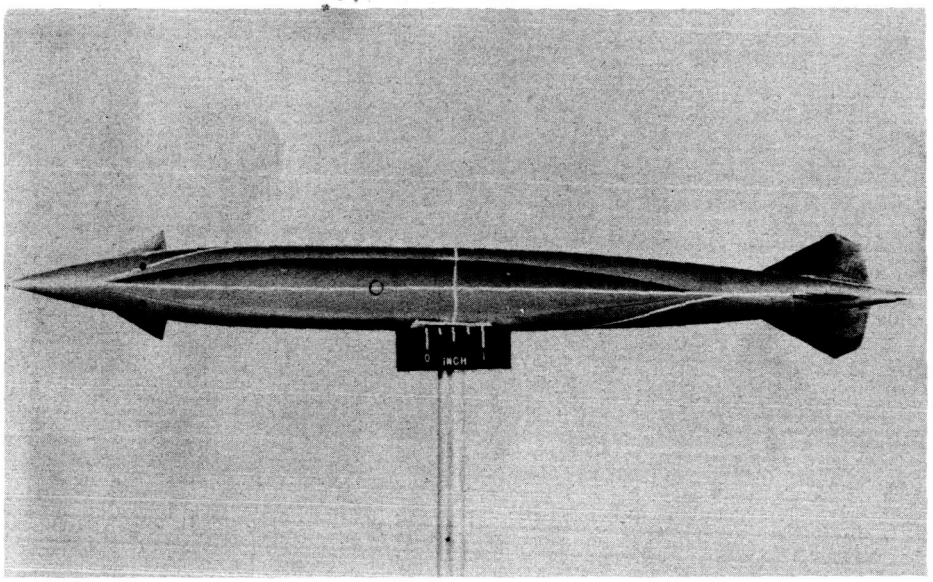

L-59-2027

Top view

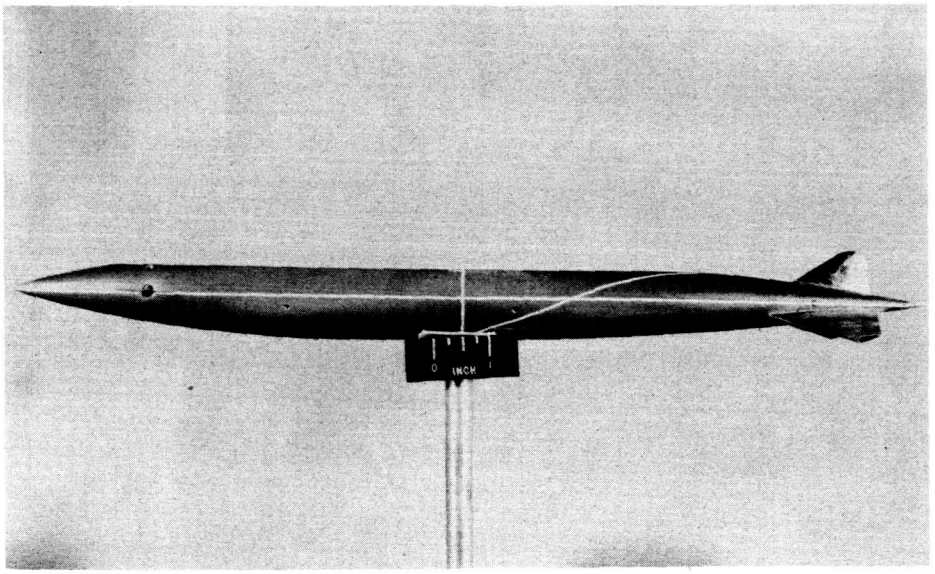

Side view

L-59-2026

Figure 3.- Photographs of the fuel-tank model with three tail fins mounted 120° apart.

[redacted]

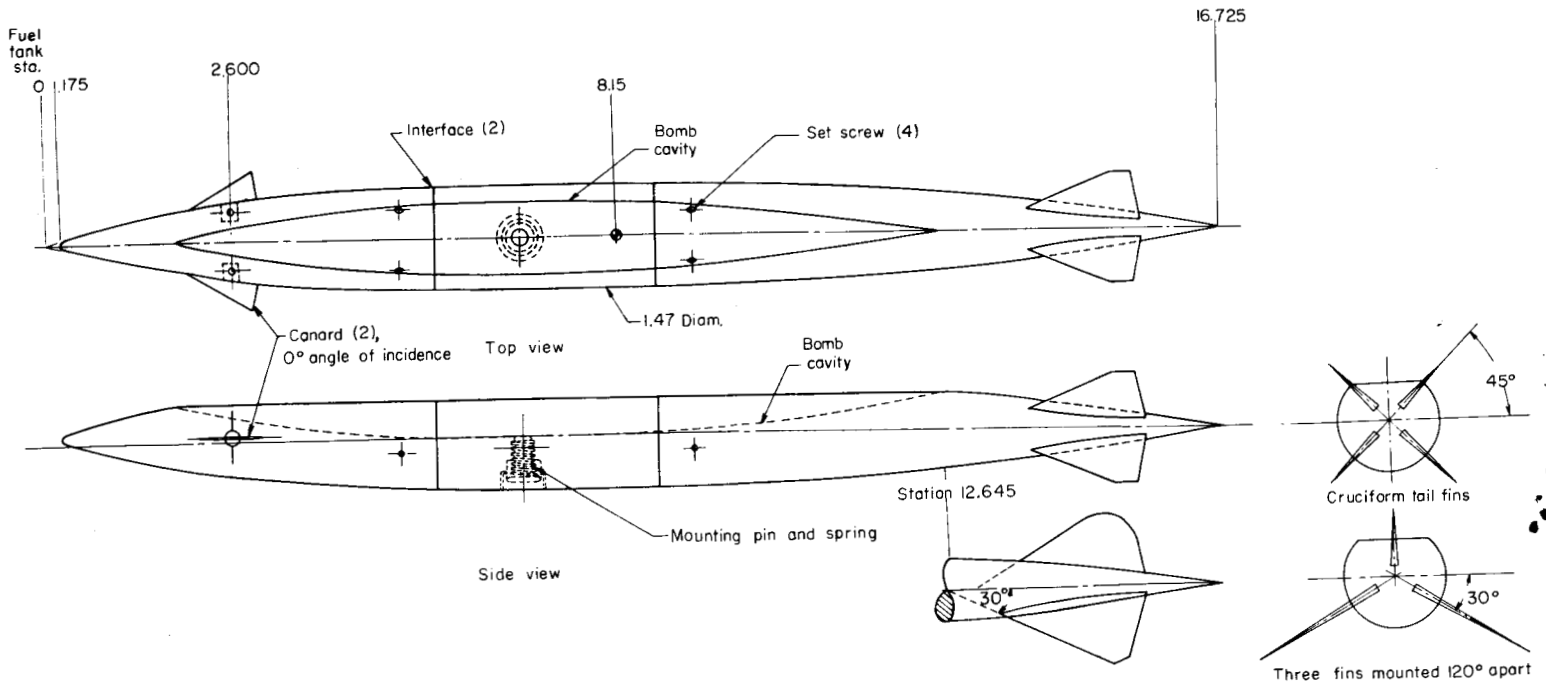

Figure 4.- Sketch of 1/40-scale fuel-tank model with tail-fin configurations. Dimensions are in inches.

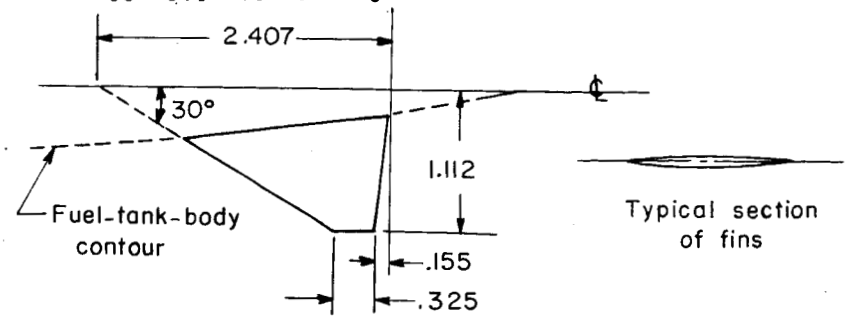

(a) Cruciform tail-fin configuration.

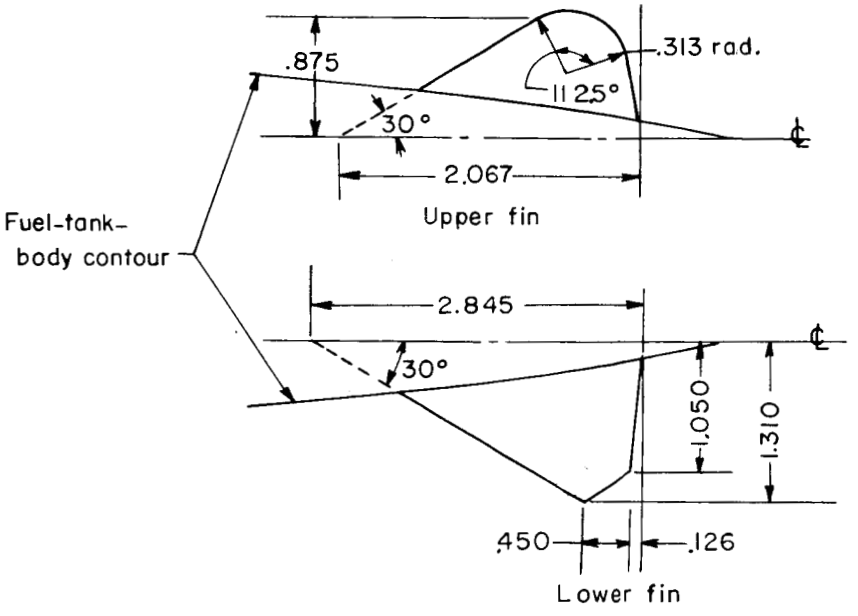

(b) Tail-fin configurations when three fins were mounted 120° apart.

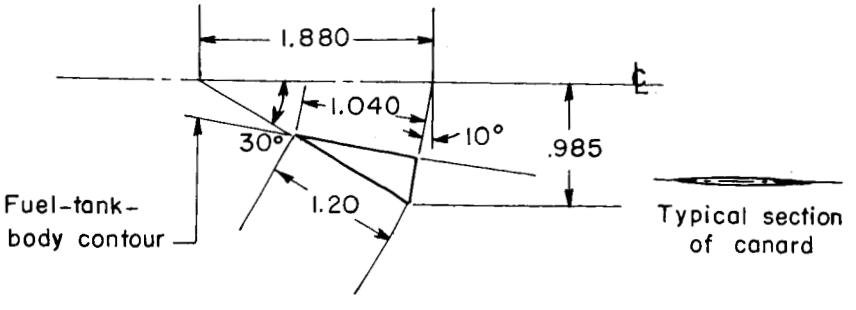

(c) Canard configuration used on all models.

Figure 5.- Details of fuel-tank canard and tail-fin configurations. Dimensions are in inches.

[redacted]

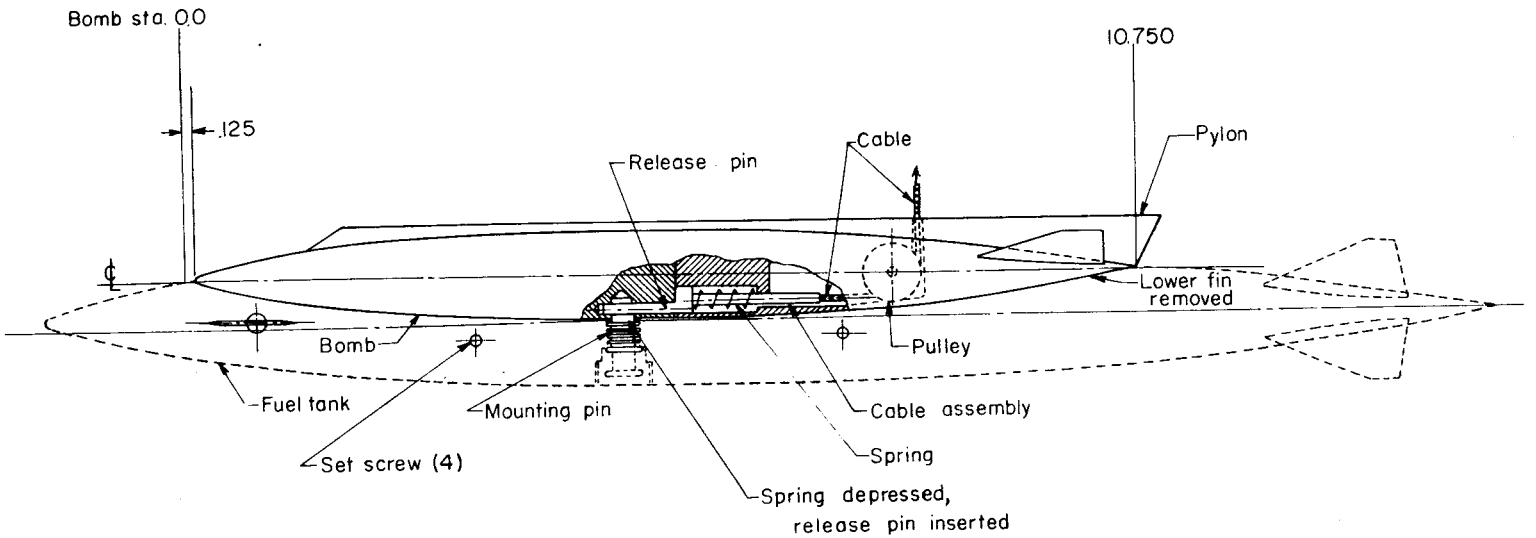

Figure 6.- Sketch showing pylon-mounted bomb and fuel tank installed, along with part of release mechanism. Dimensions are in inches.

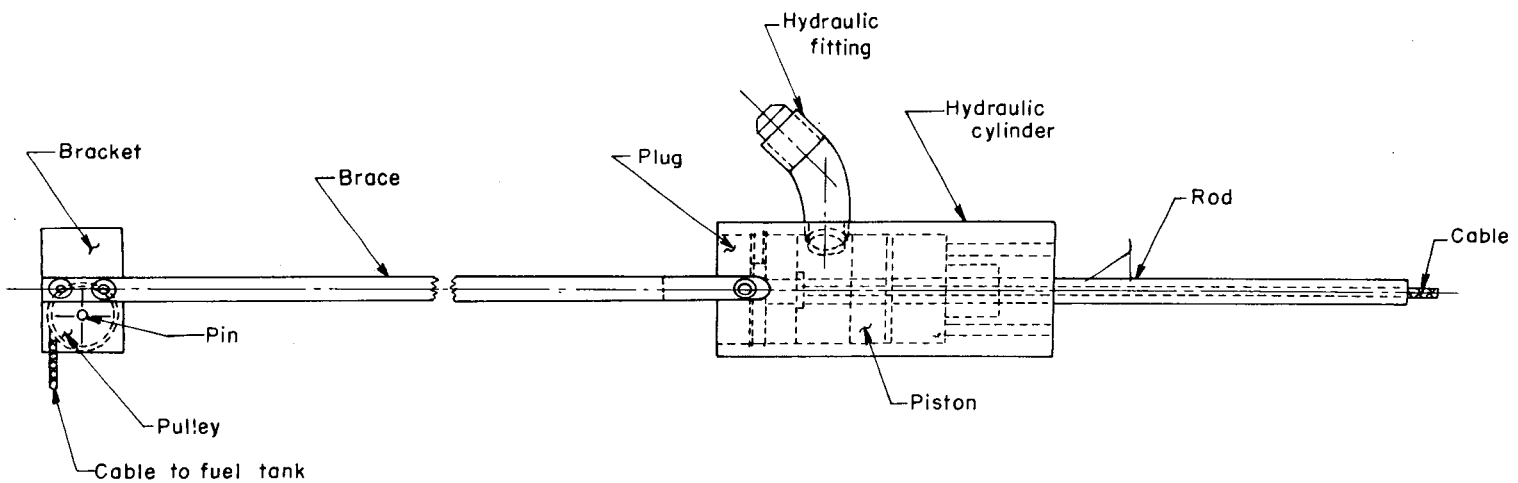

Figure 7.- Sketch of hydraulic mechanism used for fuel-tank release.

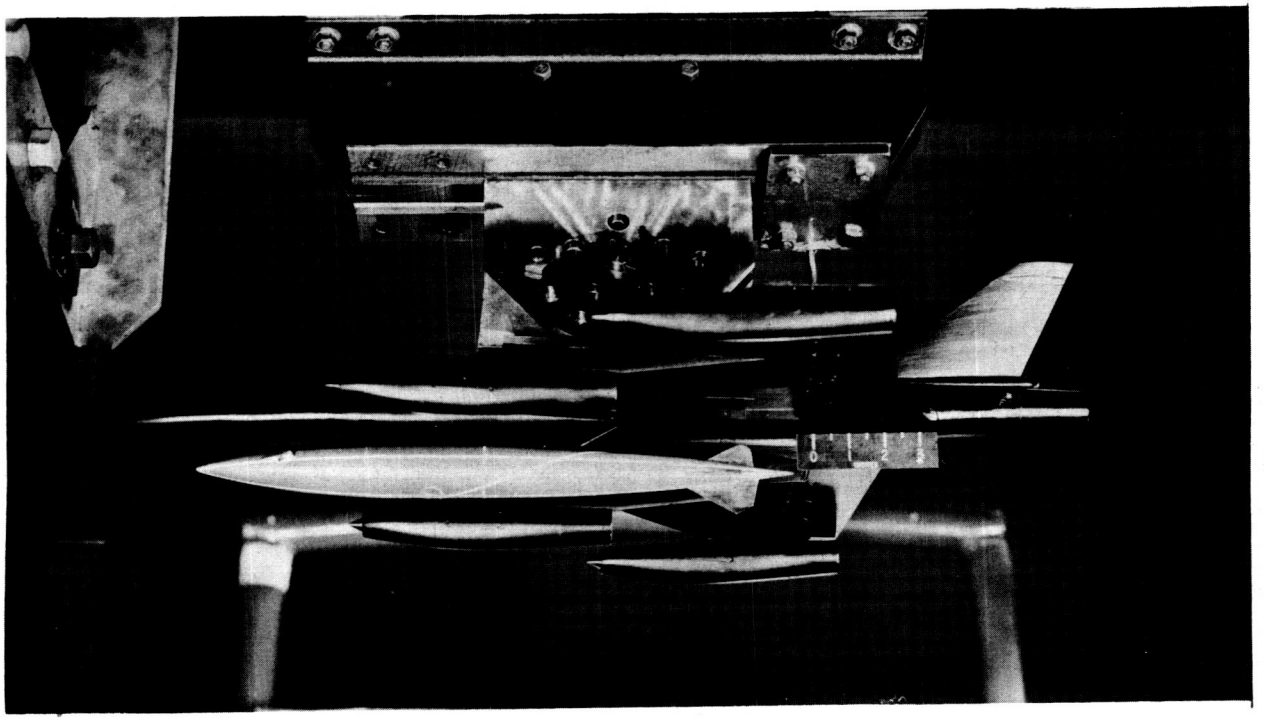

L-59-2043

Figure 8.- Photograph of 1/40-scale model of a current bomber airplane in preflight jet.

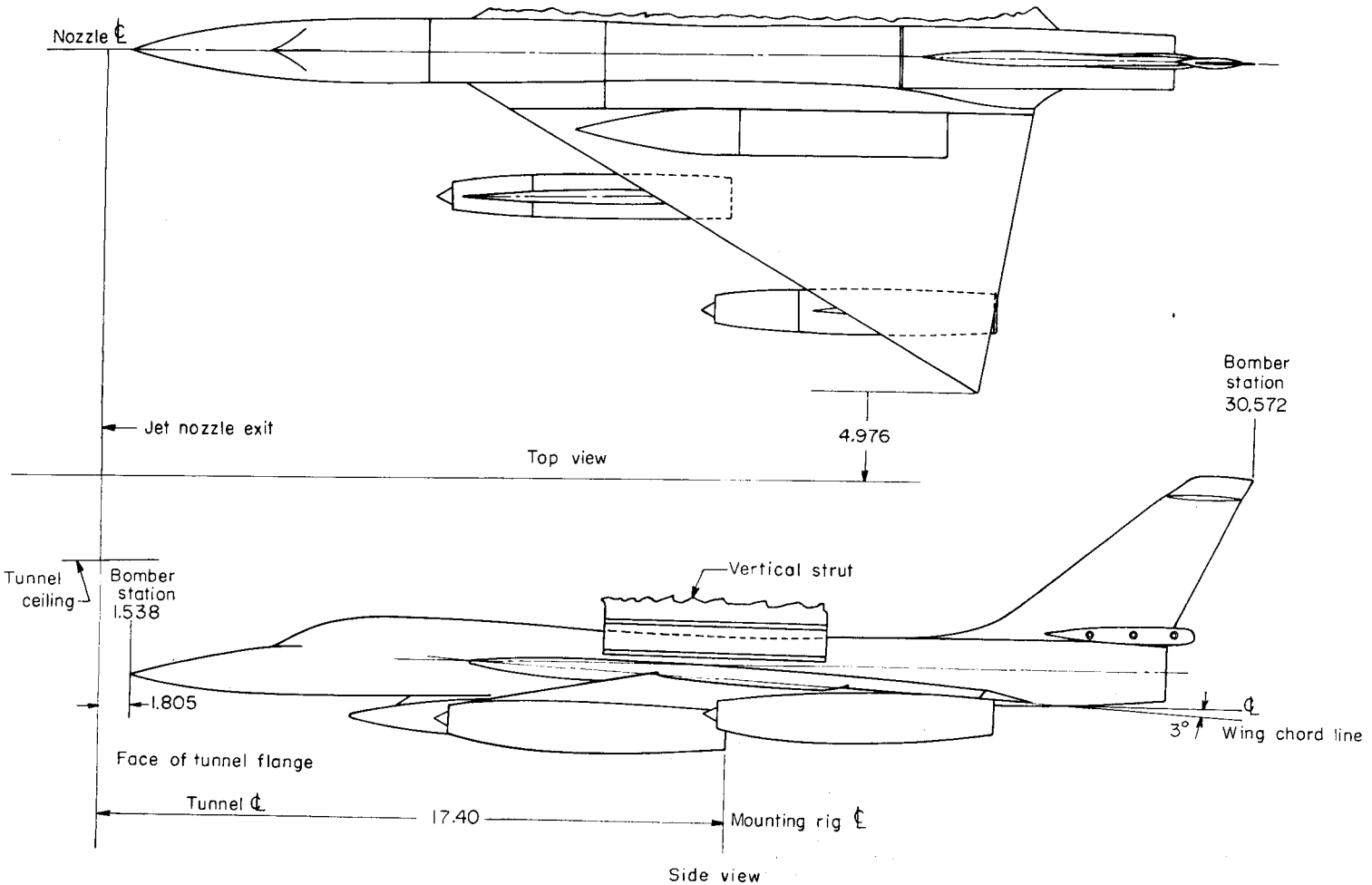

Figure 9.- Sketch of 1/40-scale model of a current bomber airplane in preflight jet. Dimensions are in inches.

[redacted]

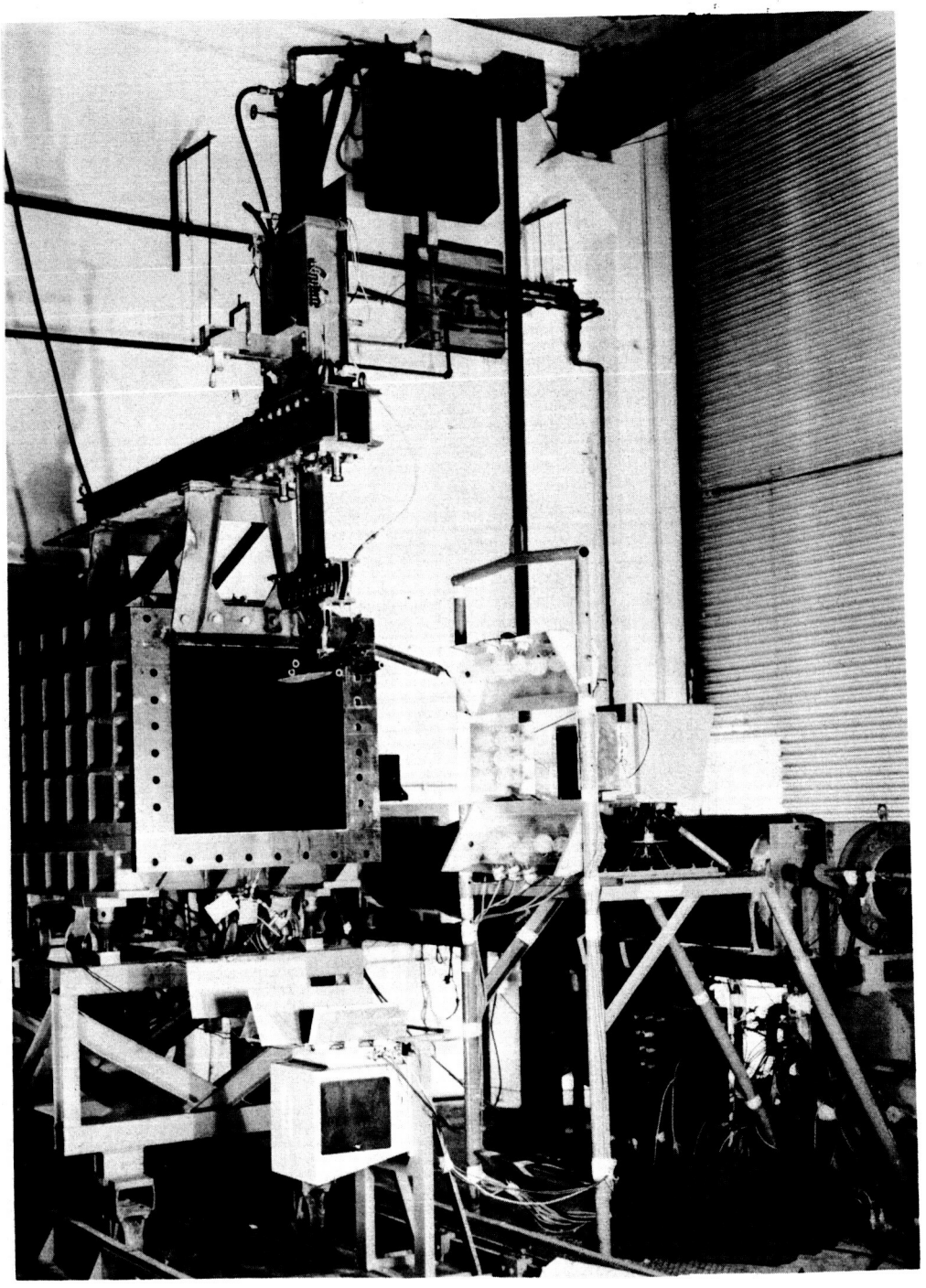

L-59-2042

Figure 10.- Equipment setup in the preflight jet of the NASA Wallops Station.

L-915

[redacted]

DEC[redacted]IFIED

L-915

Side view

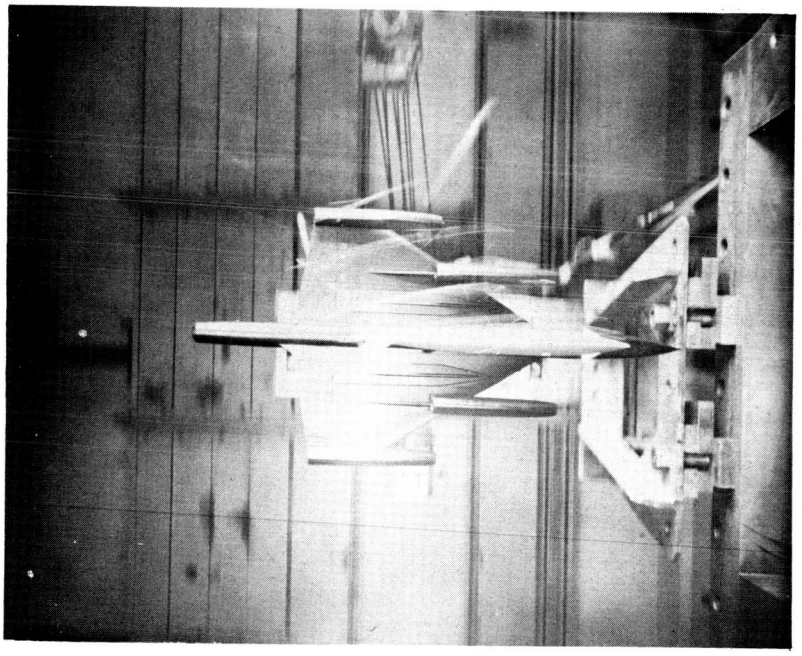

Bottom view

L-60-4354

(a) Test 1. $M = 0.91$; $h = 25{,}400$ feet; $\delta = -15^{\circ}$; $\alpha = 11^{\circ}13'$; $\beta = 0^{\circ}$; fuel tank struck airplane model.

Figure 11.- Fuel-tank releases with cruciform tail fins.

[redacted]

[redacted]

Side view

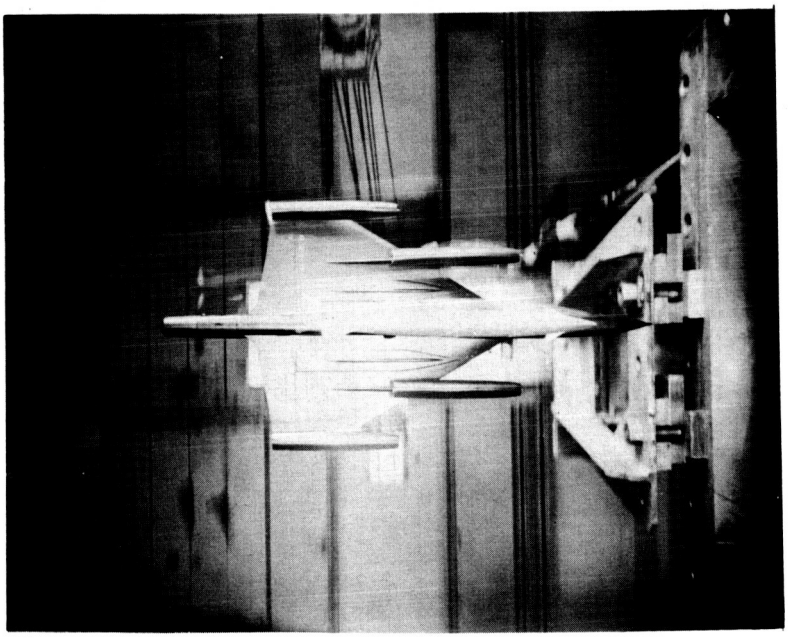

Bottom view

L-60-4355

(b) Test 2. $M = 0.91$; $h = 25{,}500$ feet; $\delta = -15^{\circ}$; $\alpha = 5^{\circ}30'$; $\beta = 0^{\circ}$.

Figure 11.- Continued.

[redacted]

L-915

DECLASSIFIED

L-915

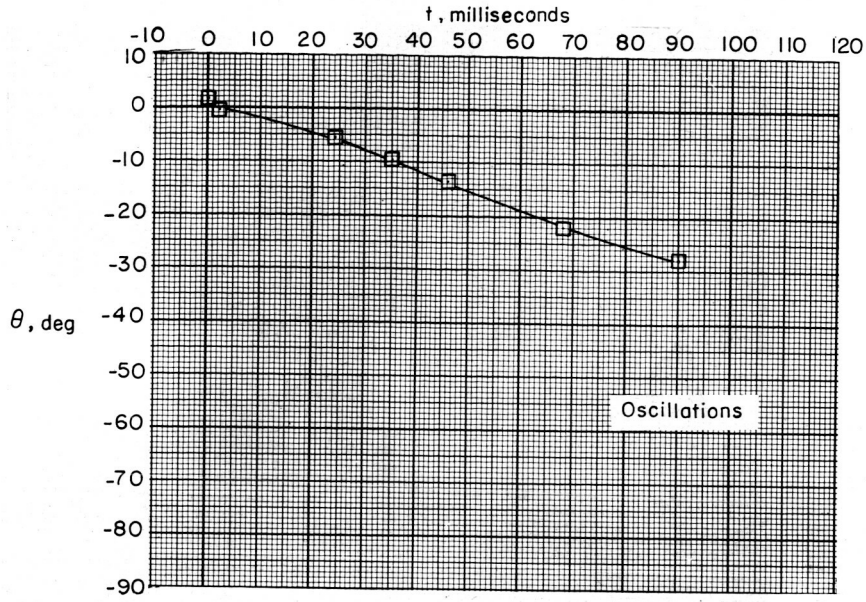

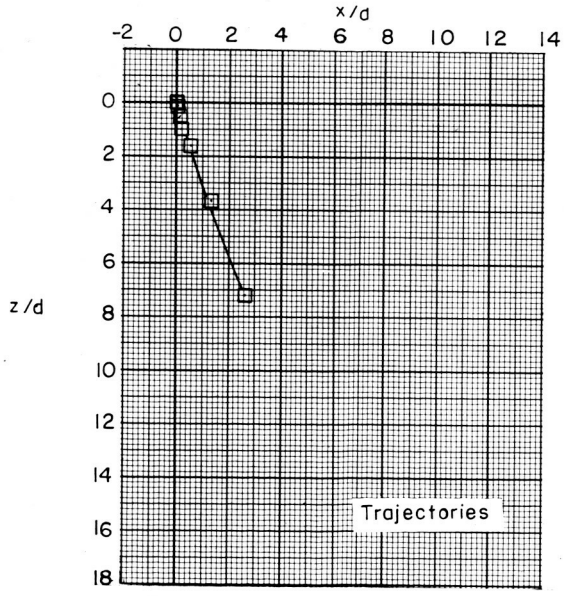

(b) Concluded.

Figure 11.- Continued.

[redacted]

[redacted]

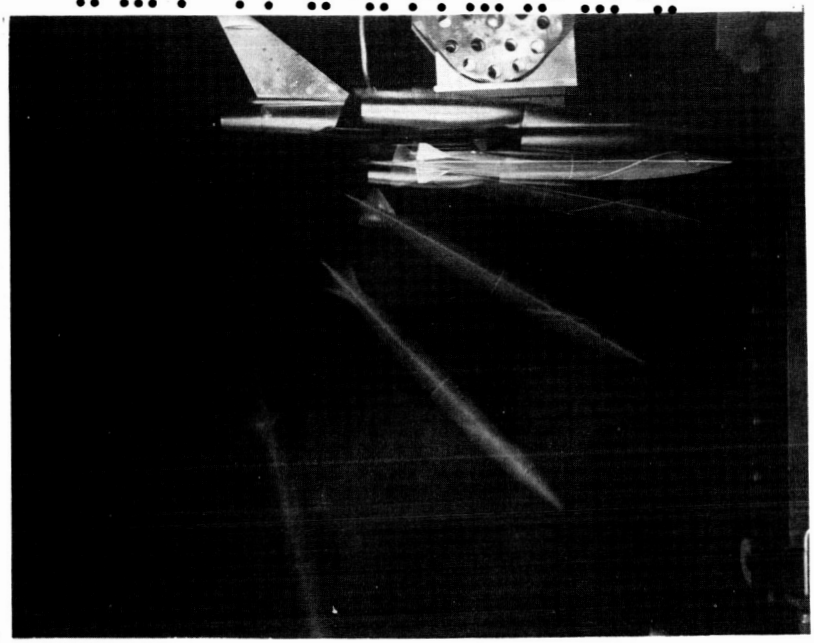

Side view

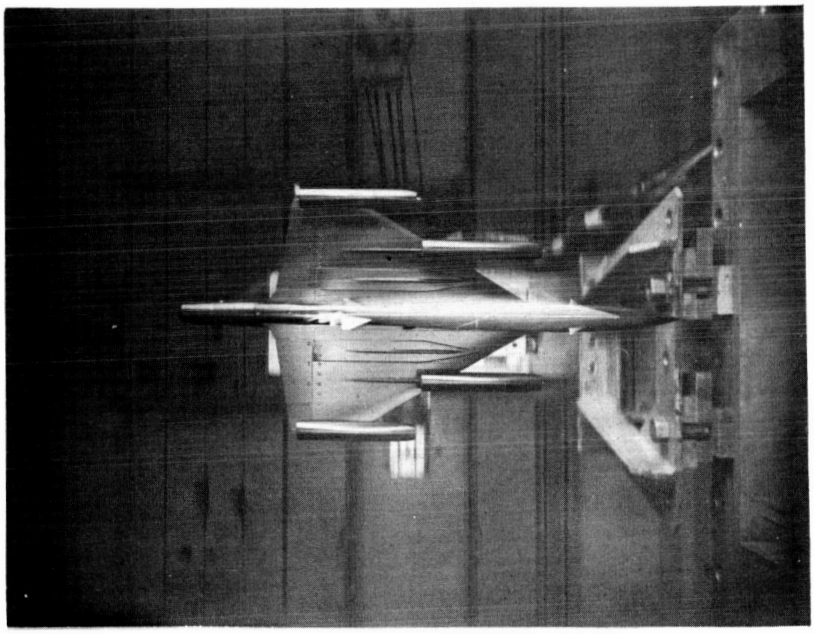

Bottom view

L-60-4356

(c) Test 3. $M = 0.89$; $h = 1{,}300$ feet; $\delta = 2^{\circ}$; $\alpha = 3^{\circ}16'$; $\beta = 0^{\circ}$.

Figure 11.- Continued.

[redacted]

L-915

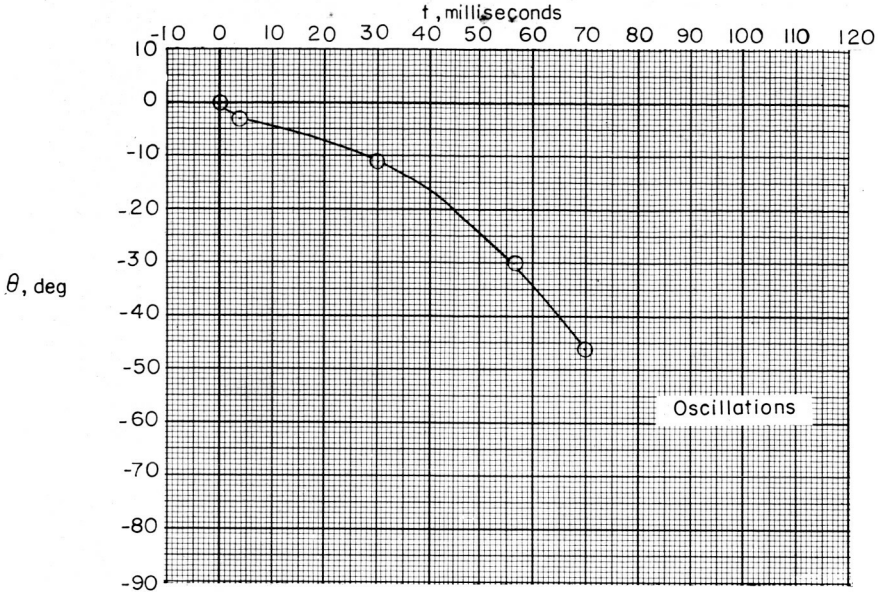

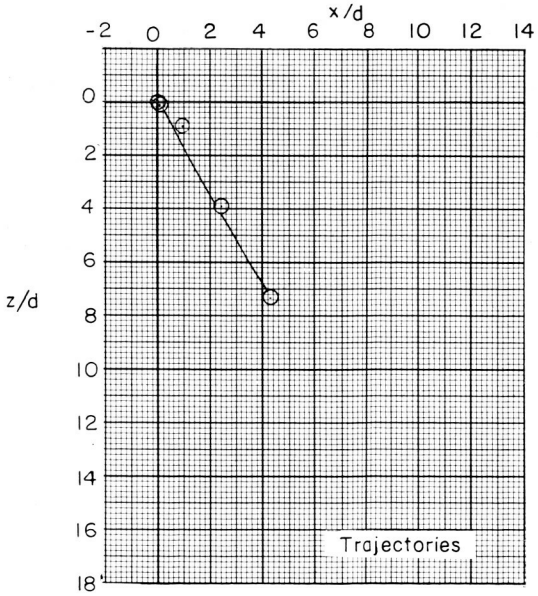

(c) Concluded.

Figure 11.- Continued.

L-915

[redacted]

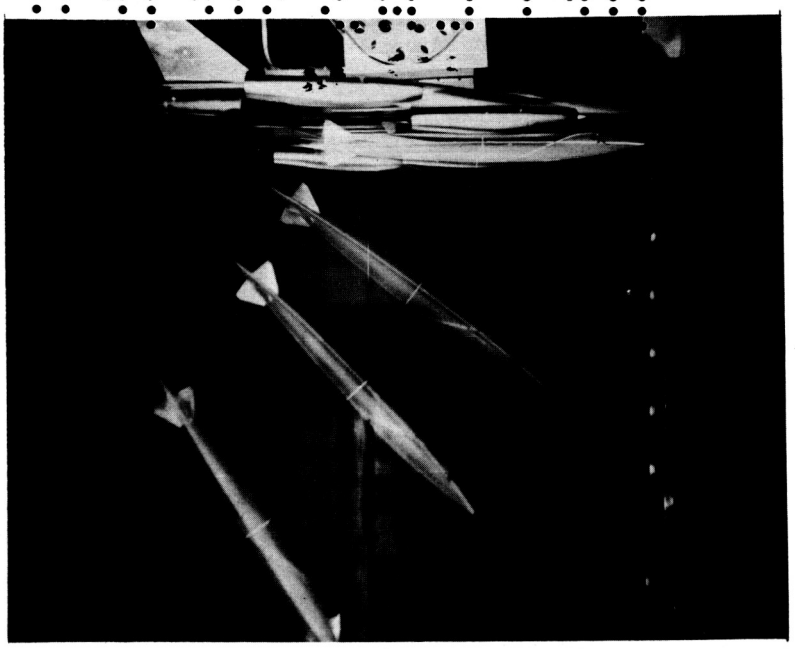

Side view

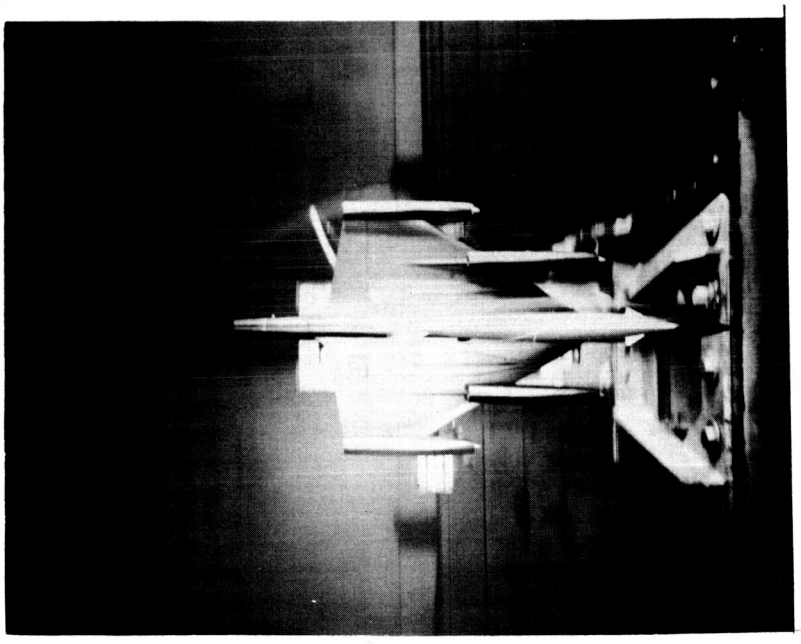

Bottom view

L-60-4357

(d) Test 4. $M = 1.39$; $h = 25{,}350$ feet; $\delta = -15^{\circ}$; $\alpha = 3^{\circ}42'$; $\beta = 0^{\circ}$.

Figure 11.- Continued.

[redacted]

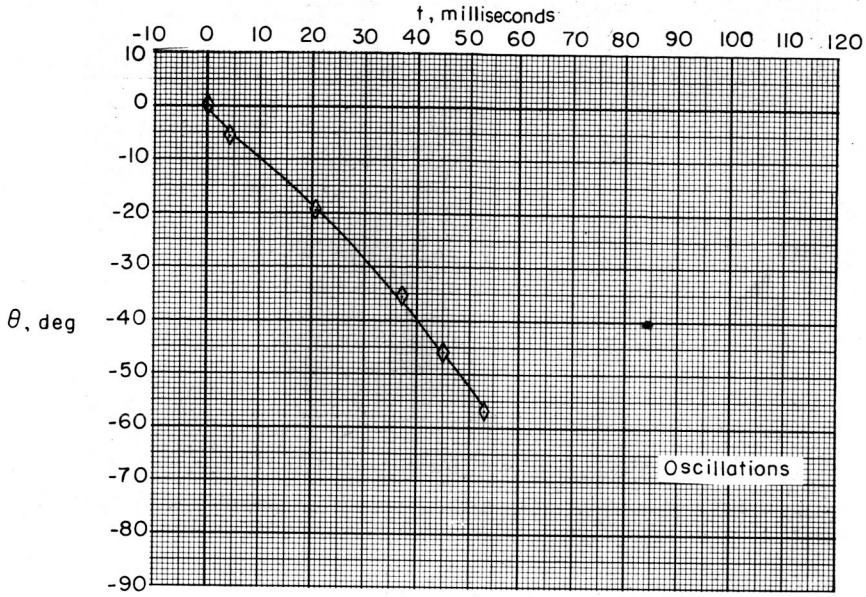

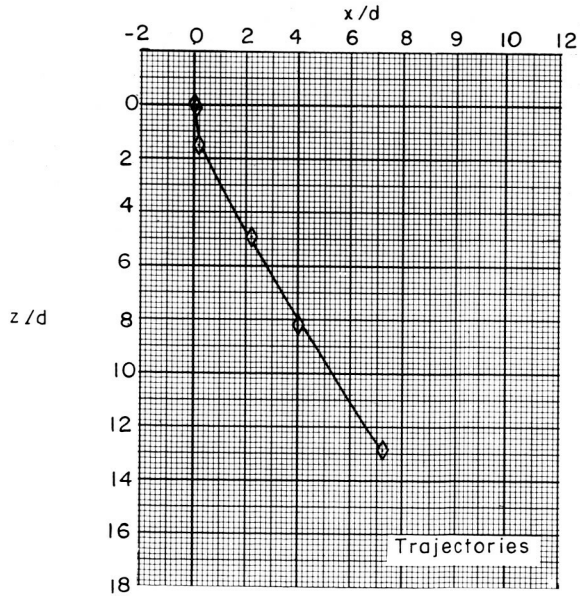

(d) Concluded.

Figure 11.- Continued.

[redacted]

Side view

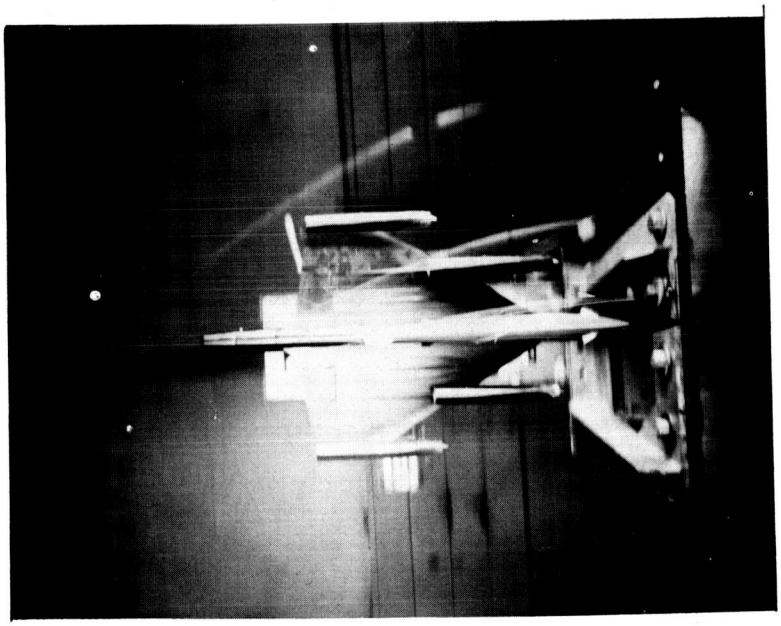

Bottom view

L-60-4358

(e) Test 5 and test 6. $M = 1.59$; $h = 25{,}600$ feet; $\delta = -15^{\circ}$; $\alpha = 5^{\circ}56'$; $\beta = 0^{\circ}$.

Figure 11.- Continued.

[redacted]

Side view

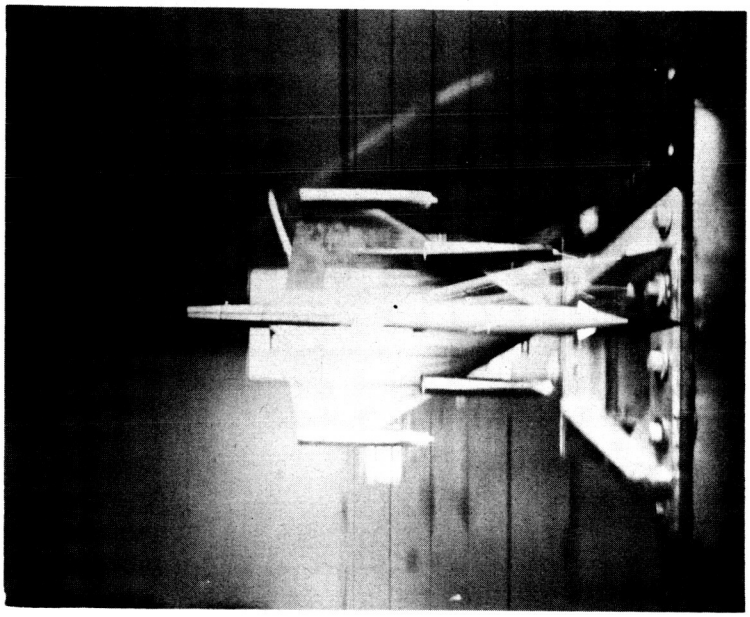

Bottom view

Test 6. Repeat of test 5.

(e) Continued.

L-60-4359

Figure 11.- Continued.

[redacted]

[redacted]

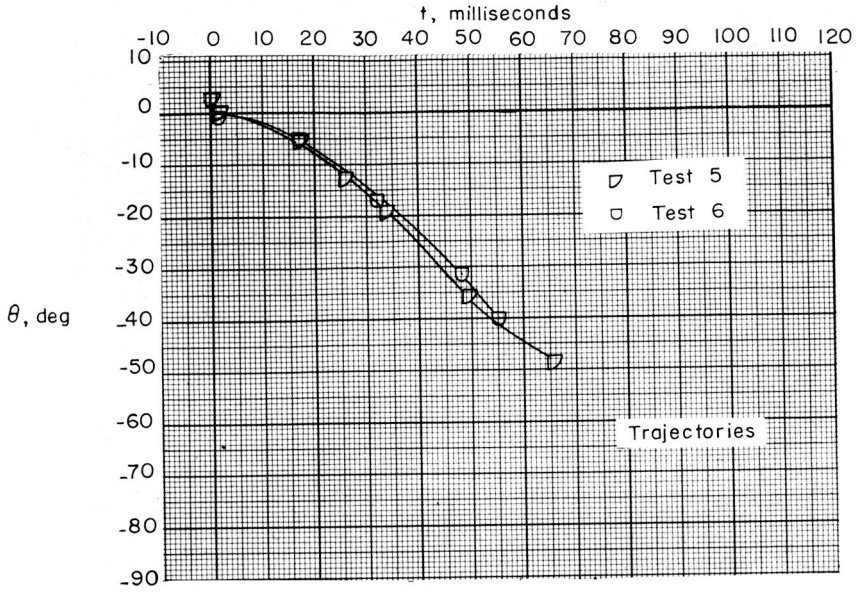

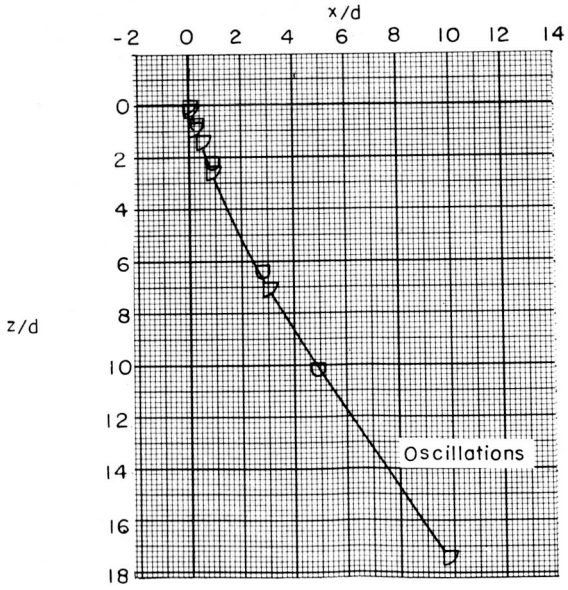

(e) Concluded.

Figure 11.- Continued.

[redacted]

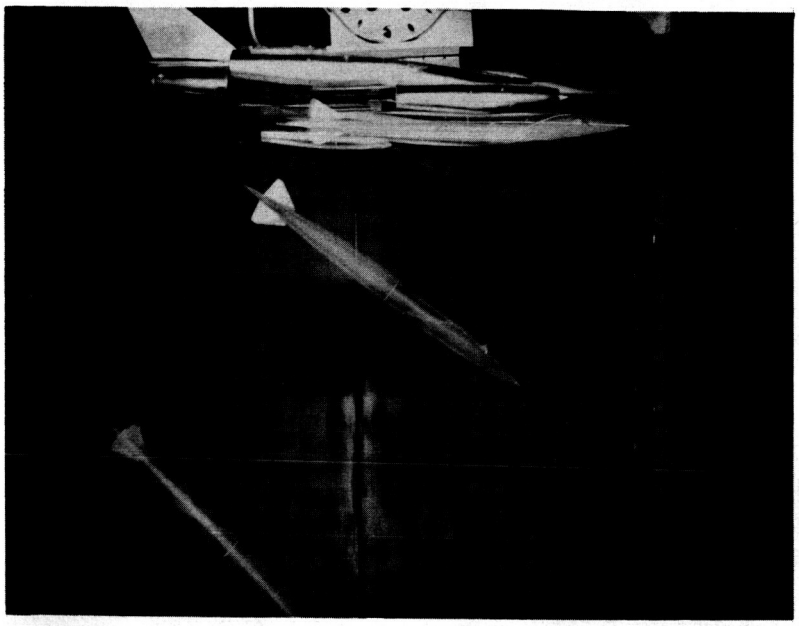

Side view

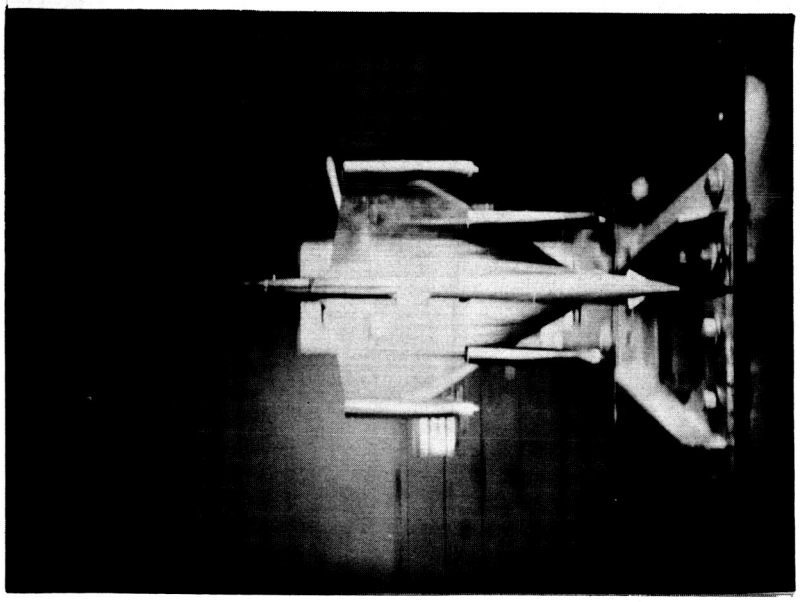

Bottom view

L-60-4360

(f) Test 7. M = 1.59; h = 25,650 feet; $\delta = -15^{\circ}$; $\alpha = 3^{\circ}16'$; $\beta = 0^{\circ}$; tail fin struck airplane model.

Figure 11.- Continued.

[redacted]

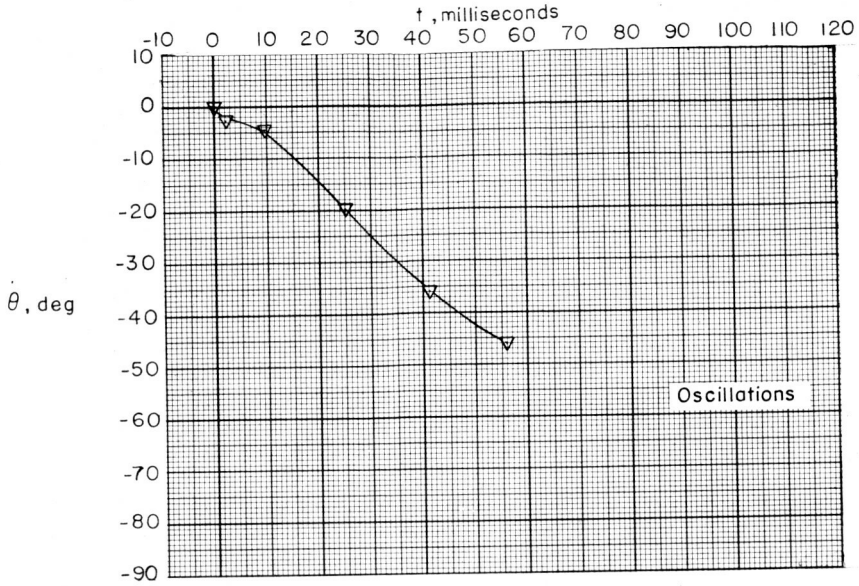

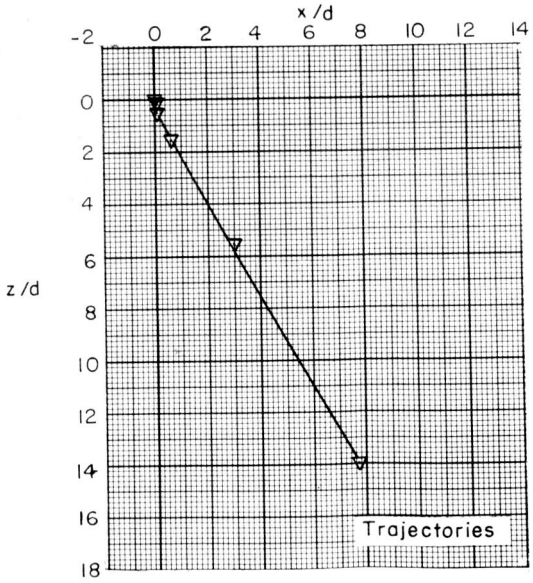

(f) Concluded.

Figure 11.- Continued.

[redacted]

DECLASSIFIED
[redacted]

L-915

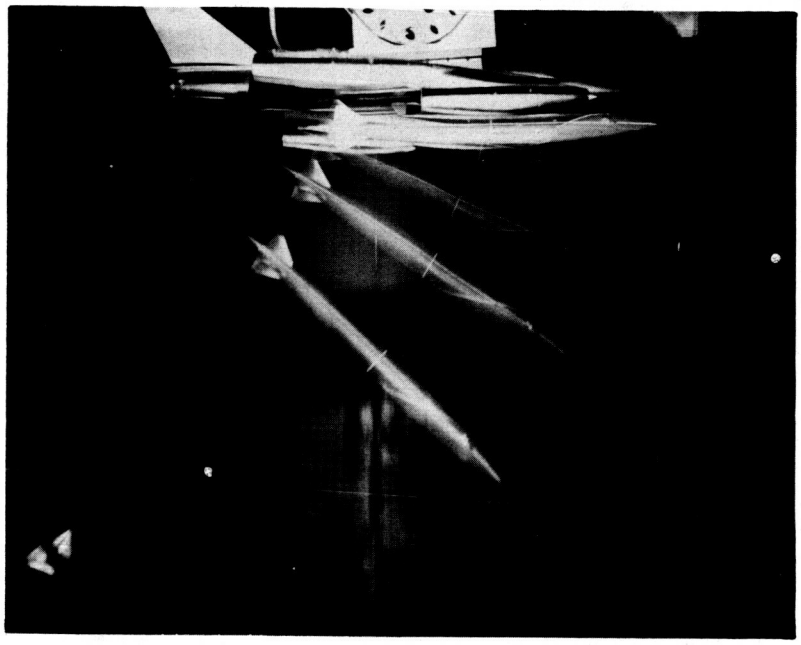

Side view

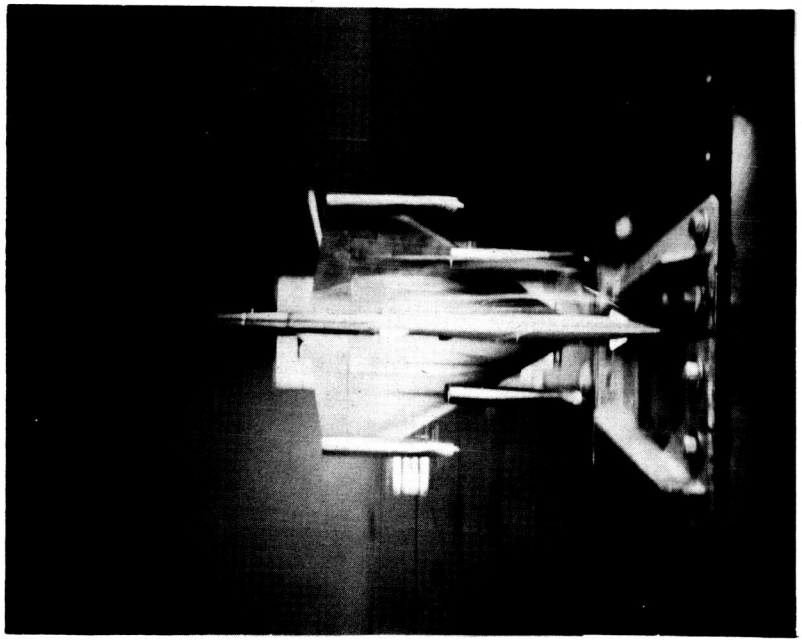

Bottom view

L-60-4361

(g) Test 8. $M = 1.59$; $h = 25{,}650$ feet; $\delta = -15^{\circ}$; $\alpha = 4^{\circ}30'$; $\beta = 0^{\circ}$.

Figure 11.- Continued.

[redacted]

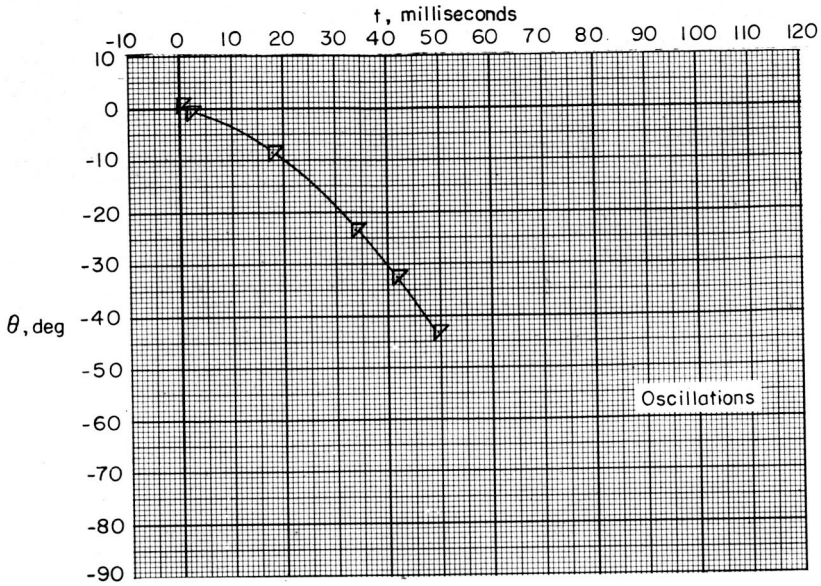

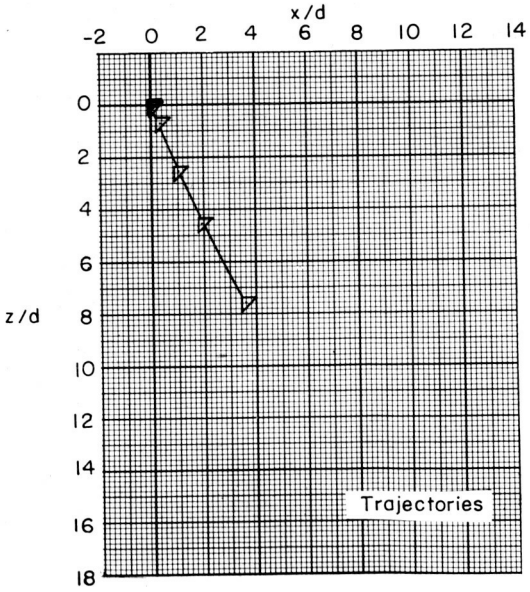

(g) Concluded.

Figure 11.- Continued.

L-915

[redacted]

DECLASSIFIED
[redacted]

L-915

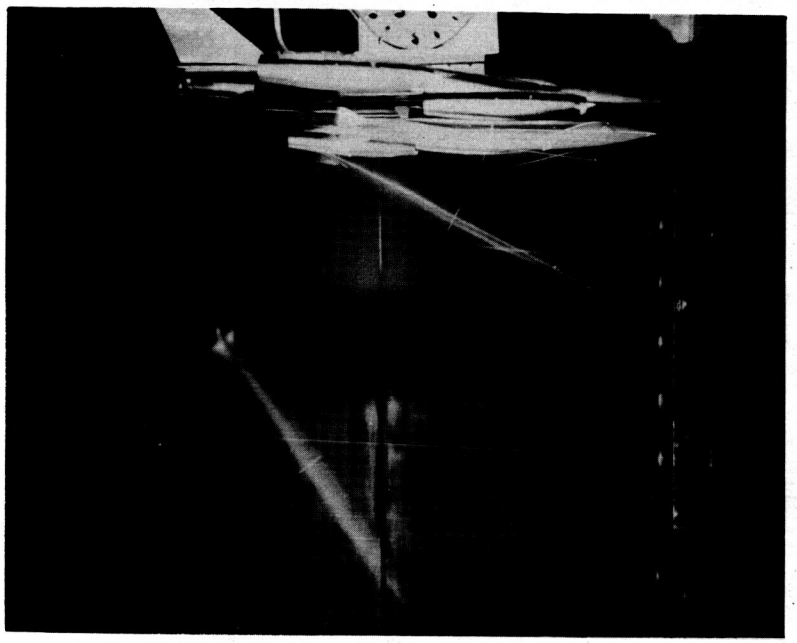

Side view

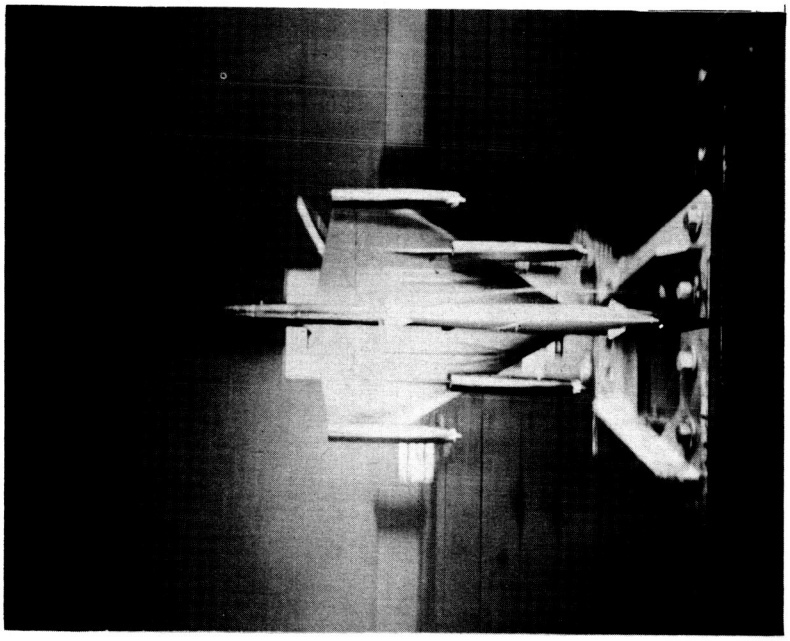

Bottom view

L-60-4362

(h) Test 9. $M = 1.98$; $h = 25{,}700$ feet; $\delta = -15^{\circ}$; $\alpha = 3^{\circ}16'$; $\beta = 0^{\circ}$.

Figure 11.- Continued.

[redacted]

[redacted]

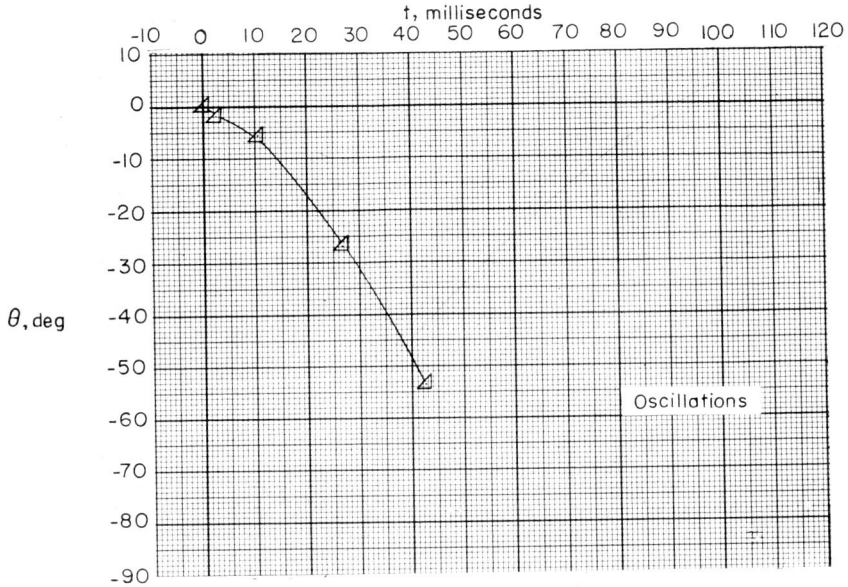

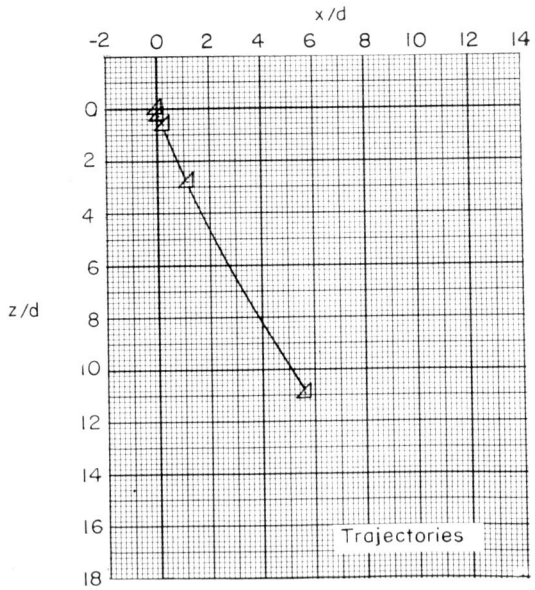

(h) Concluded.

Figure 11.- Continued.

L-915

[redacted]

DECLASSIFIED

[redacted]

L-915

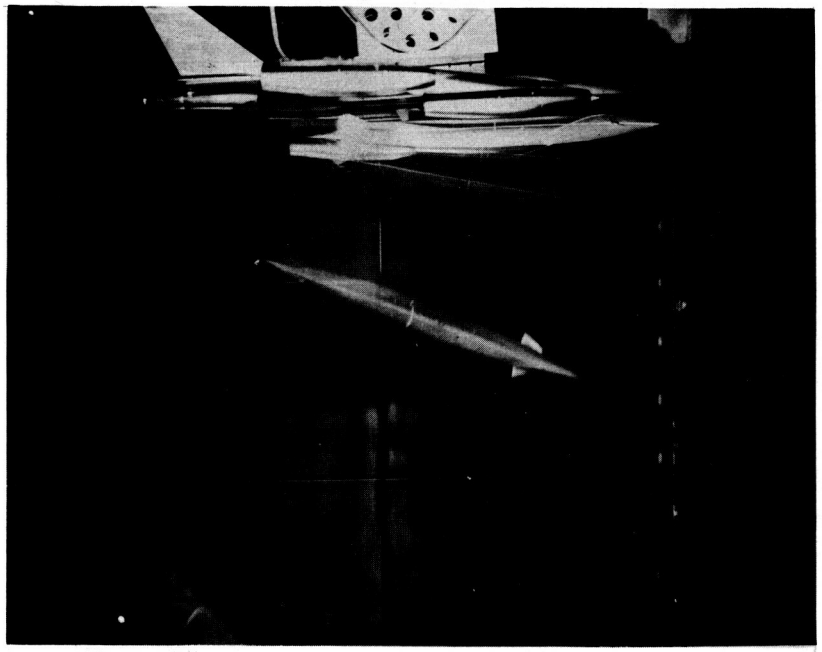

Side view

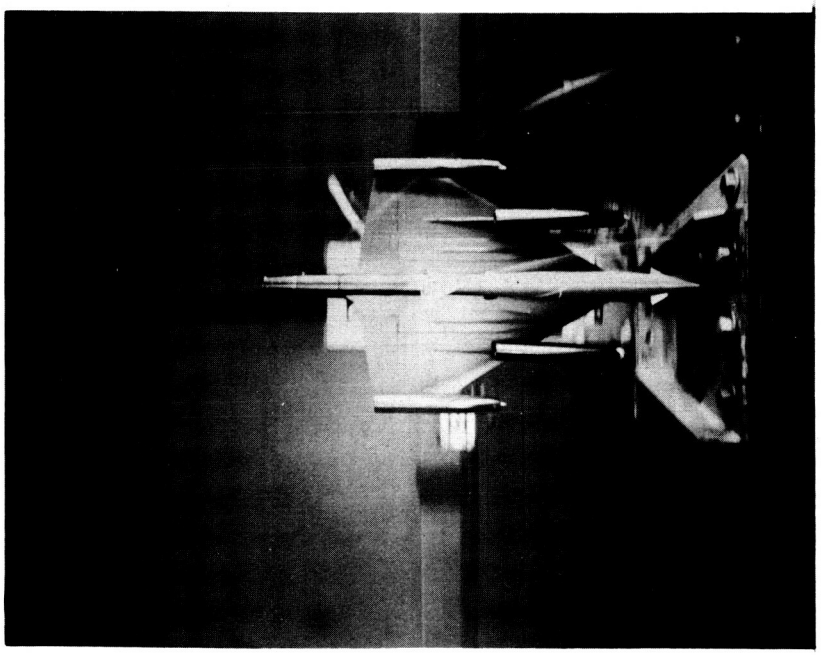

Bottom view

L-60-4363

(i) Test 10. M = 1.98; h = 25,700 feet; $\delta = -15^{\circ}$; $\alpha = 5^{\circ}06'$; $\beta = 0^{\circ}$.

Figure 11.- Continued.

[redacted]

[redacted]

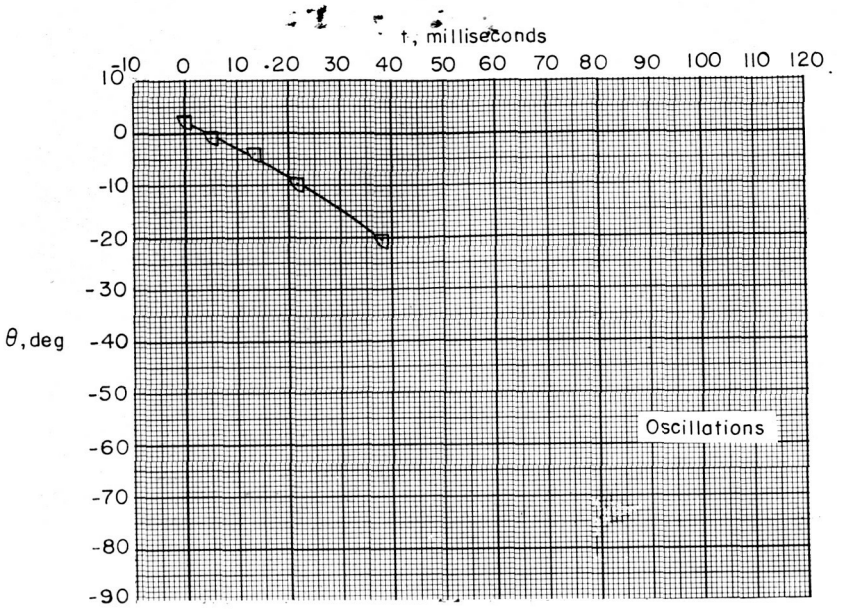

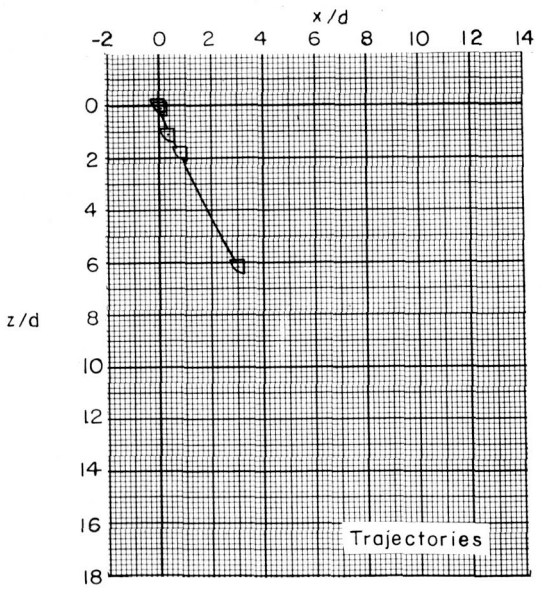

(i) Concluded.

Figure 11.- Continued.

[redacted]

L-915

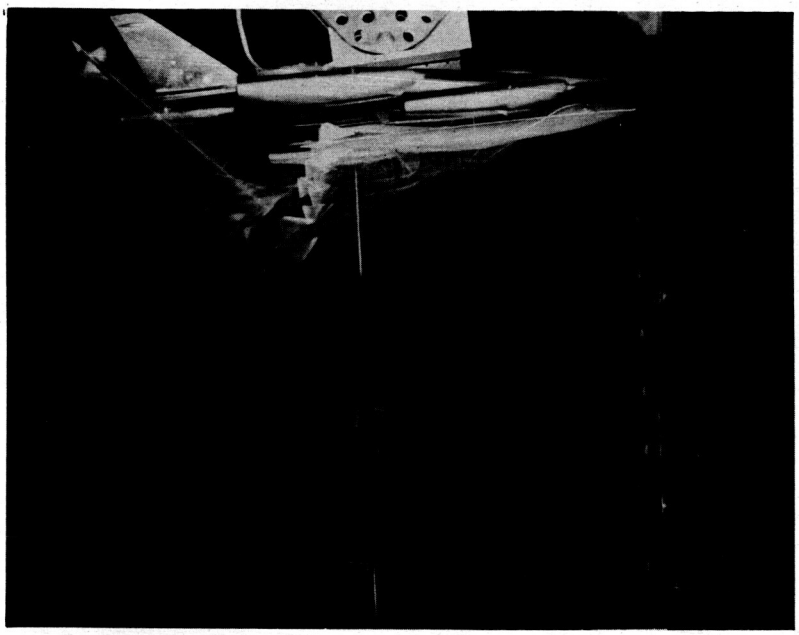

Side view

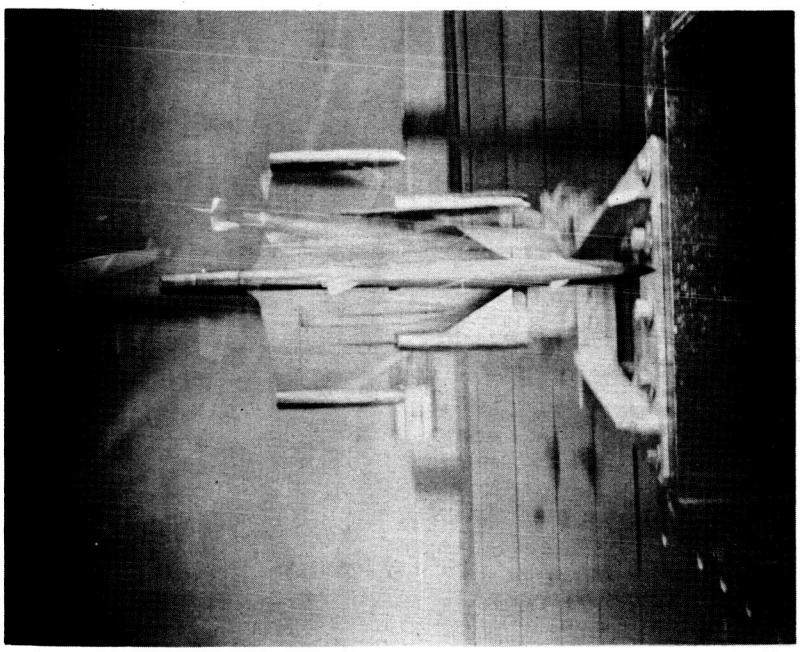

Bottom view

L-60-4364

(j) Test 11. $M = 1.98$; $h = 36{,}000$ feet; $\delta = -15^{\circ}$; $\alpha = 6^{\circ}37'$; $\beta = 0^{\circ}$; fuel tank hit airplane model.

Figure 11.- Concluded.

[redacted]

[redacted]

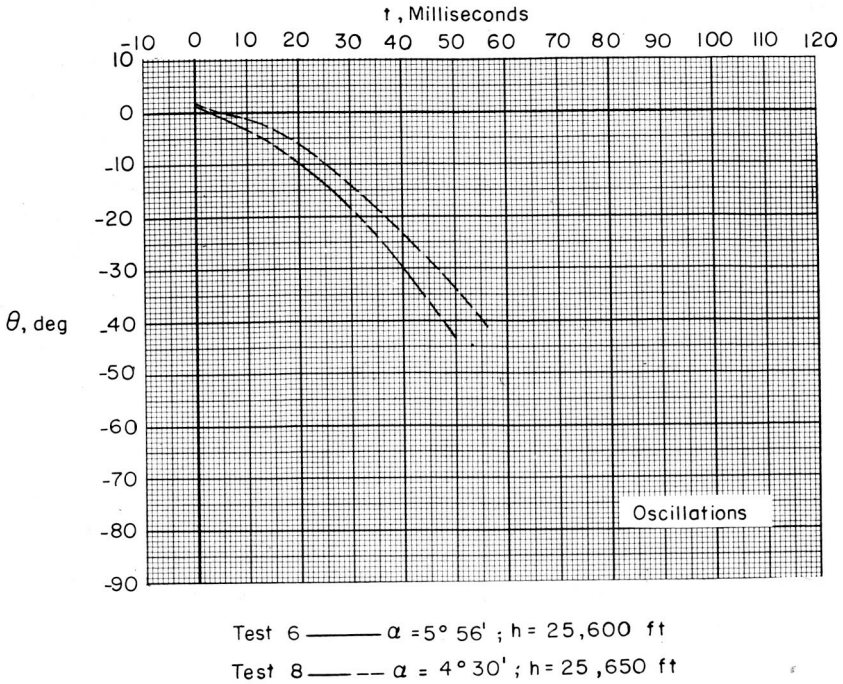

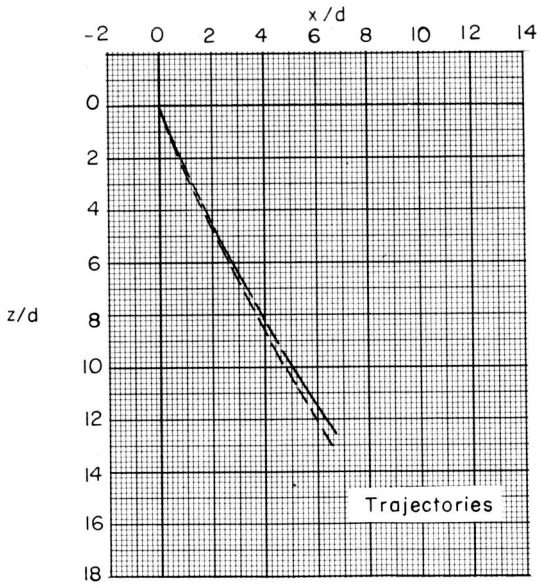

(a) Effect of change in wing angle of attack at $M = 1.59$; $\delta = -15^{\circ}$; $\beta = 0^{\circ}$.

Figure 12.- Comparison plots with cruciform tail fins.

L-915

[redacted]

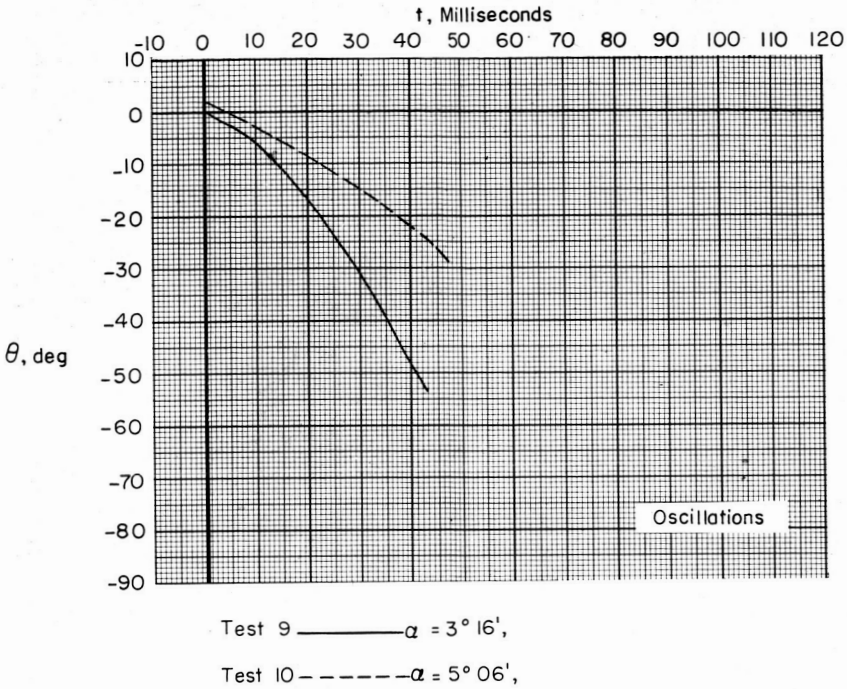

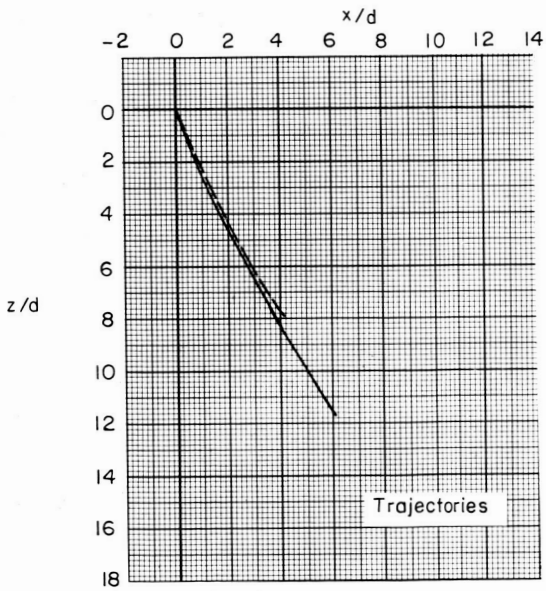

(b) Effect of change in wing angle of attack at $M = 1.98$; $\delta = -15^{\circ}$.

Figure 12.- Concluded.

L-915

[redacted]

Side view

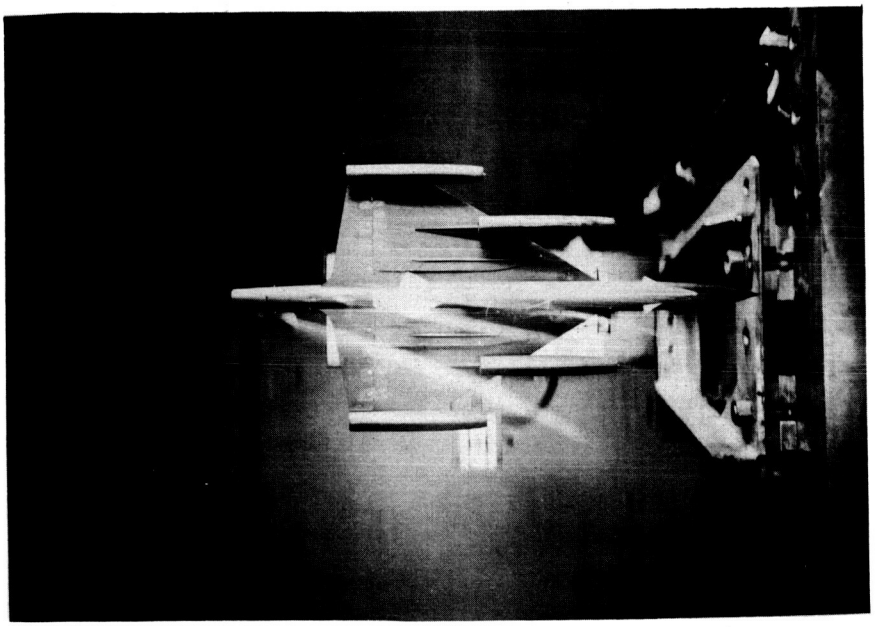

Bottom view

L-60-4365

(a) Test 12. $M = 0.69$; h = sea level; $\delta = -6^{\circ}$; $\alpha = 5^{\circ}11'$; $\beta = 0^{\circ}$.

Figure 13.- Fuel-tank releases with three tail fins mounted 120° apart.

DECLASSIFIED

[redacted]

L-915

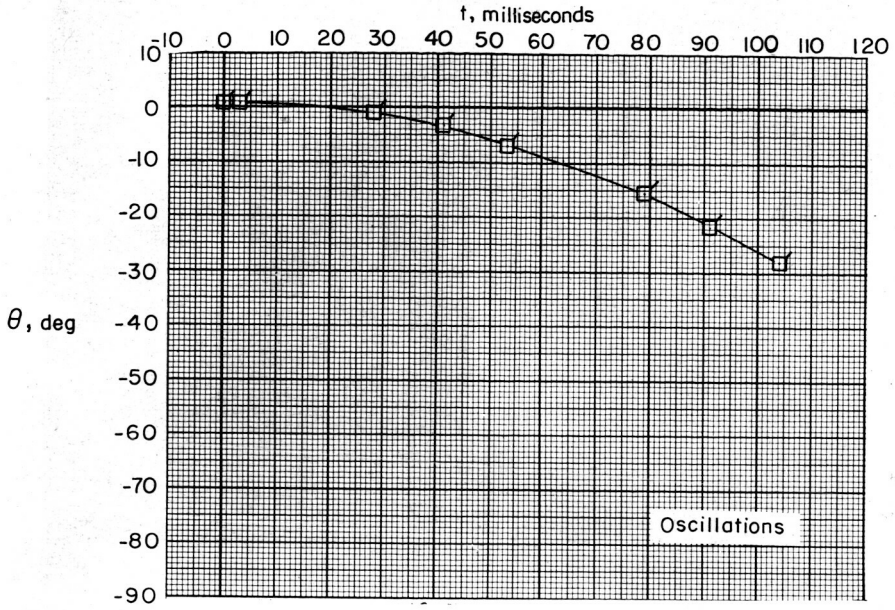

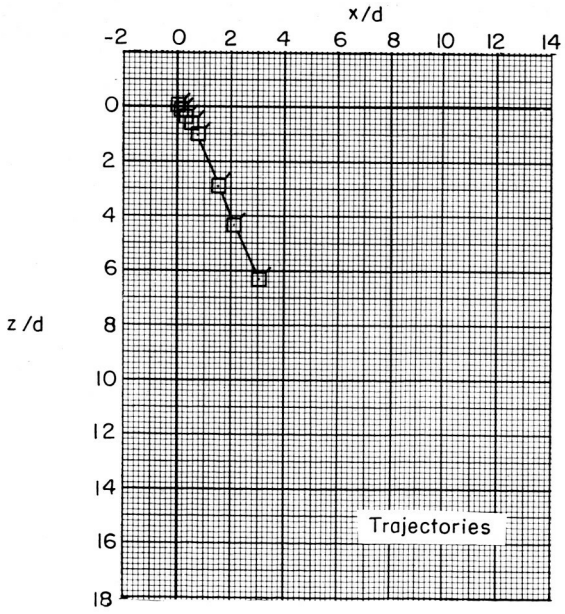

(a) Concluded.

Figure 13.- Continued.

[redacted]

[redacted]

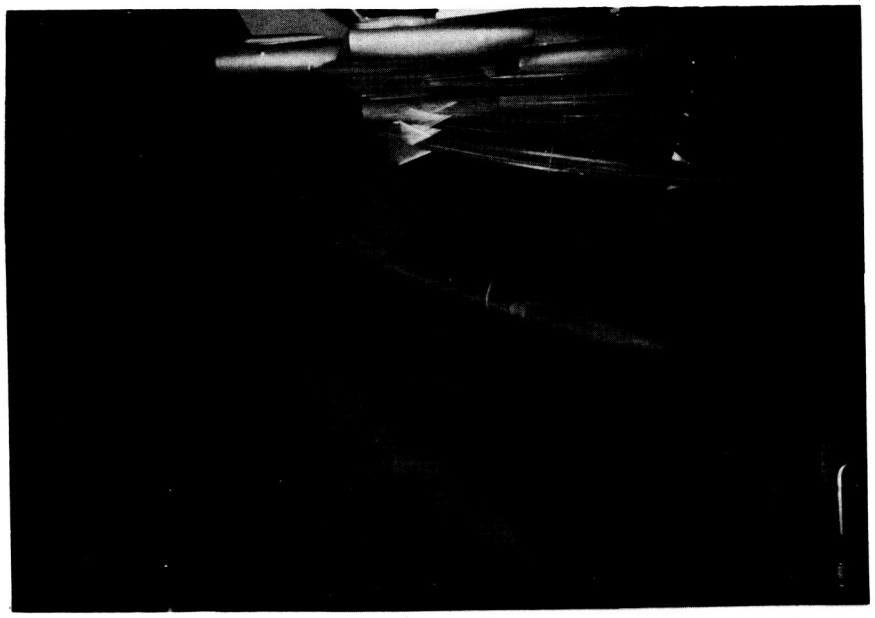

Side view

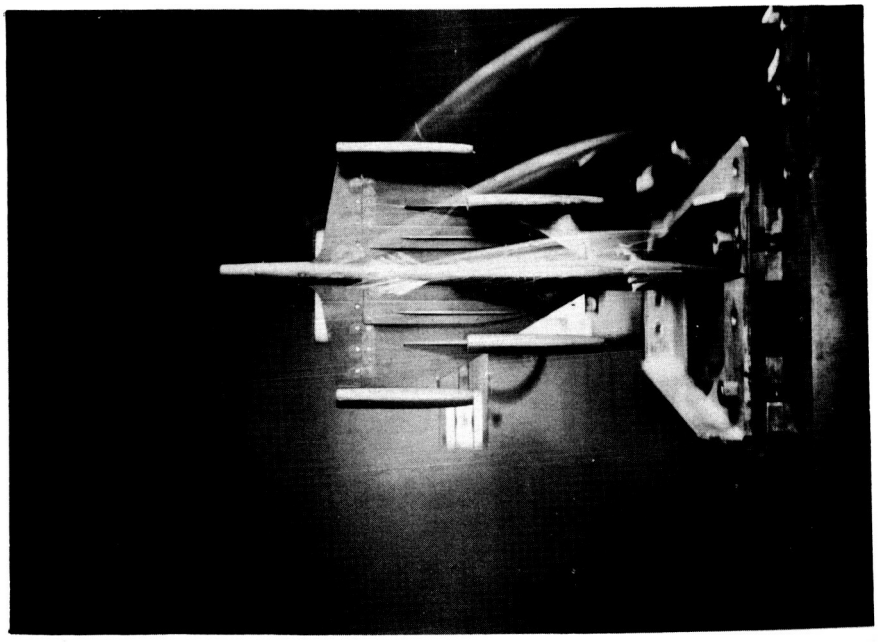

Bottom view

L-60-4366

(b) Test 13. $M = 0.69$; $h = 2{,}200$ feet; $\delta = -4^{\circ}$; $\alpha = 5^{\circ}11'$; $\beta = 0^{\circ}$; fuel-tank model rolled.

Figure 13.- Continued.

[redacted]

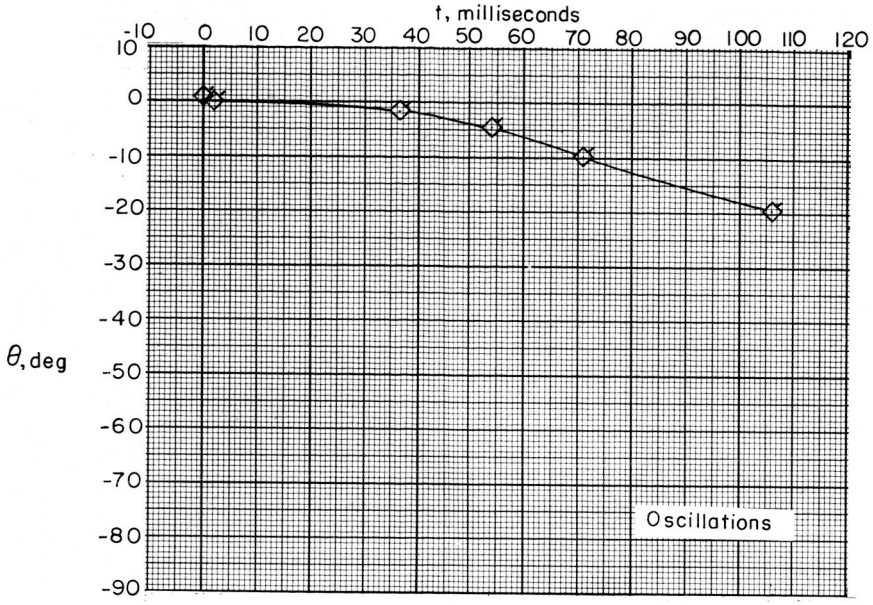

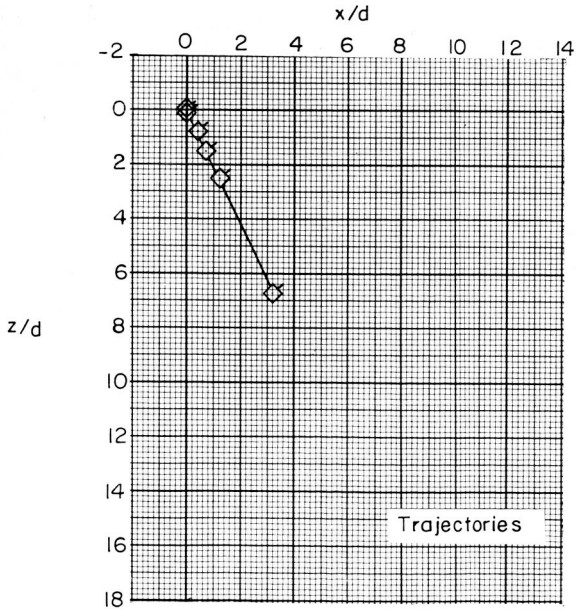

(b) Concluded.

Figure 13.- Continued.

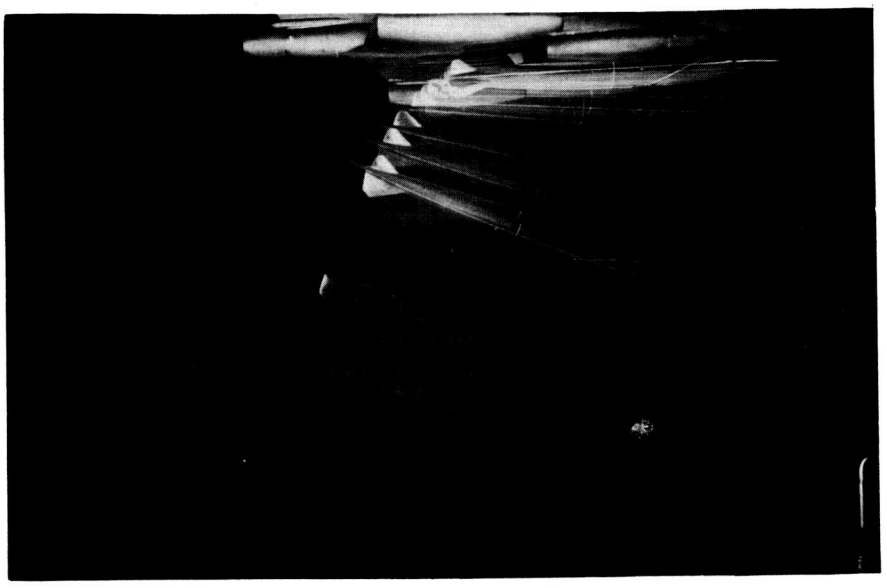

Side view

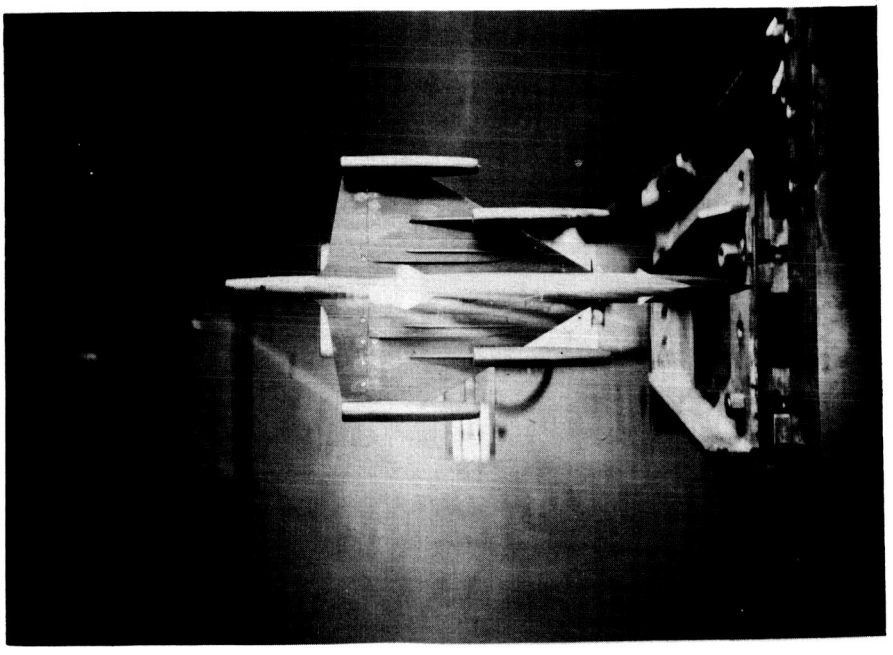

Bottom view

L-60-4367

(c) Test 14. $M = 0.70$; $h = 100$ feet; $\delta = -2^{\circ}$; $\alpha = 5^{\circ}11'$; $\beta = 0^{\circ}$.

Figure 13.- Continued.

DECLASSIFIED
[redacted]

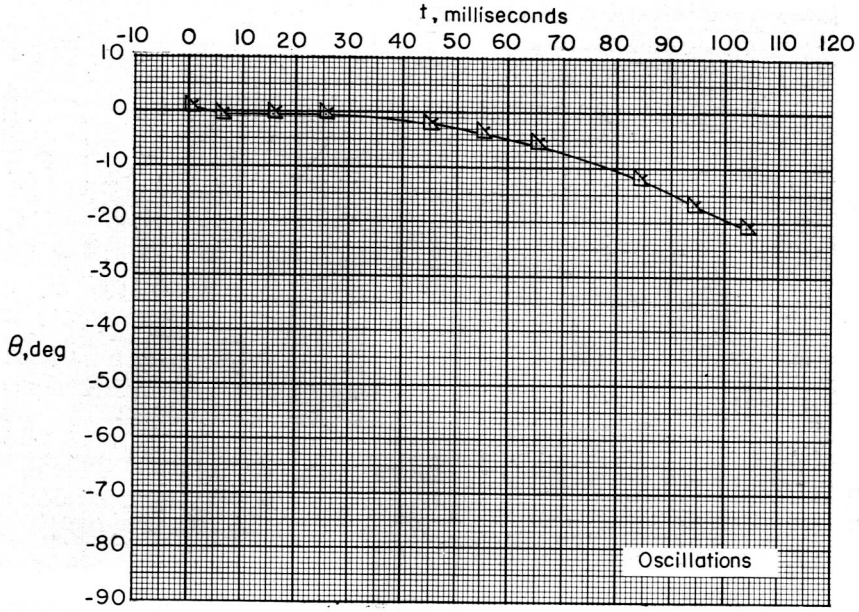

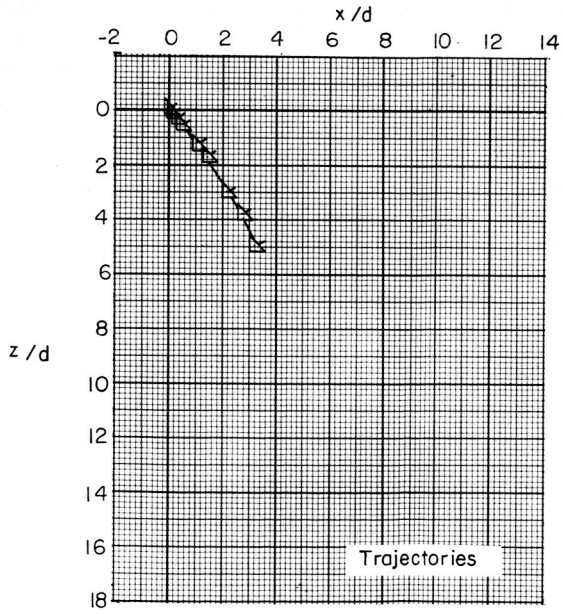

(c) Concluded.

Figure 13.- Continued.

[redacted]

[redacted]

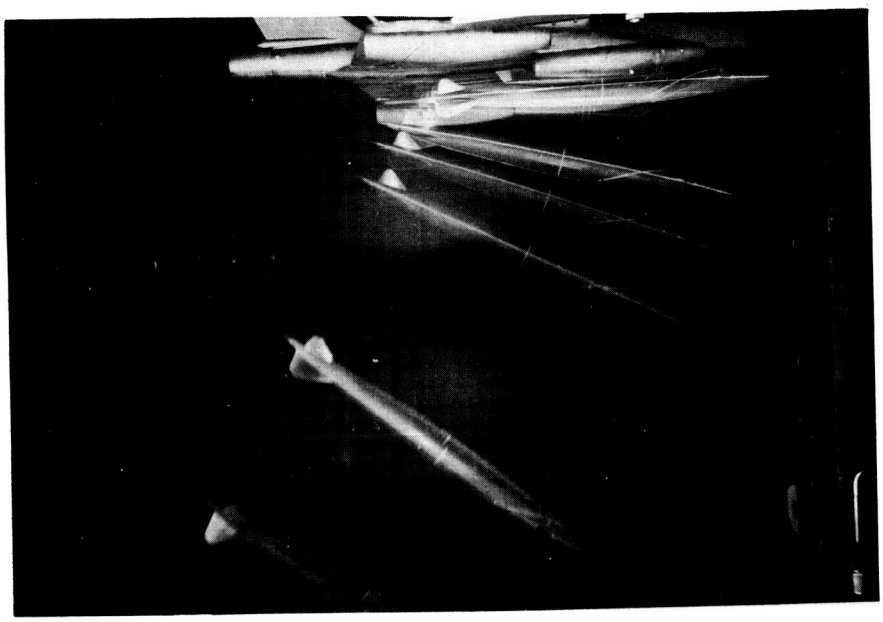

Side view

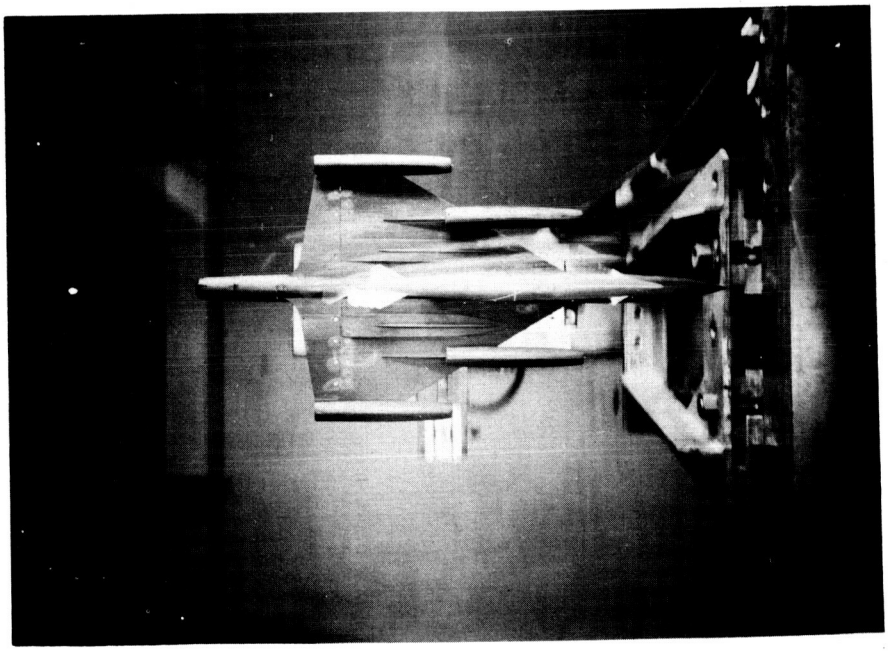

Bottom view

L-60-4368

(d) Test 15. $M = 0.72$; $h = 100$ feet; $\delta = -4^{\circ}$; $\alpha = 5^{\circ}11'$; $\beta = 0^{\circ}$.

Figure 13.- Continued.

[redacted]

L-915

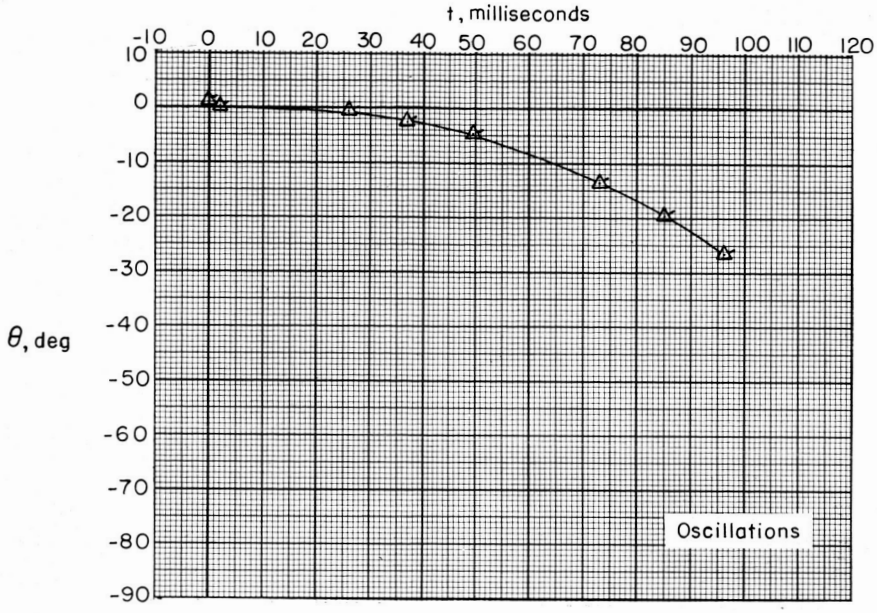

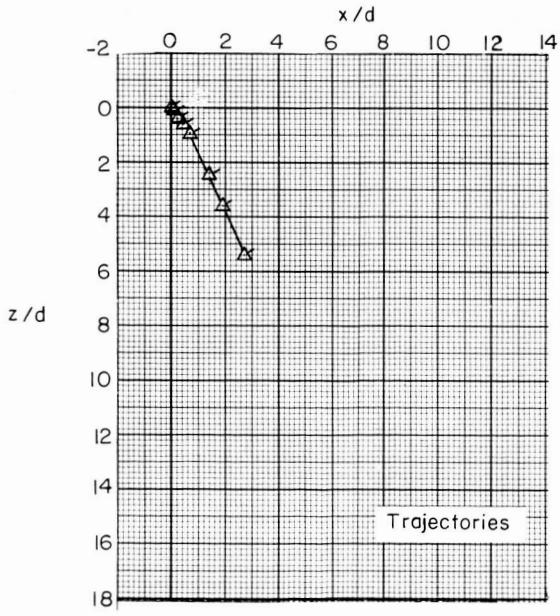

(d) Concluded.

Figure 13.- Continued.

[redacted]

Side view

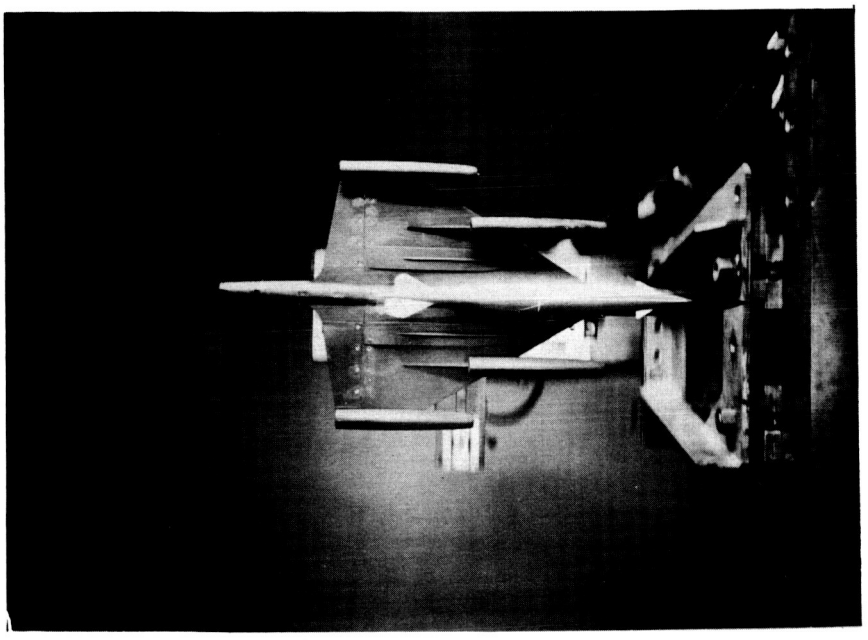

Bottom view

L-60-4369

(e) Test 16. $M = 0.80$; $h = 26{,}200$ feet; $\delta = -20^{\circ}$; $\alpha = 6^{\circ}45'$; $\beta = 0^{\circ}$.

Figure 13.- Continued.

[redacted]

L-915

DECLASSIFIED
[redacted]

L-915

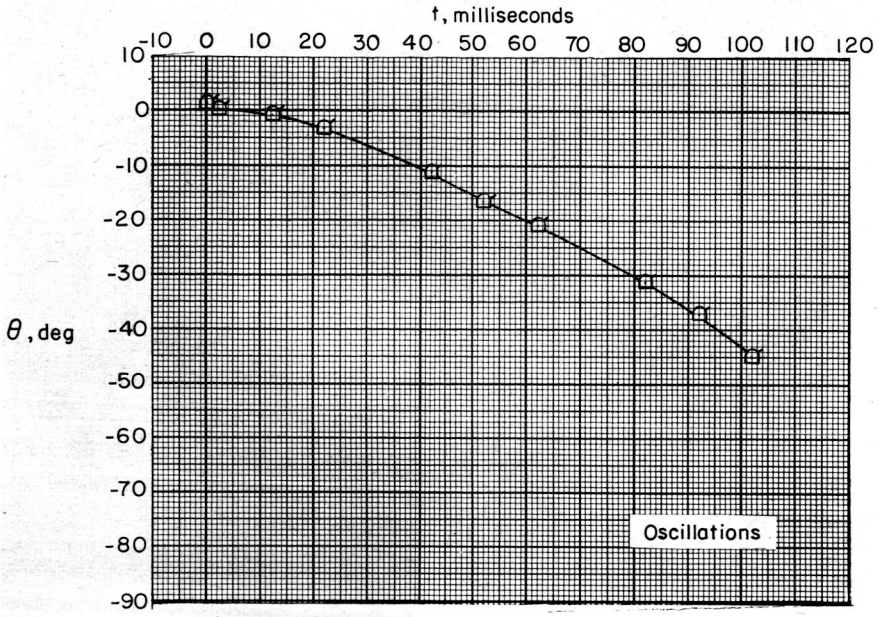

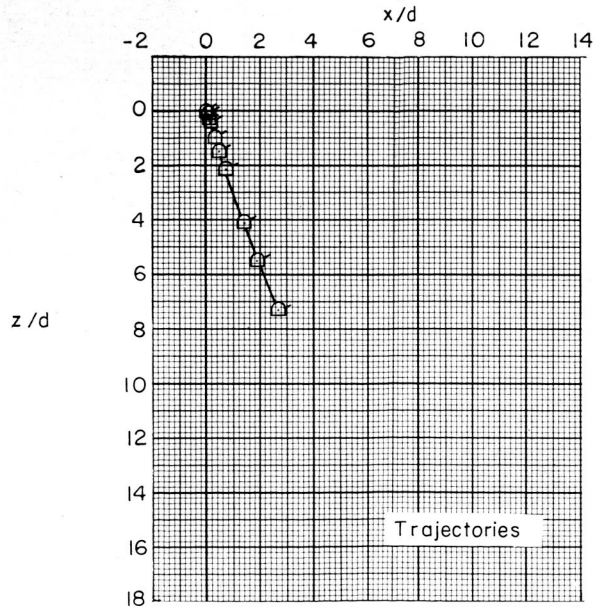

(e) Concluded.

Figure 13.- Continued.

[redacted]

[redacted]

Side view

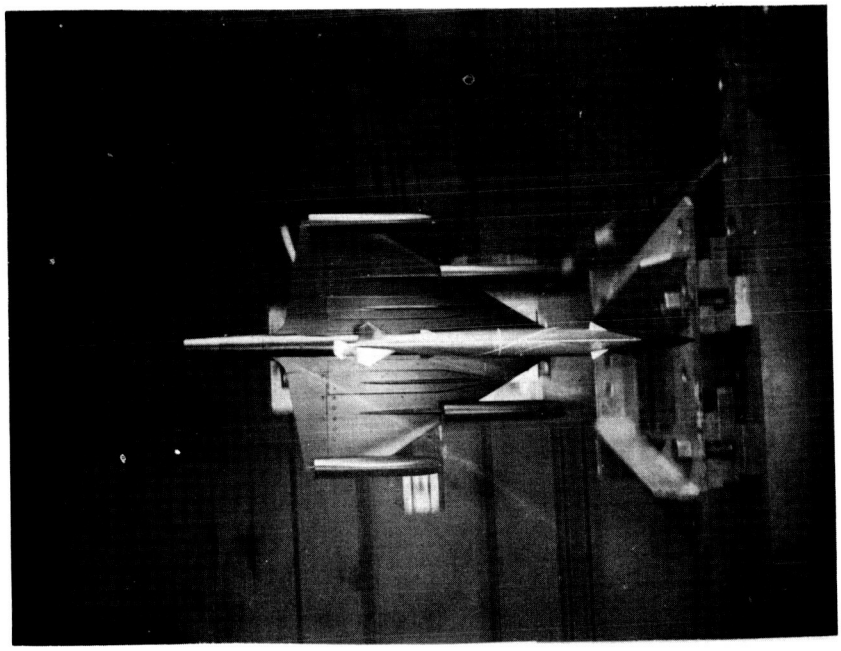

Bottom view

L-60-4370

(f) Test 17. $M = 0.90$; $h = 26{,}150$ feet; $\delta = -20^{\circ}$; $\alpha = 9^{\circ}20'$; $\beta = 1^{\circ}$.

Figure 13.- Continued.

[redacted]

L-915

DECLASSIFIED [redacted]

L-915

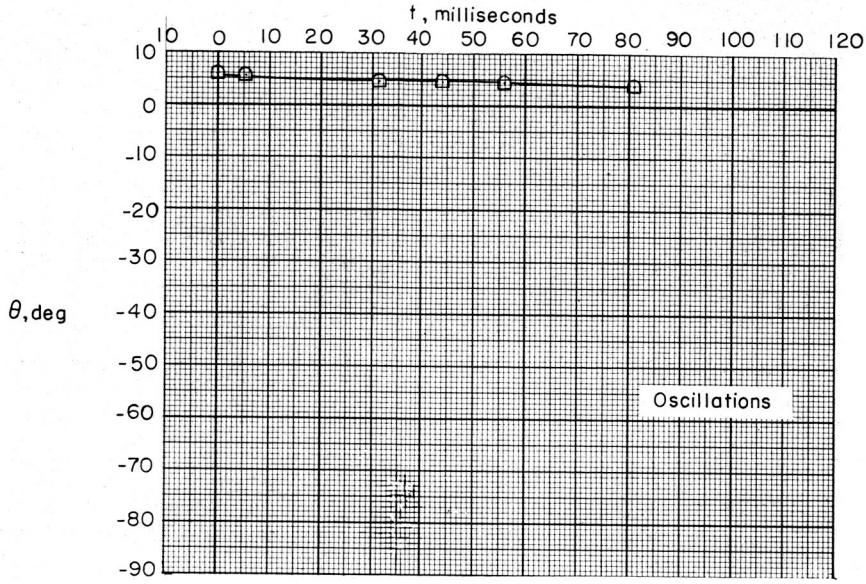

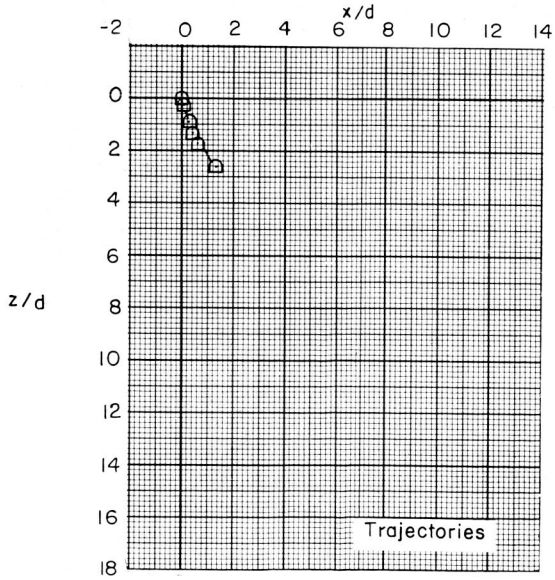

(f) Concluded.

Figure 13.- Continued.

[redacted]

[redacted]

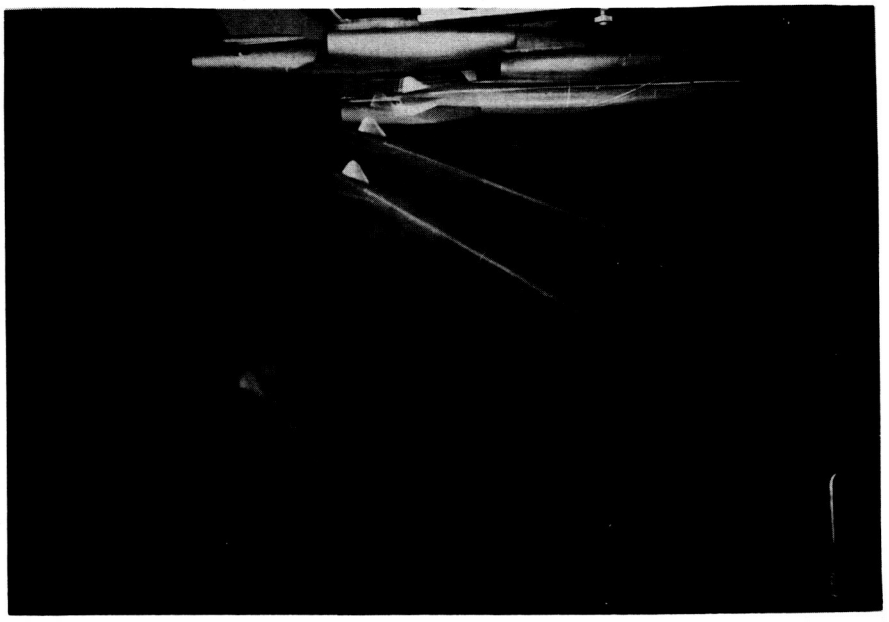

Side view

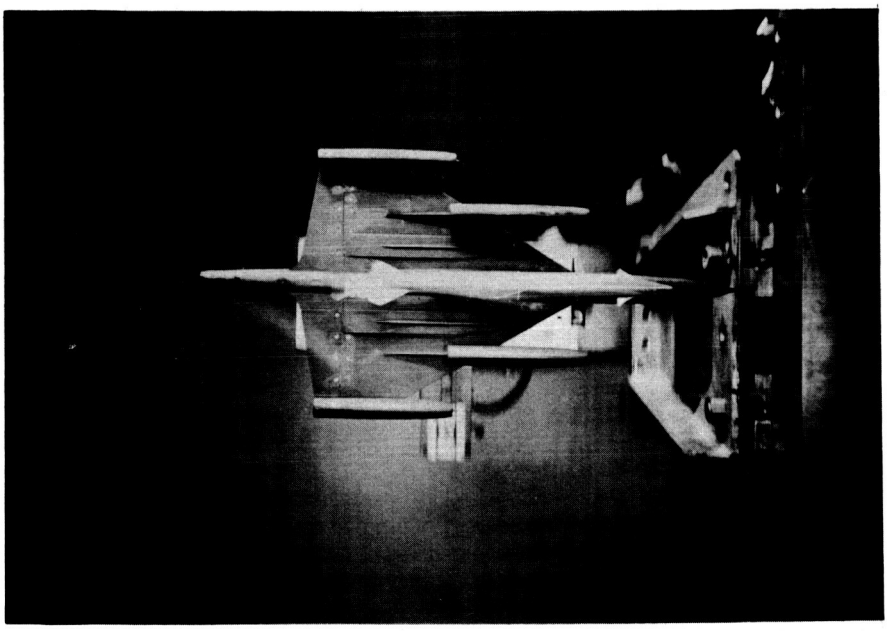

Bottom view

L-60-4371

(g) Test 18. $M = 0.90$; h = sea level; $\delta = -2^{\circ}$; $\alpha = 3^{\circ}36'$; $\beta = 0^{\circ}$.

Figure 13.- Continued.

L-915

[redacted]

L-915

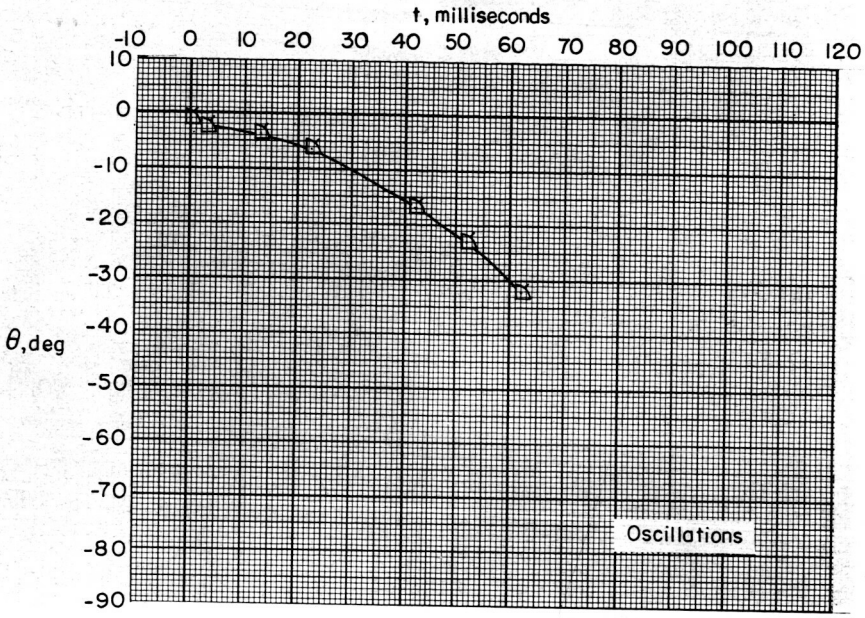

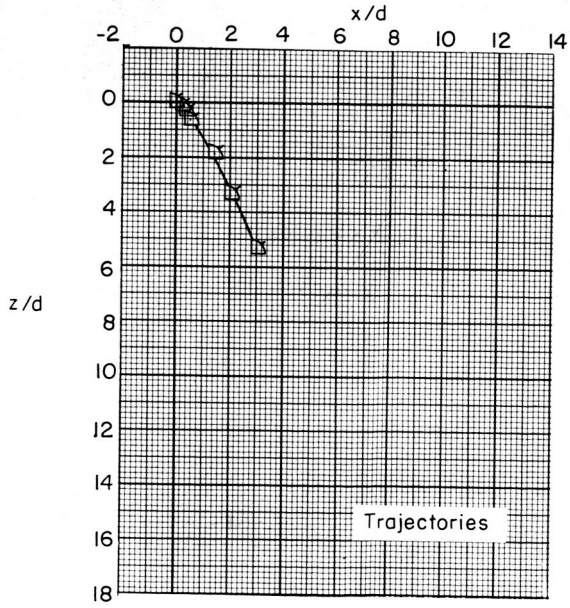

(g) Concluded.

Figure 13.- Continued.

[redacted]

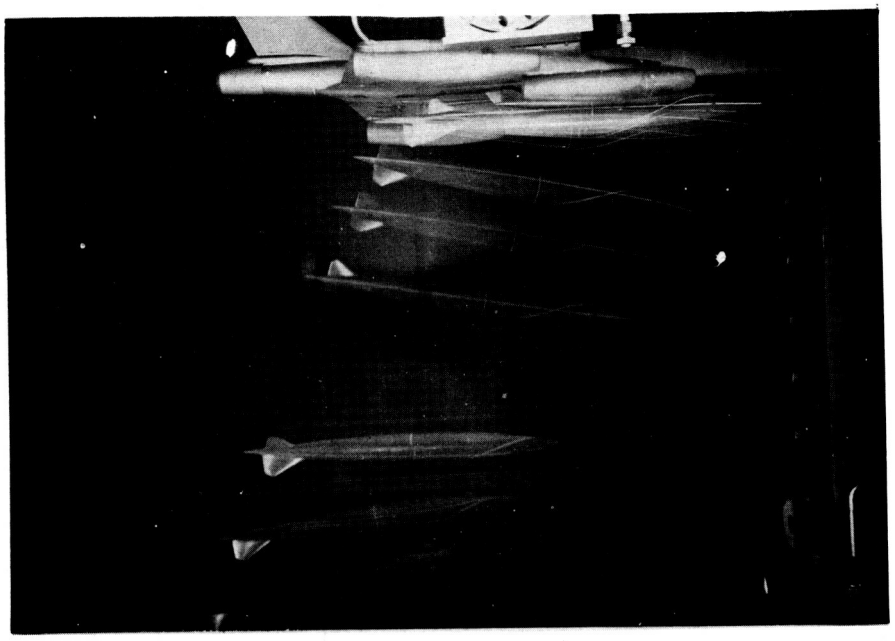

Side view

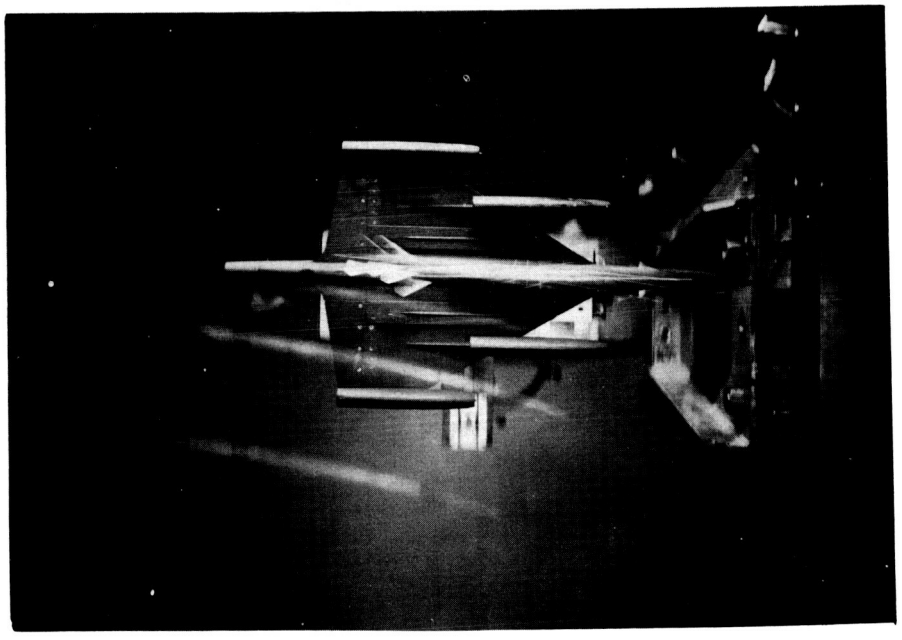

Bottom view

L-60-4372

(h) Test 19. $M = 0.91$; h = sea level; $\delta = 0^{\circ}$; $\alpha = 3^{\circ}36'$; $\beta = 0^{\circ}$.

Figure 13.- Continued.

[redacted]

L-915

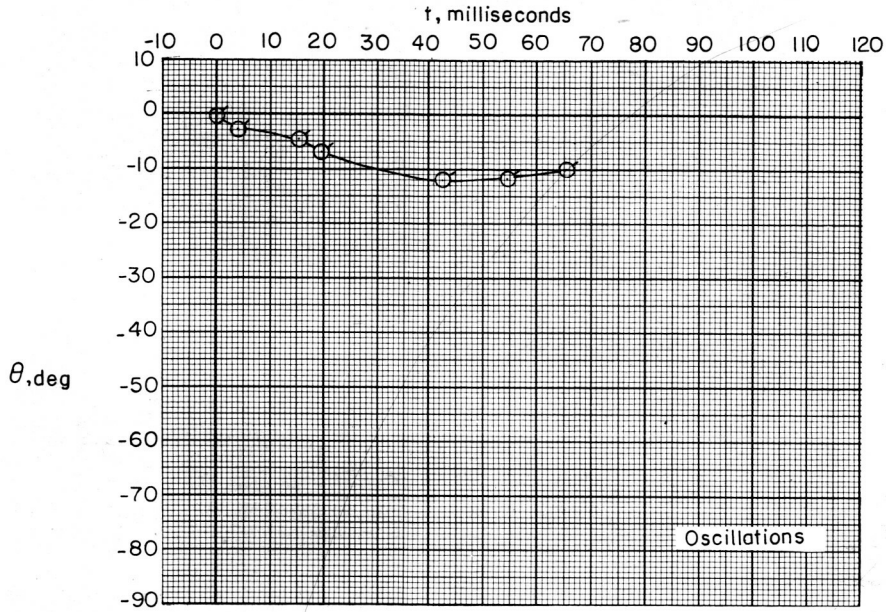

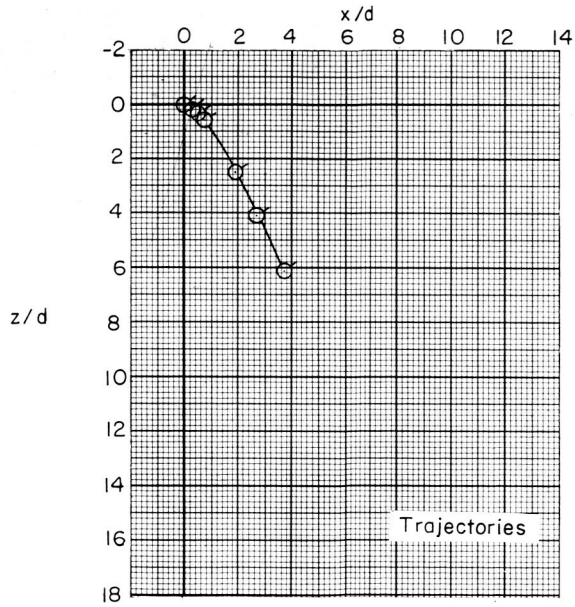

(h) Concluded.

Figure 13.- Continued.

L-915

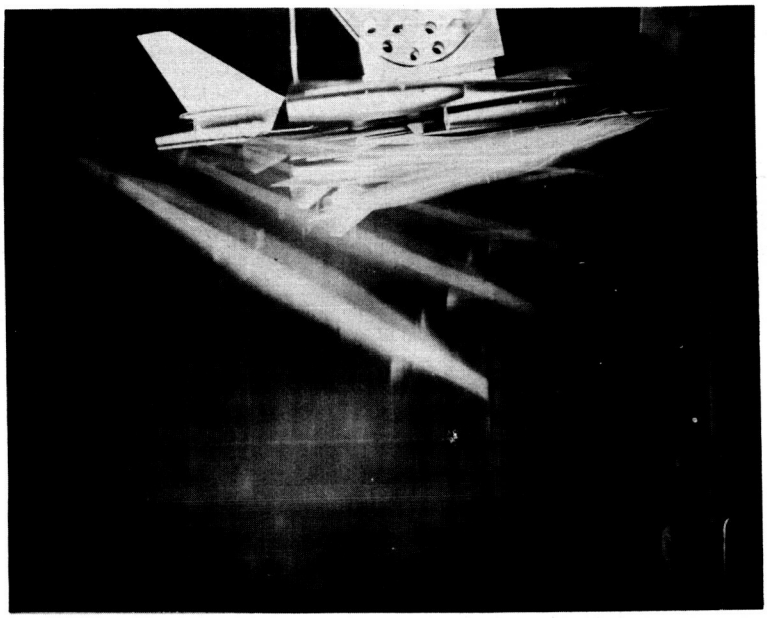

Side view

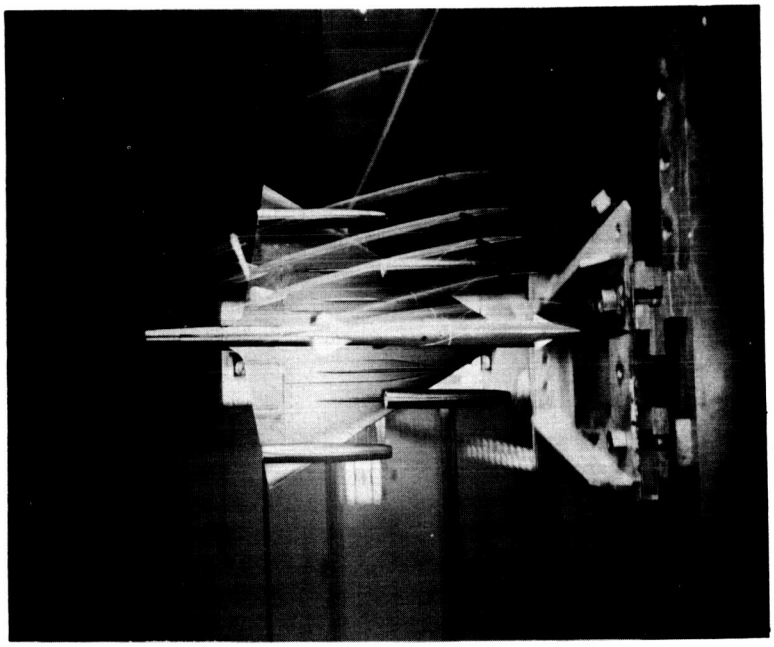

Bottom view

L-60-4373

(i) Test 20. $M = 0.91$; $h = 25{,}950$ feet; $\delta = -20^{\circ}$; $\alpha = 11^{\circ}13'$; $\beta = 0^{\circ}$; fuel tank struck airplane model.

Figure 13.- Continued.

[redacted]

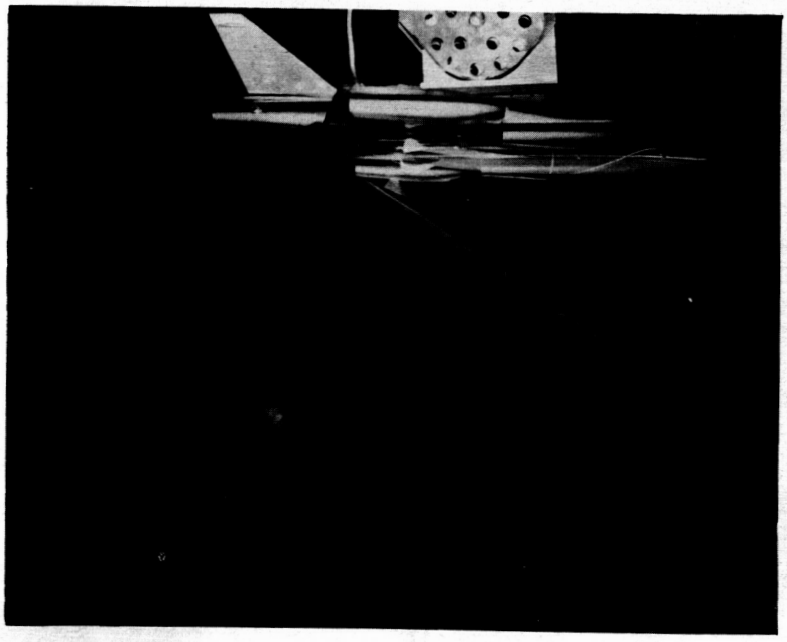

Side view

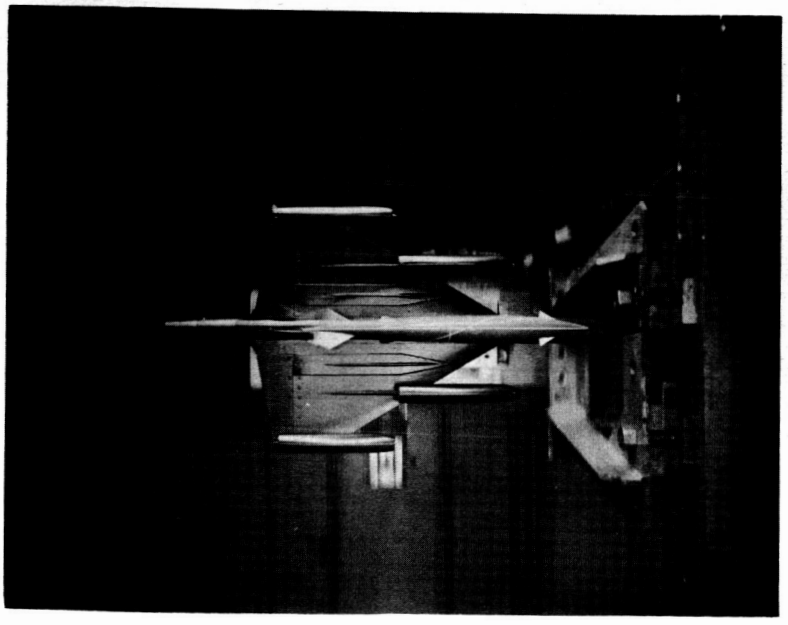

Bottom view

Test 21 ; $\beta = 0°$

L-60-4374

(j) Test 21 and test 22. M = 0.91; h = 2,450 feet; $\delta = -6°$; $\alpha = 3°16'$.

Figure 13.- Continued.

[redacted]

L-913

Side view

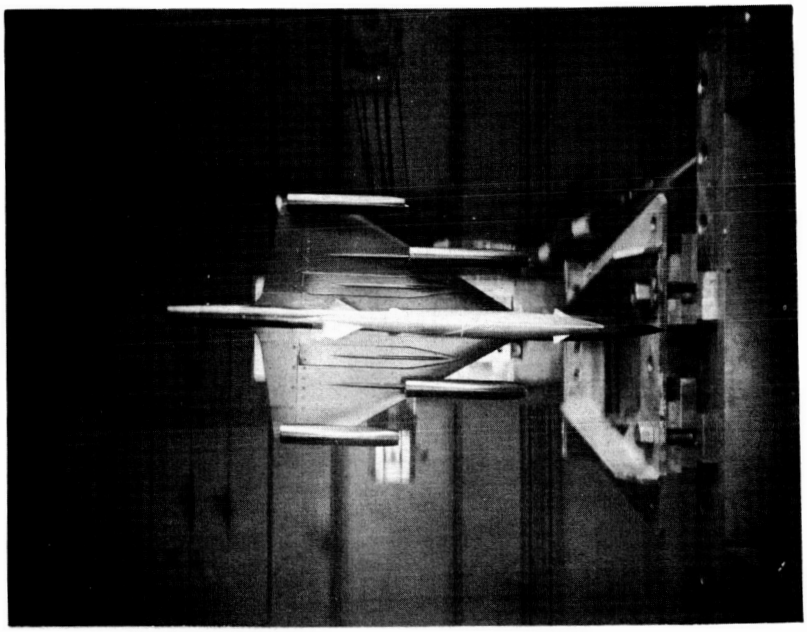

Bottom view

Test 22; $\beta = 1°$

(j) Continued.

L-60-4375

Figure 13.- Continued.

L-915

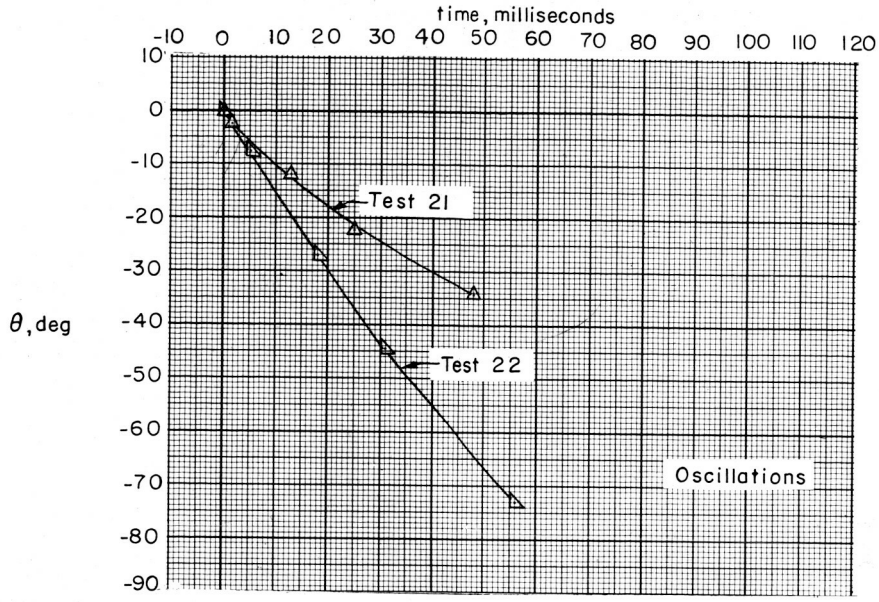

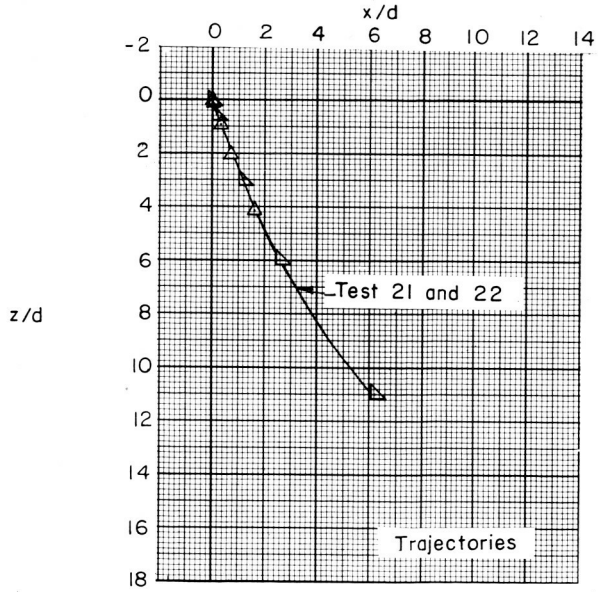

(j) Concluded.

Figure 13.- Continued.

[redacted]

 [redacted]

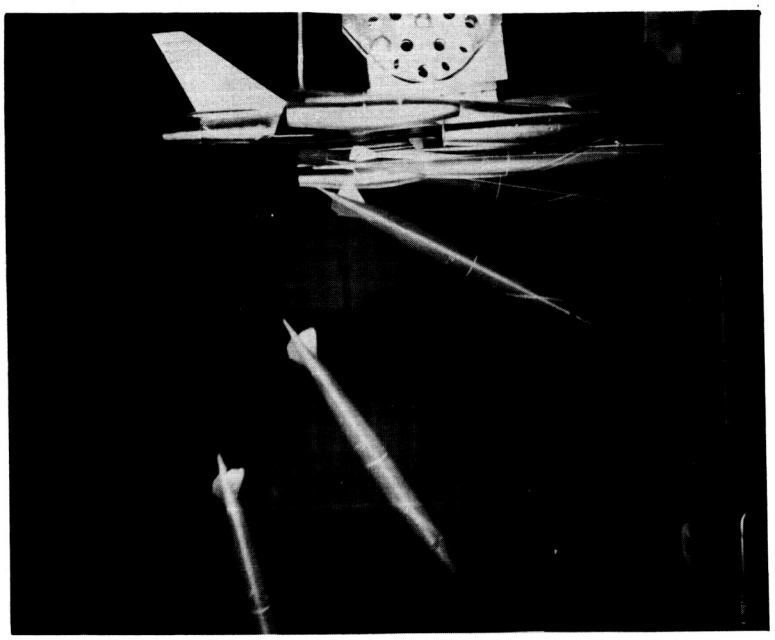

Side view

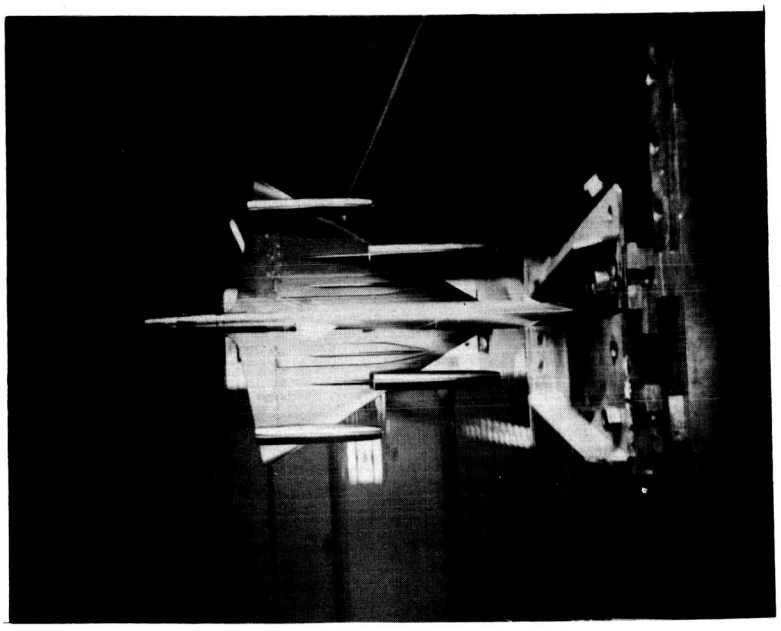

Bottom view

L-60-4376

(k) Test 23. $M = 0.92$; $h = 25{,}650$ feet; $\delta = -20^{\circ}$; $\alpha = 5^{\circ}30'$; $\beta = 0^{\circ}$.

Figure 13.- Continued.

[redacted]

L-915

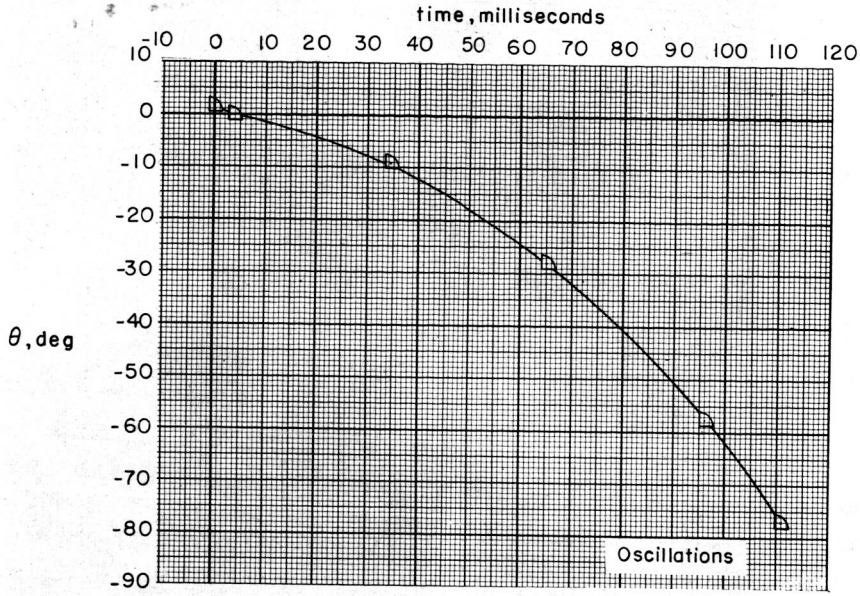

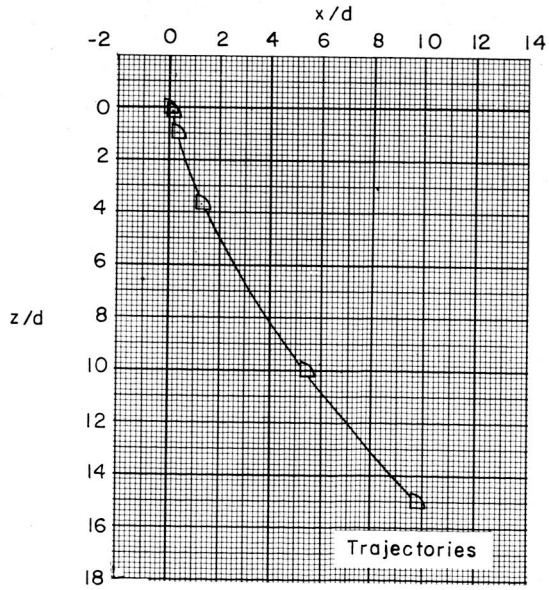

(k) Concluded.

Figure 13.- Continued.

[redacted]

Side view

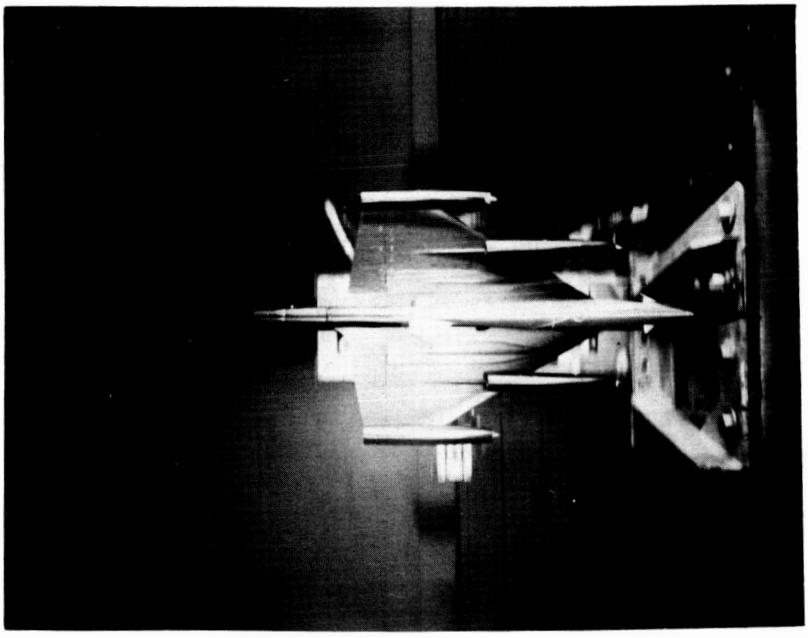

Bottom view

L-60-4377

(*l*) Test 24. M = 1.39; h = 26,000 feet; $\delta = -6^{\circ}$; $\alpha = 4^{\circ}30'$; $\beta = 0^{\circ}$.

Figure 13.- Continued.

[redacted]

L-915

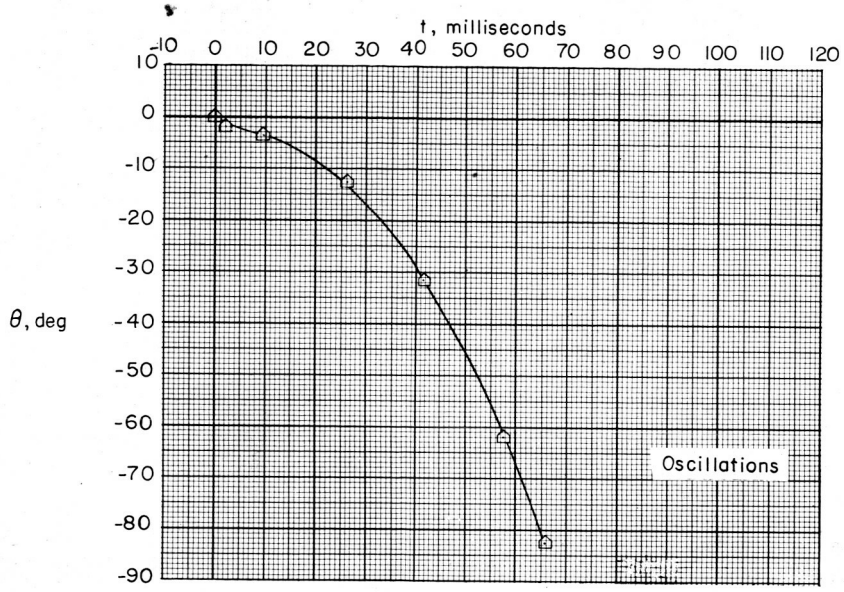

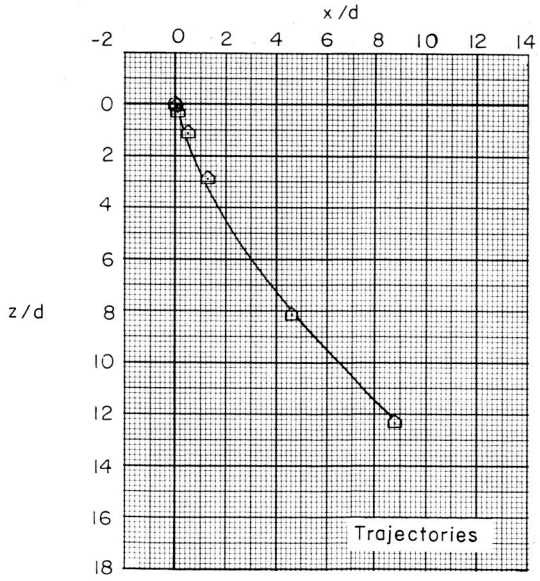

(l) Concluded.

Figure 13.- Continued.

DECLASSIFIED
[redacted]

Side view

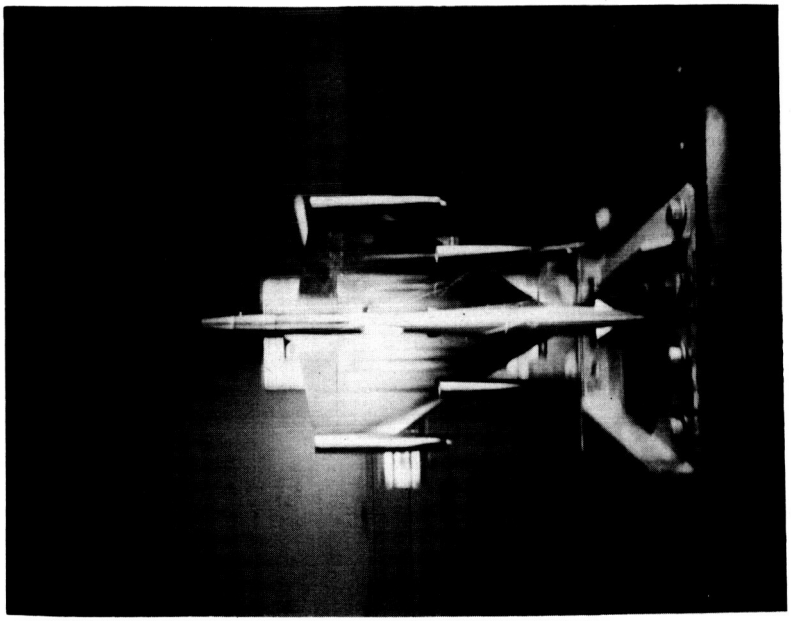

Bottom view

L-60-4378

(m) Test 25. $M = 1.59$; $h = 25{,}650$ feet; $\delta = -20^{\circ}$; $\alpha = 5^{\circ}56'$; $\beta = 0^{\circ}$; upper tail fin of fuel-tank model struck airplane model.

Figure 13.- Continued.

[redacted]

L-915

L-915

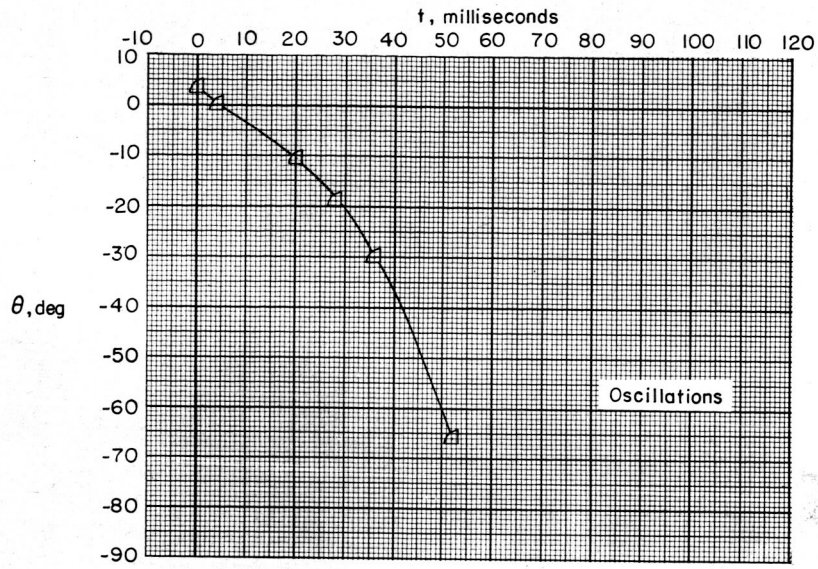

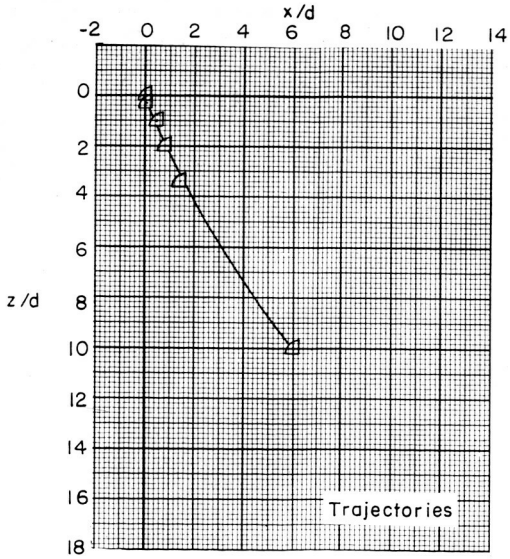

(m) Concluded.

Figure 13.- Continued.

DECLASSIFIED

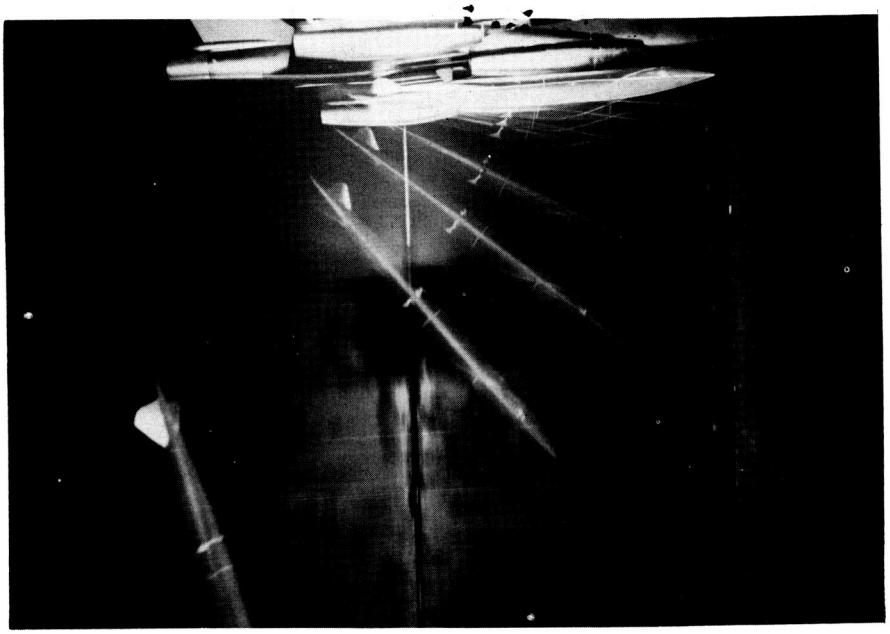

Side view

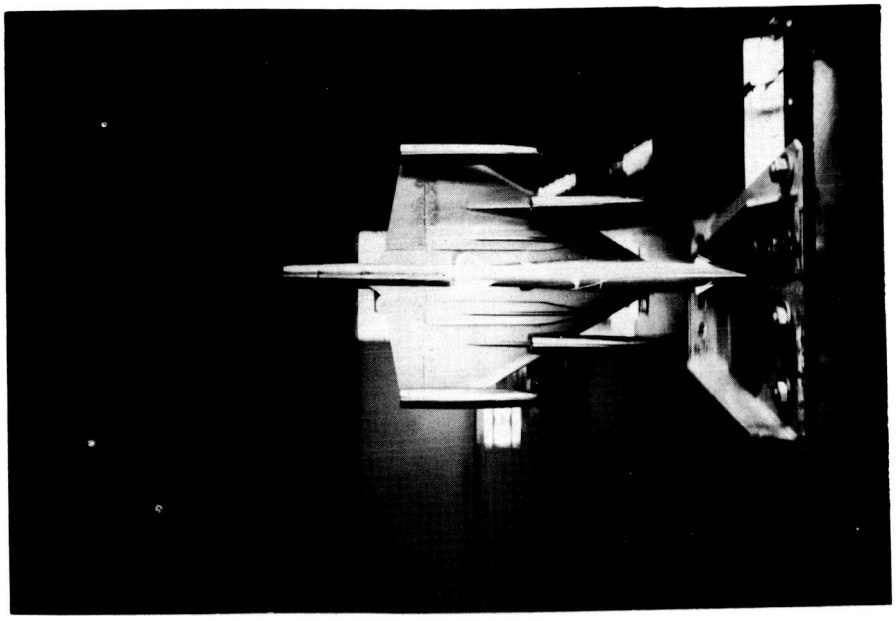

Bottom view

L-60-4379

(n) Test 26. $M = 1.59$; $h = 26{,}000$ feet; $\delta = -20^{\circ}$; $\alpha = 6^{\circ}30'$; $\beta = 0^{\circ}$. upper tail fin of fuel-tank model struck airplane model.

Figure 13.- Continued.

[redacted]

L-915

DE[redacted]SIFIED

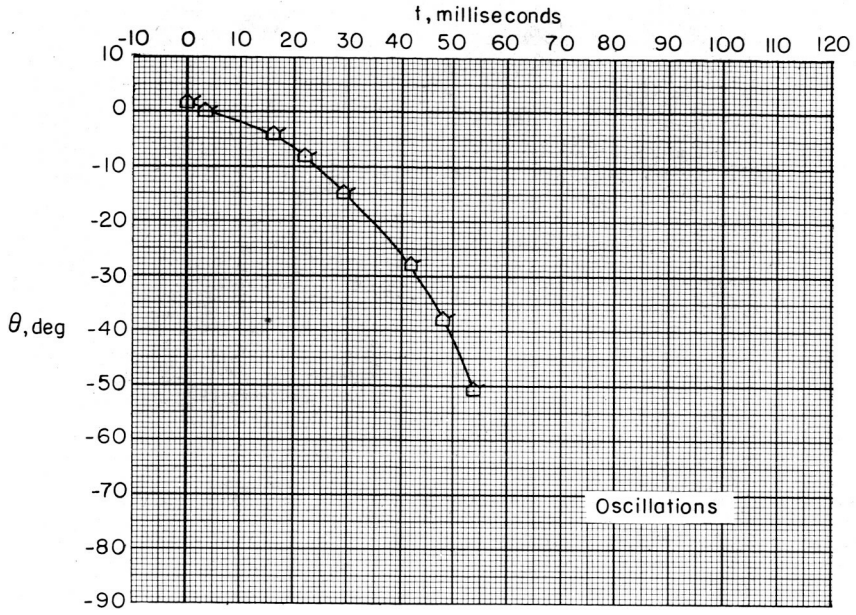

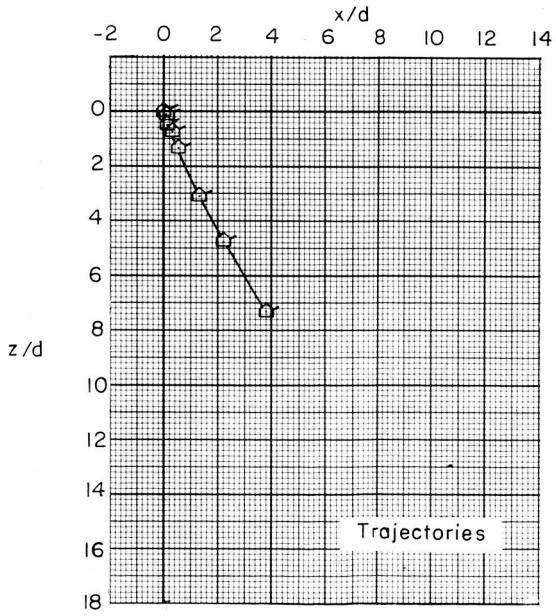

(n) Concluded.

Figure 13.- Continued.

[redacted]

[redacted]

Side view

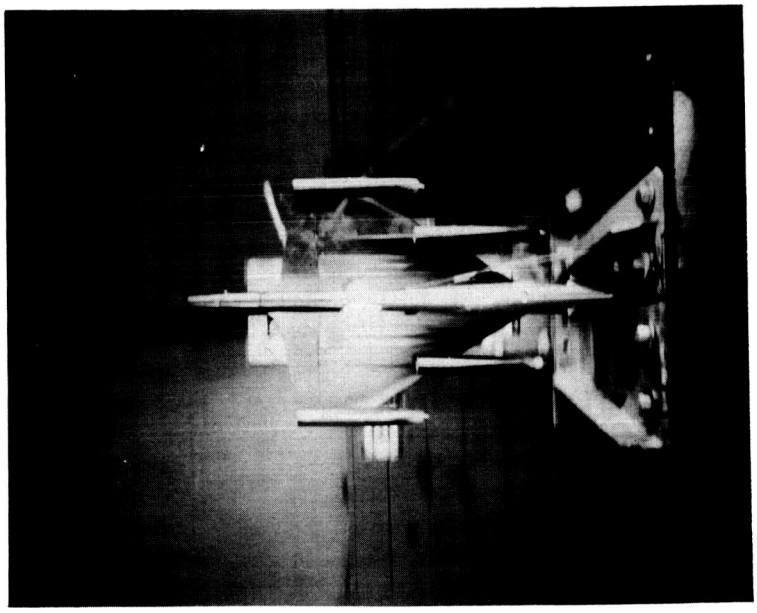

Bottom view

L-60-4380

(o) Test 27. $M = 1.59$; $h = 25{,}950$ feet; $\delta = -6^{\circ}$; $\alpha = 5^{\circ}56'$; $\beta = 0^{\circ}$.

Figure 13.- Continued.

L-915

[redacted]

L-915

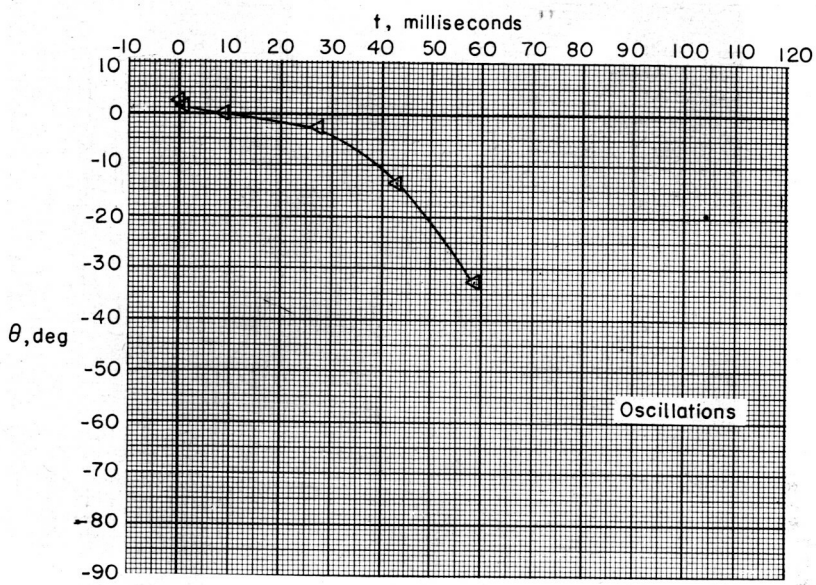

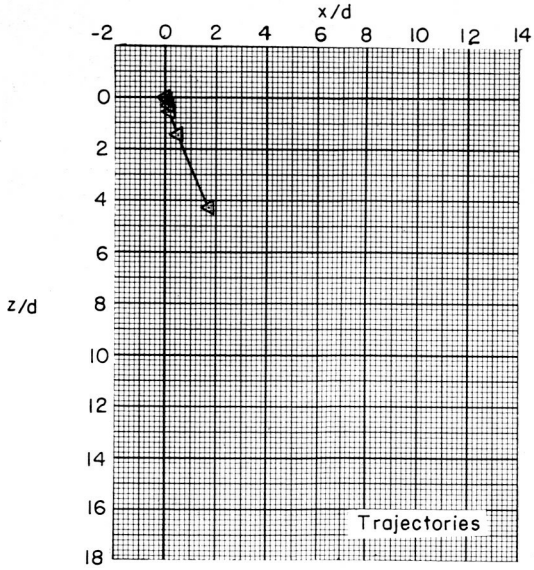

(o) Concluded.

Figure 13.- Continued.

DECLASSIFIED [redacted]

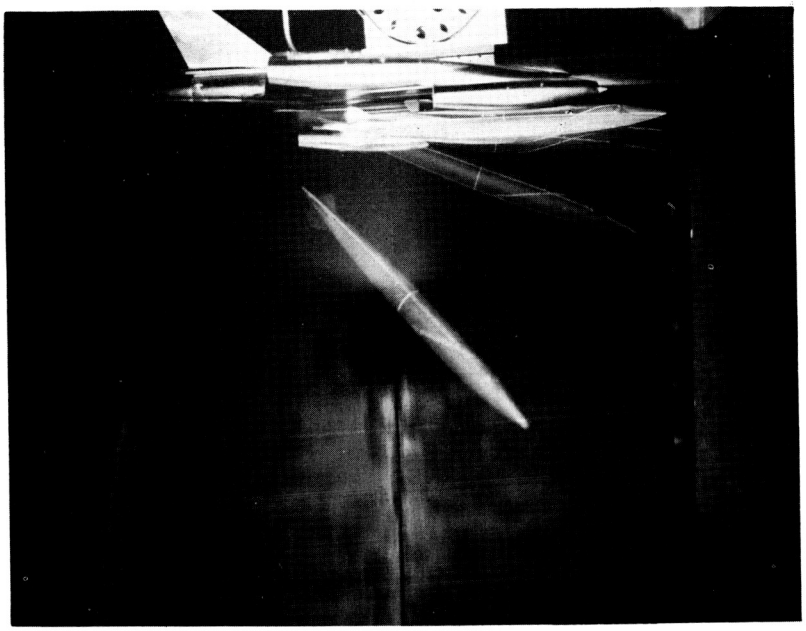

Side view

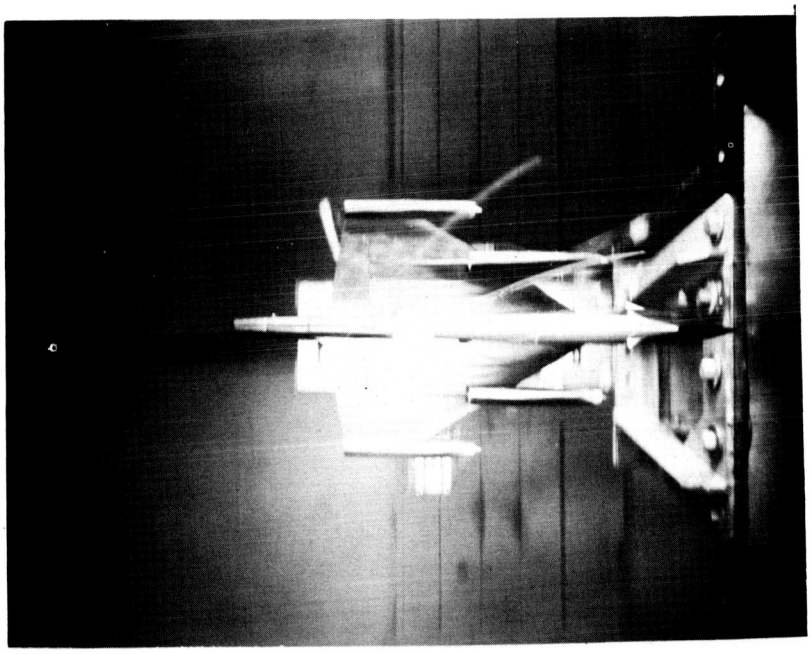

Bottom view

L-60-5501

(p) Test 28. $M = 1.59$; $h = 25{,}950$ feet; $\delta = -6^{\circ}$; $\alpha = 4^{\circ}30'$; $\beta = 0^{\circ}$; upper tail fin of fuel-tank model struck airplane model.

Figure 13.- Continued.

[redacted]

L-915

L-915

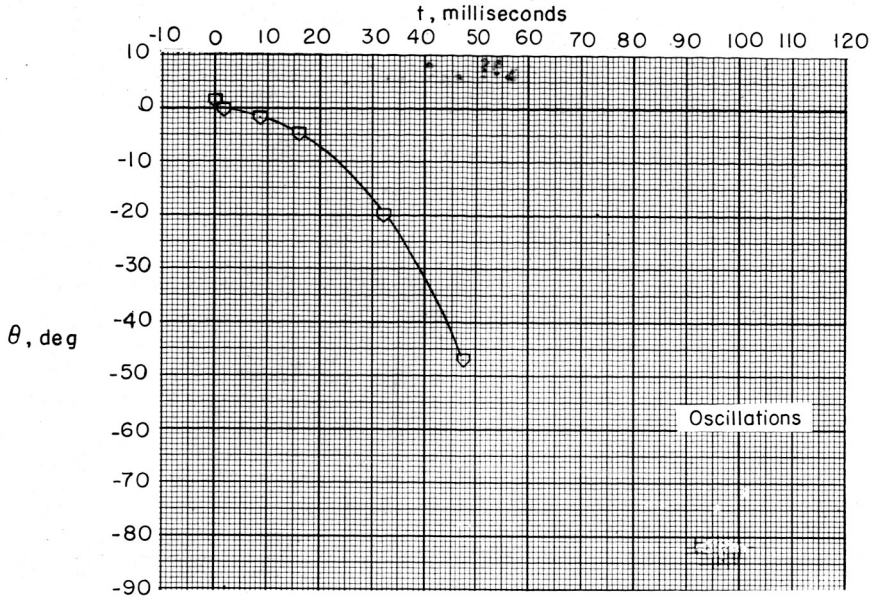

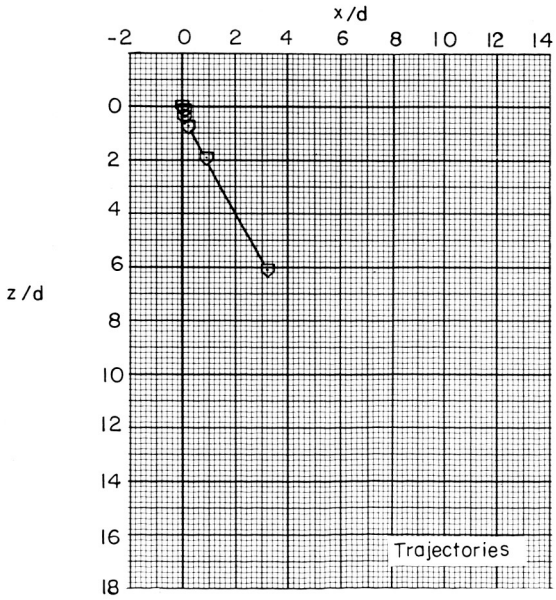

(p) Concluded.

Figure 13.- Continued.

[redacted]

[redacted]

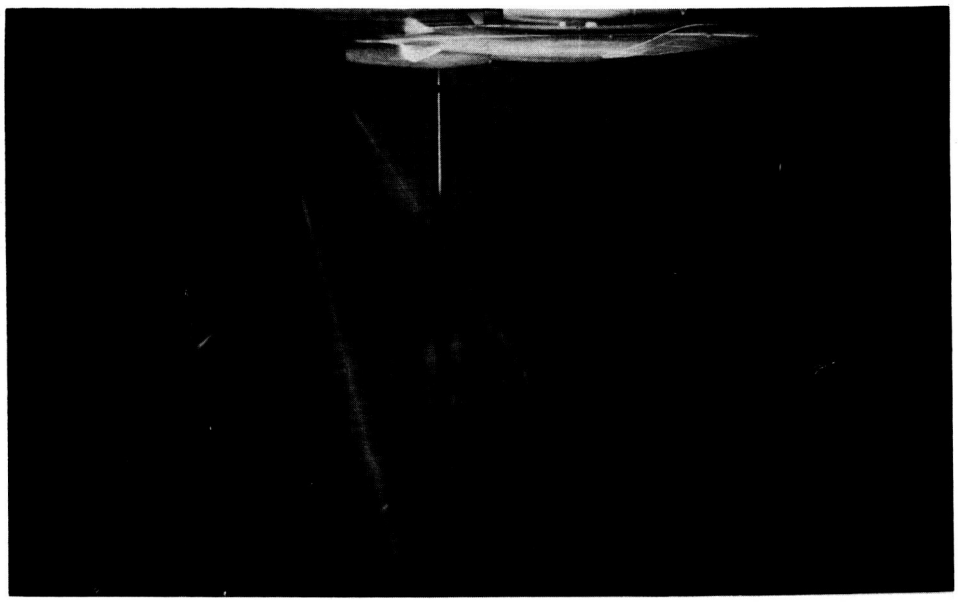

Side view

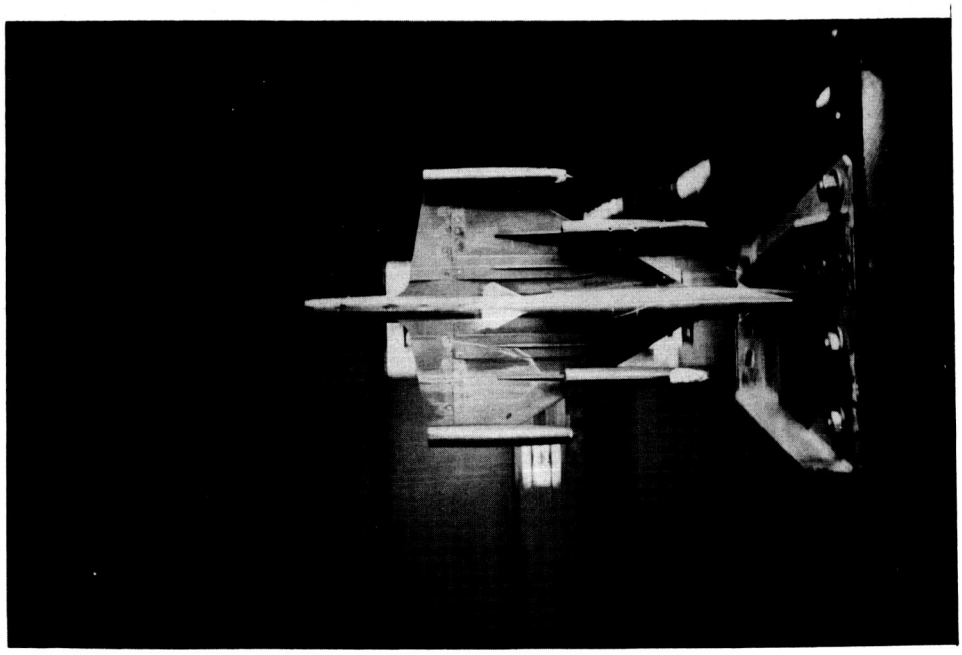

Bottom view

L-60-5502

(q) Test 29. $M = 1.59$; $h = 25{,}850$ feet; $\delta = 0^{\circ}$; $\alpha = 4^{\circ}03'$; $\beta = 0^{\circ}$; upper tail fin of fuel-tank model struck airplane model.

Figure 13.- Continued.

[redacted]

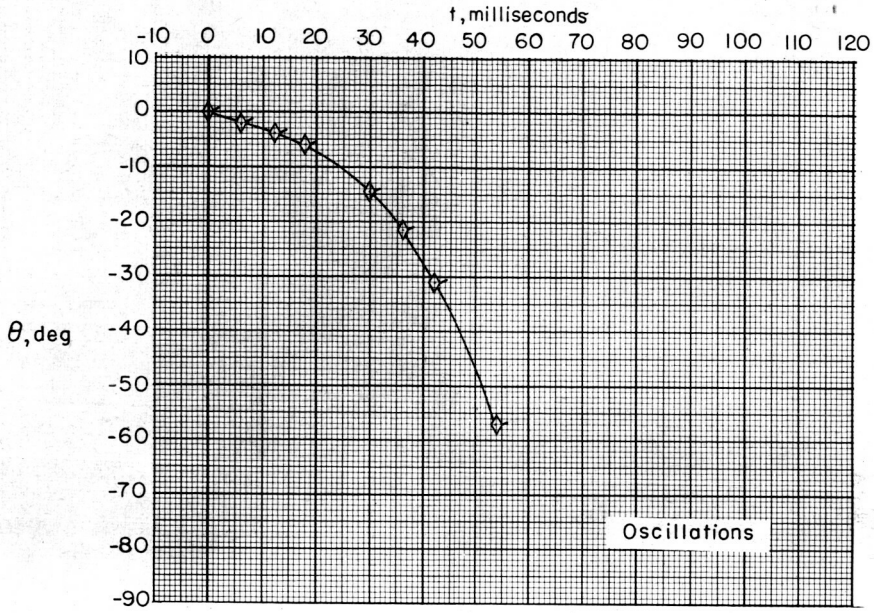

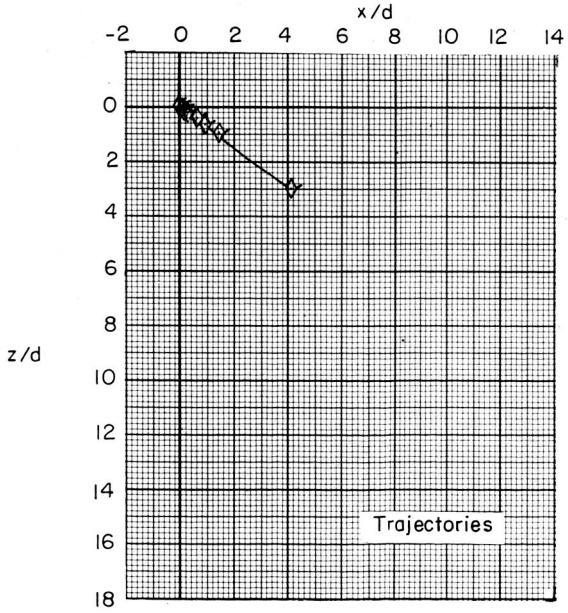

(q) Concluded.

Figure 13.- Continued.

[redacted]

[redacted]

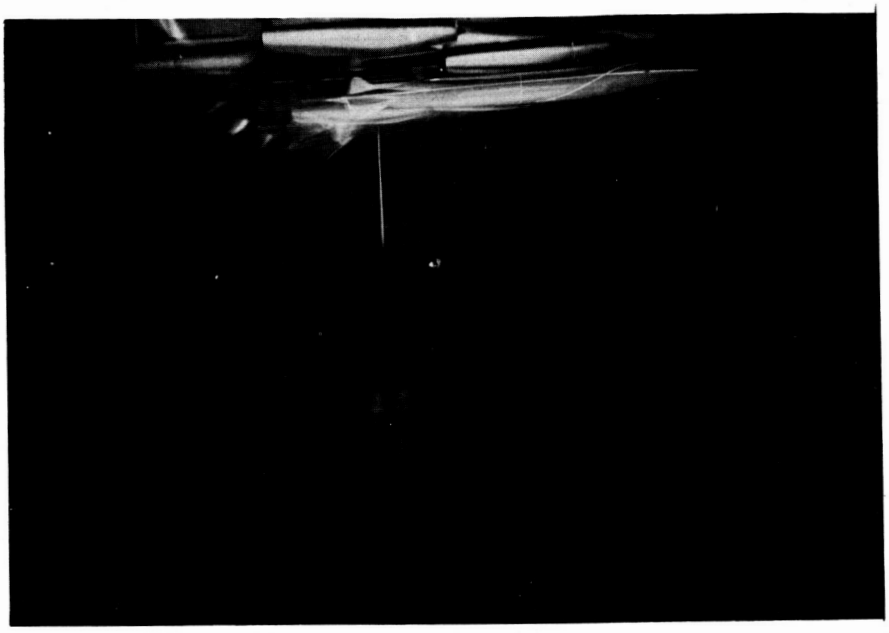

Side view

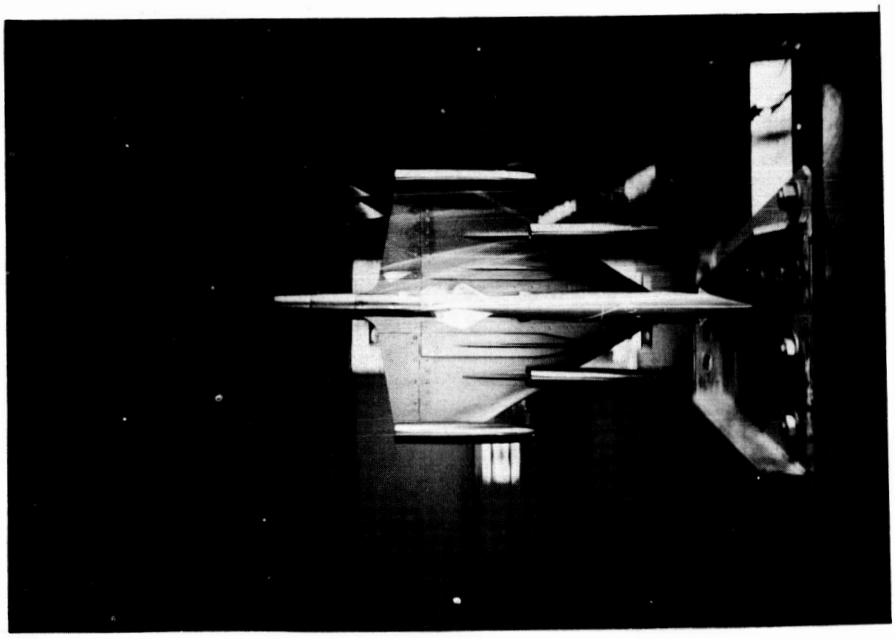

Bottom view

L-60-5503

(r) Test 30. $M = 1.59$; $h = 25{,}600$ feet; $\delta = 0^{\circ}$; $\alpha = 6^{\circ}07'$; $\beta = 0^{\circ}$; fuel-tank model rolled and struck airplane model.

Figure 13.- Continued.

[redacted]

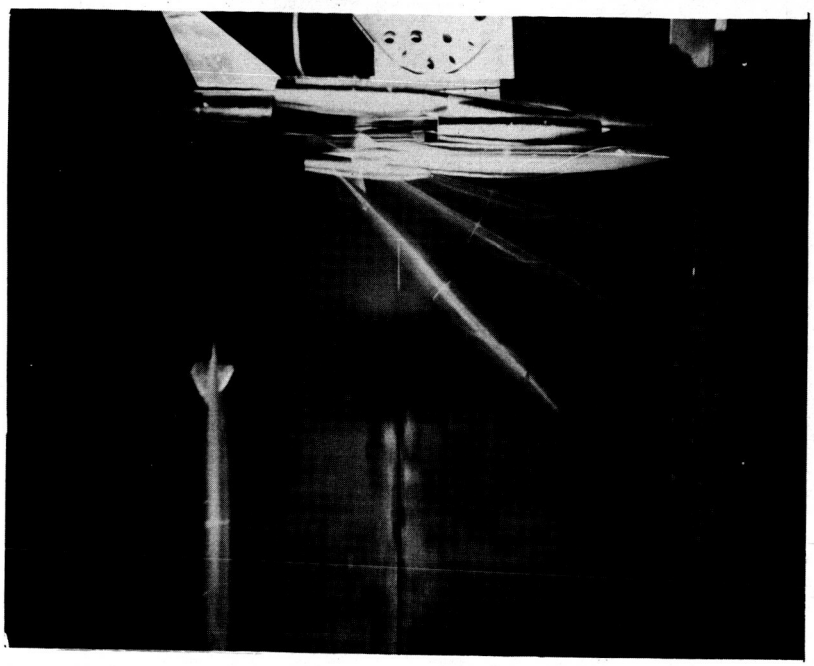

Side view

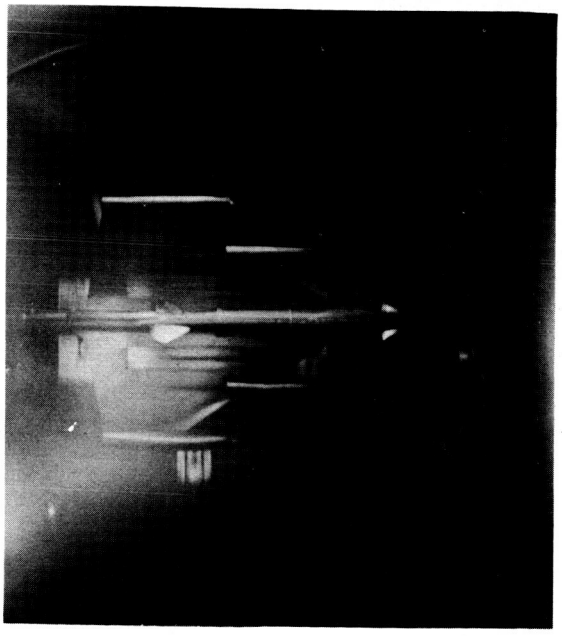

Bottom view

L-60-5504

(s) Test 31. M = 1.59; h = 25,650 feet; $\delta = -20^{\circ}$; $\alpha = 3^{\circ}16'$; $\beta = 0^{\circ}$; upper tail fin of fuel-tank model struck airplane model.

Figure 13.- Continued.

[redacted]

[redacted]

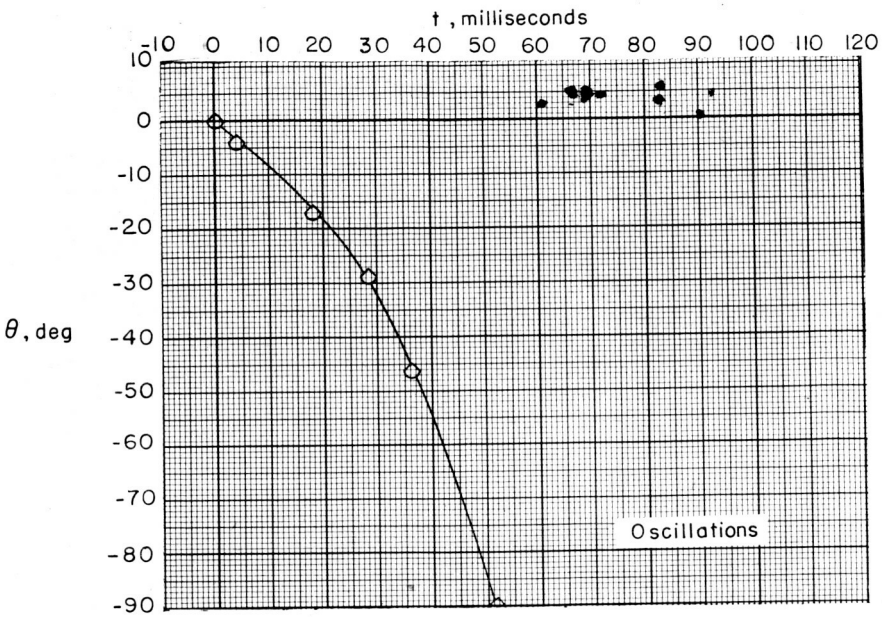

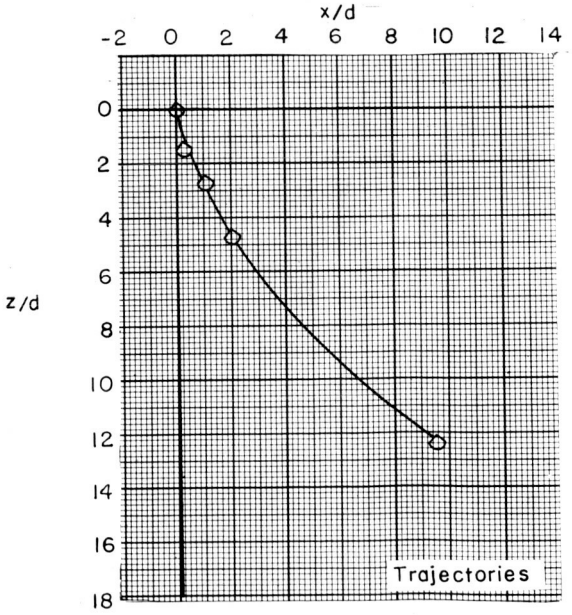

(s) Concluded.

Figure 13.- Continued.

[redacted]

L-915

Side view

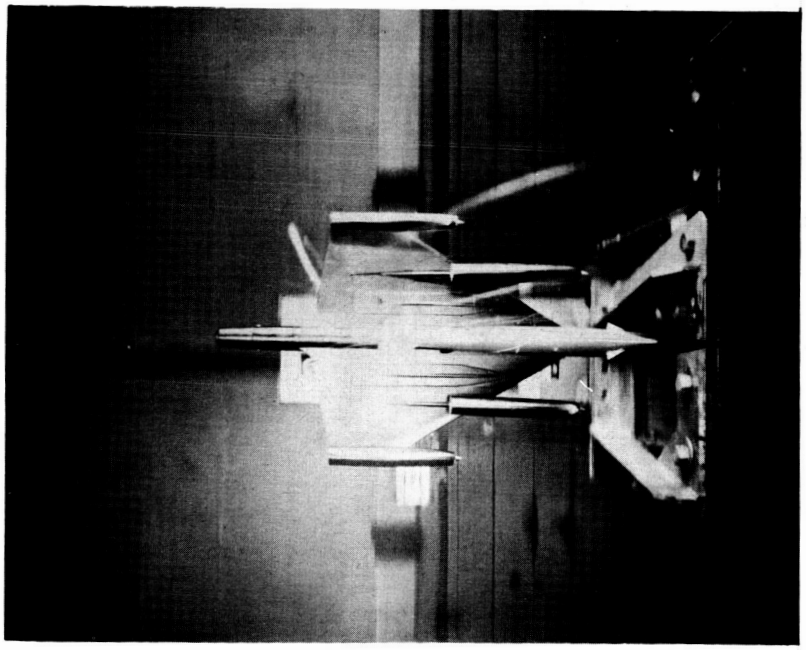

Bottom view

L-60-5505

(t) Test 32. $M = 1.98$; $h = 25{,}900$ feet; $\delta = -20^{\circ}$; $\alpha = 5^{\circ}06'$; $\beta = 0^{\circ}$.

Figure 13.- Continued.

[redacted]

[redacted]

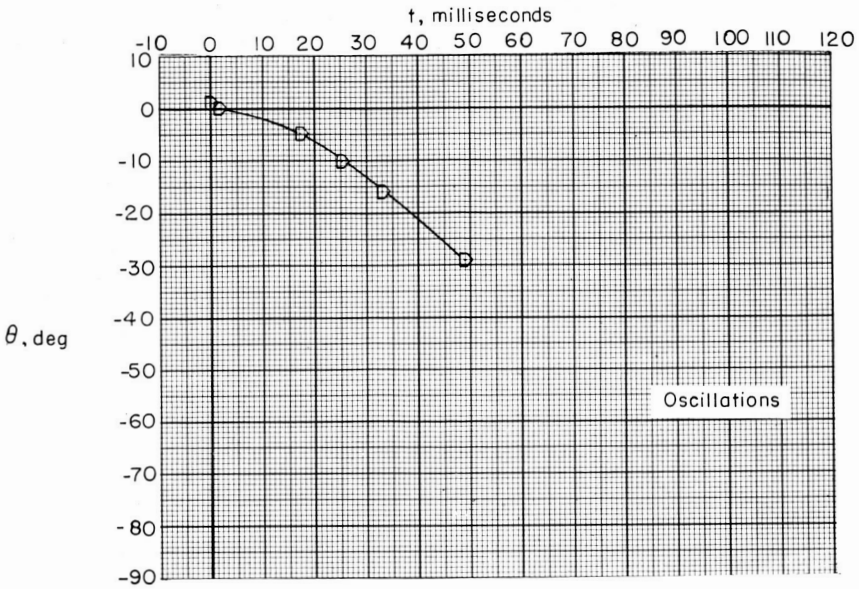

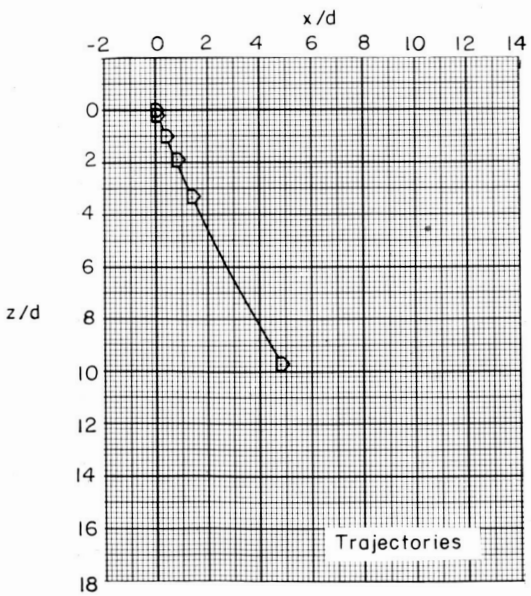

(t) Concluded.

Figure 13.- Continued.

[redacted]

L-915

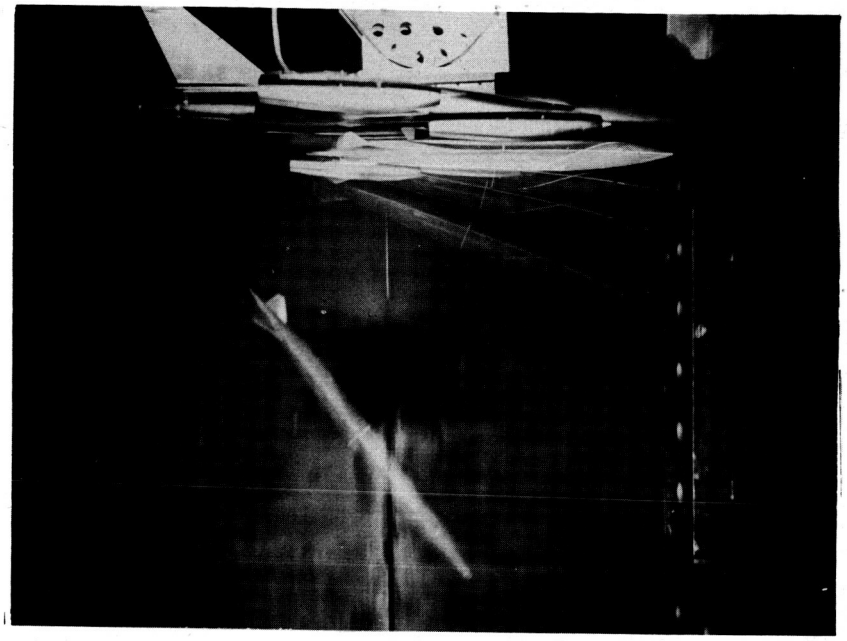

Side view

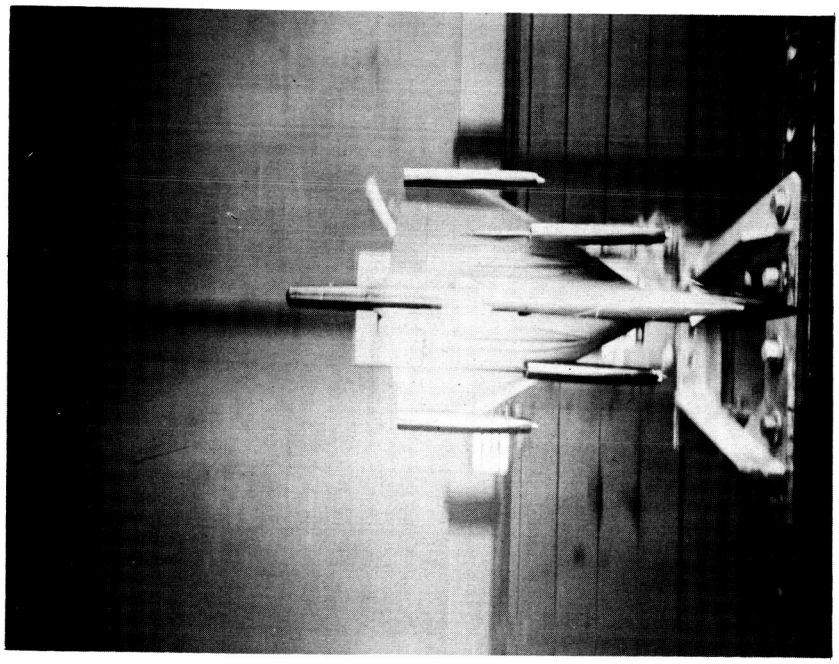

Bottom view

L-60-5506

(u) Test 33. M = 1.98; h = 25,400 feet; $\delta = -6^{\circ}$; $\alpha = 3^{\circ}16'$; $\beta = 0^{\circ}$.

Figure 13.- Continued.

[redacted]

[redacted]

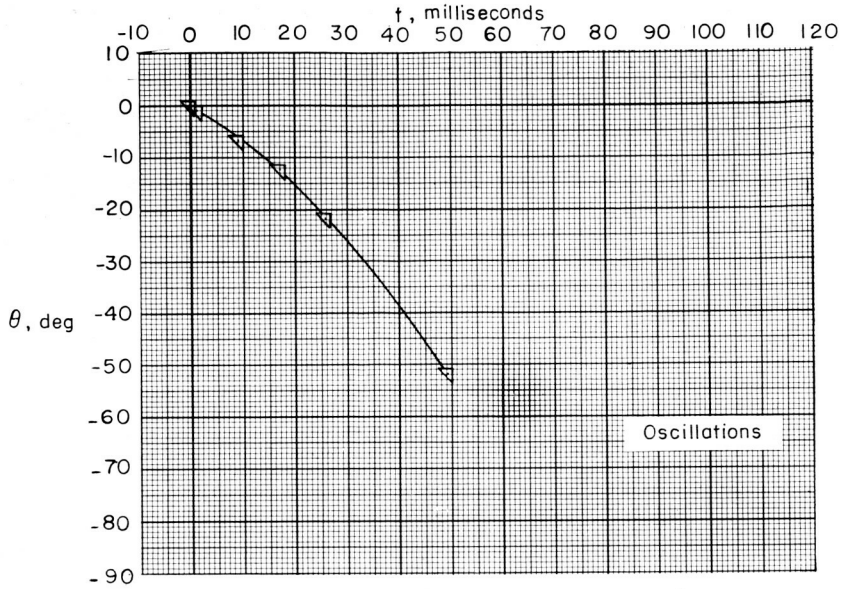

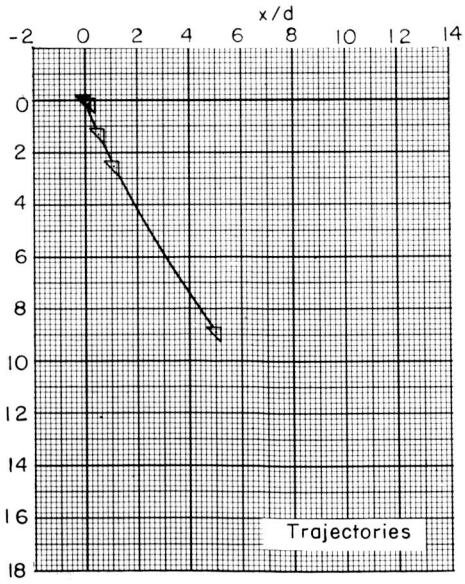

(u) Concluded.

Figure 13.- Continued.

[redacted]

L-915

L-915

Side view

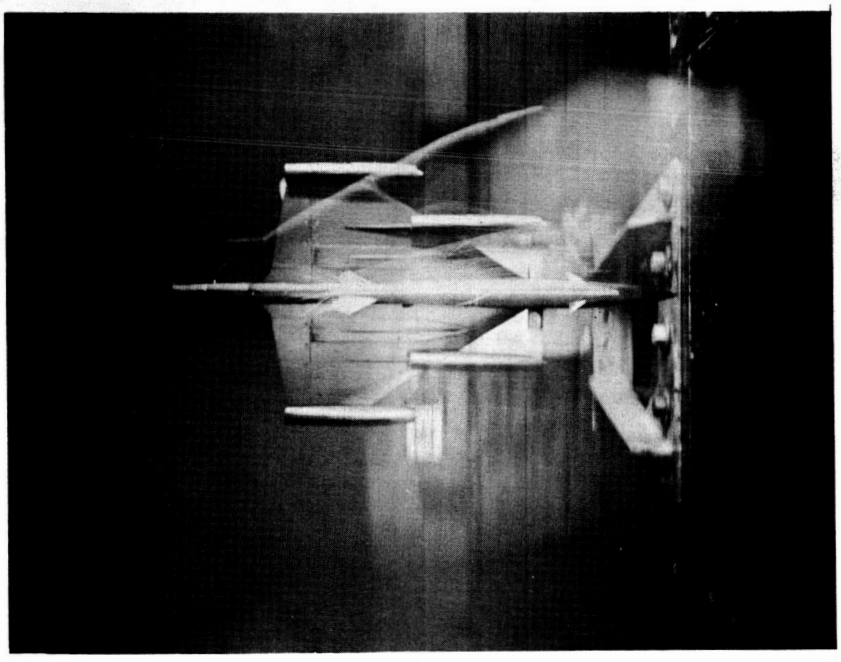

Bottom view

L-60-5507

(v) Test 34. $M = 1.98$; $h = 35{,}600$ feet; $\delta = -20^{\circ}$; $\alpha = 6^{\circ}37'$; $\beta = 0^{\circ}$.

Figure 13.- Continued.

[redacted]

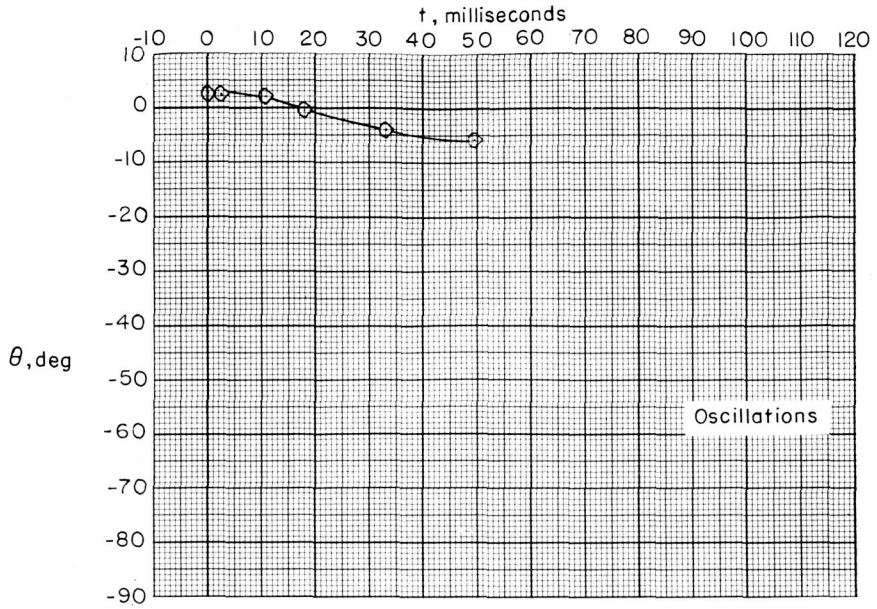

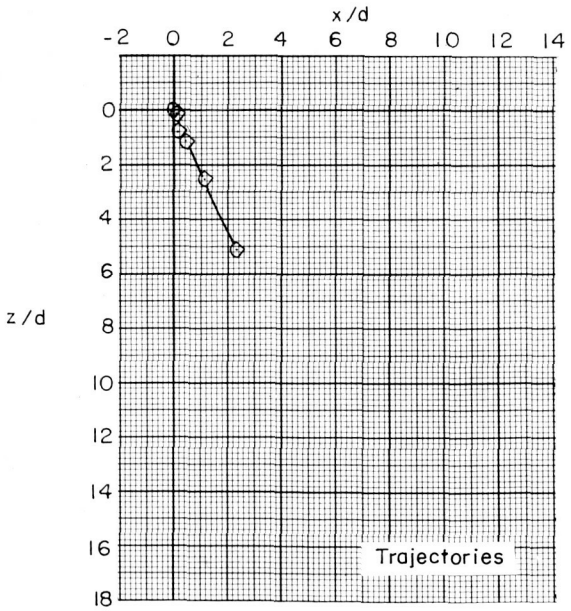

(v) Concluded.

Figure 13.- Concluded.

[redacted]

L-915

DE[redacted]SIFIED

L-915

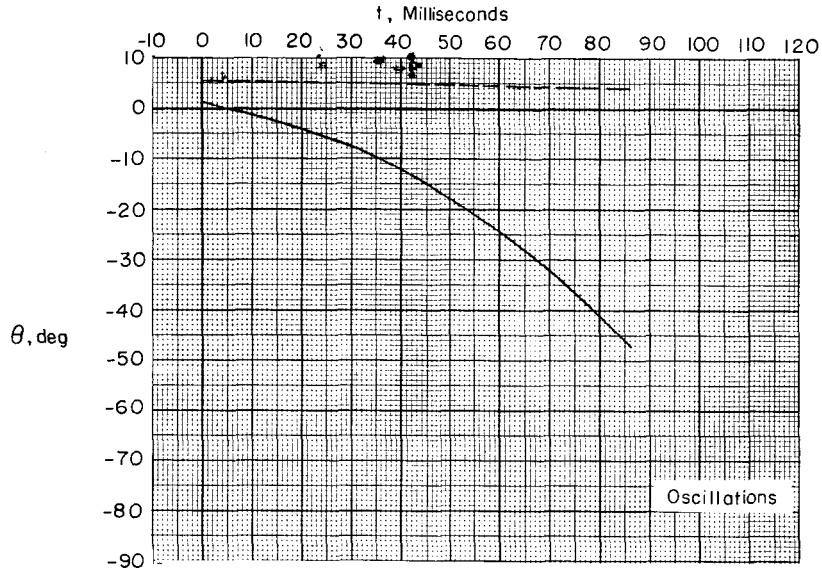

Test 17 ——— M = 0.90 ; α = 9° 20' ; β = 1° ;
h = 26,150 ft
Test 23 - - - - - M = 0.92 ; α = 5° 30' ; β = 0° ;
h = 25,650 ft

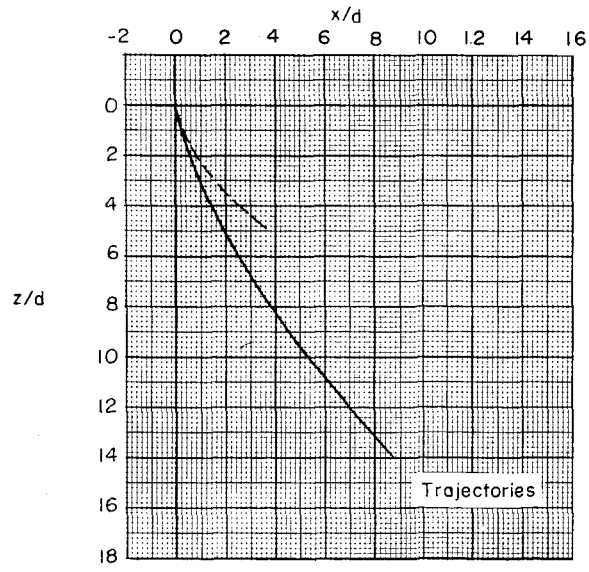

(a) Effect of change in wing angle of attack with $\delta = -20^{\circ}$.

Figure 14.- Comparison plots of fuel-tank releases incorporating three tail fins.

[redacted]

[redacted]

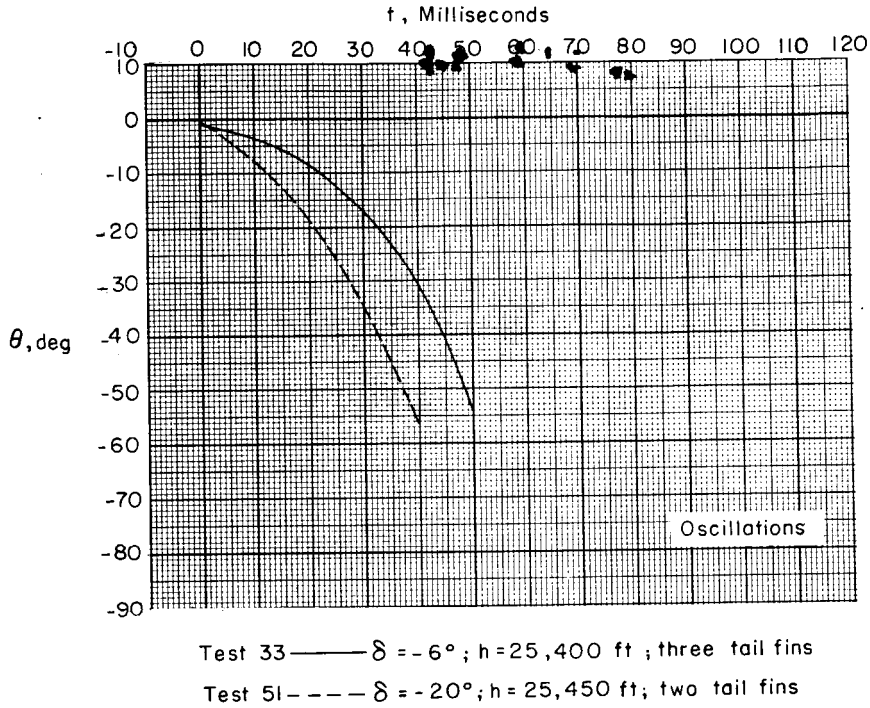

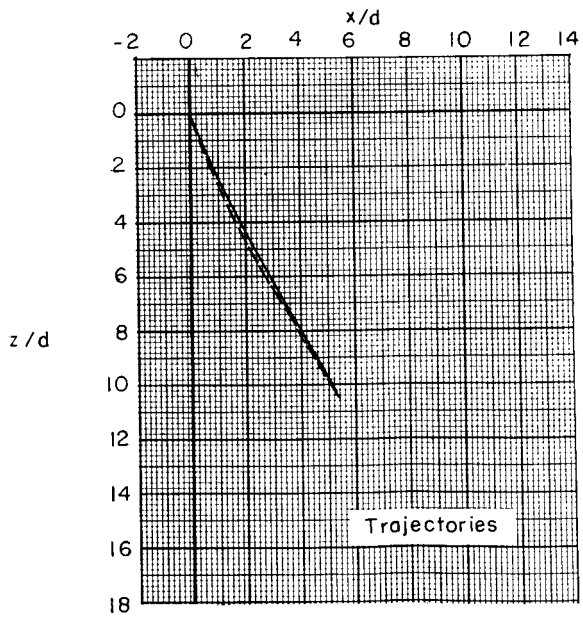

(b) Effect of change in canard-surface deflection at $M = 1.98$; $\alpha = 3^{\circ}16'$; $\beta = 0^{\circ}$.

Figure 14.- Concluded.

[redacted]

L-915

L-915

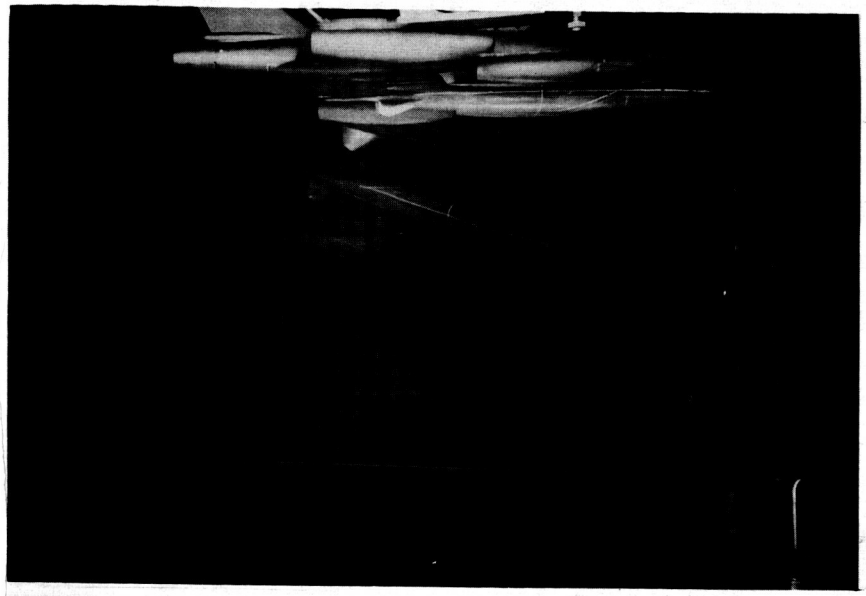

Side view

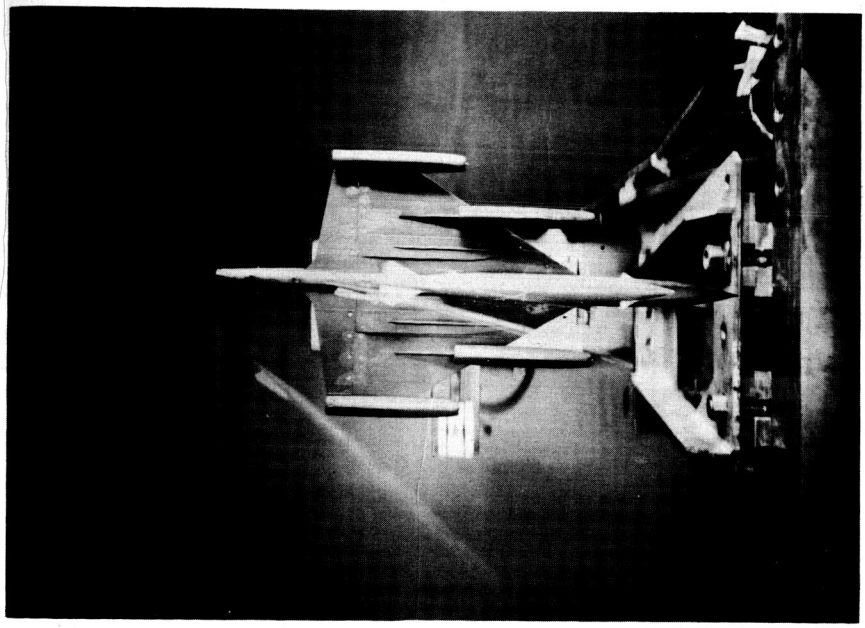

Bottom view

L-60-5508

(a) Test 35. $M = 0.92$; h = sea level; $\delta = -2^{\circ}$; $\alpha = 3^{\circ}36'$; $\beta = 1^{\circ}$.

Figure 15.- Fuel-tank releases with two tail fins mounted 30° downward of the horizontal.

[redacted]

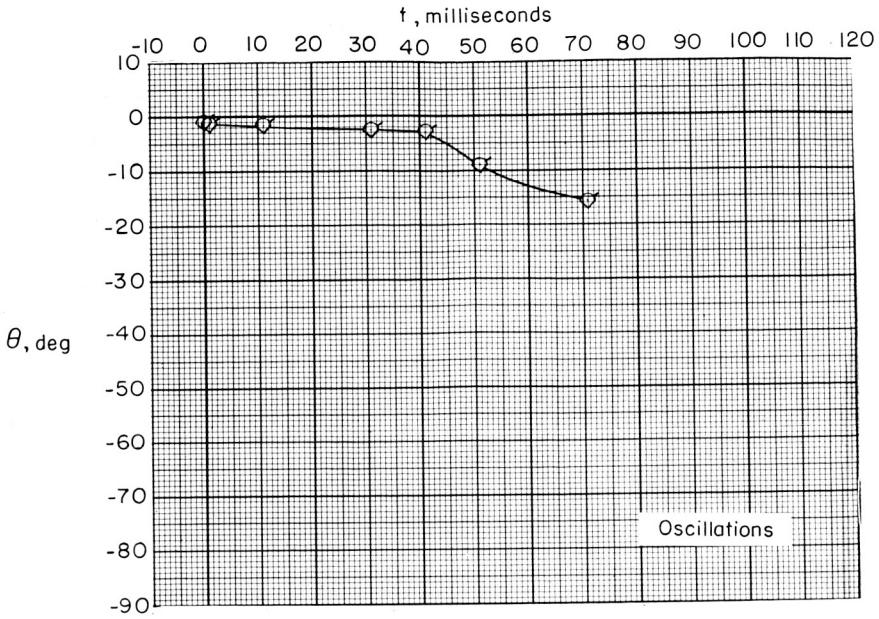

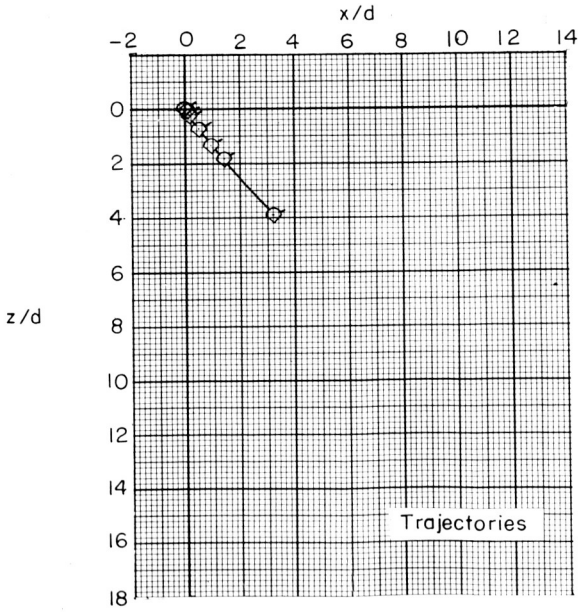

(a) Concluded.

Figure 15.- Continued.

L-915

[redacted]

L-915

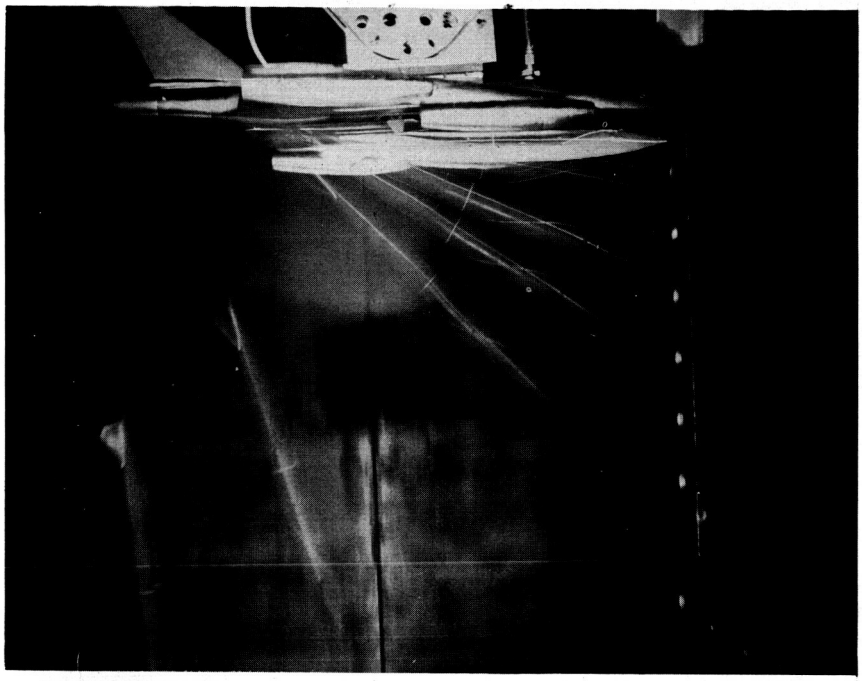

Side view

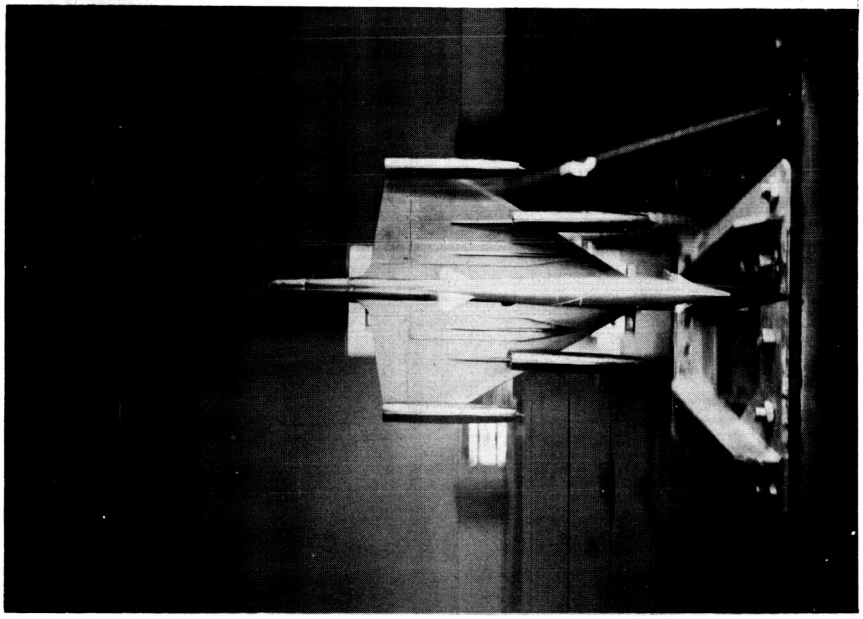

Bottom view

L-60-5509

(b) Test 36. $M = 1.39$; $h = 26{,}250$ feet; $\delta = -2^{\circ}$; $\alpha = 3^{\circ}21'$; $\beta = 0^{\circ}$; tail cone of fuel-tank model struck airplane model.

Figure 15.- Continued.

[redacted]

[redacted]

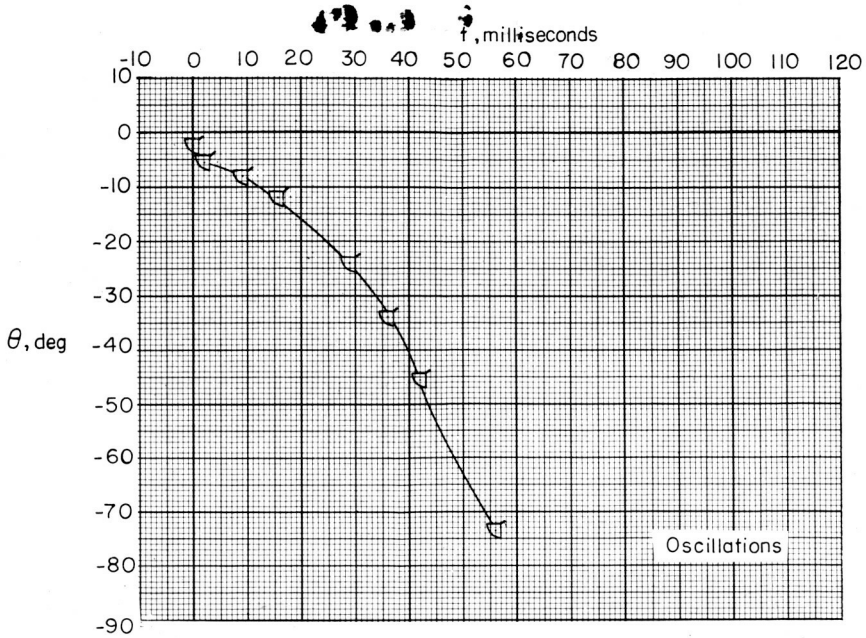

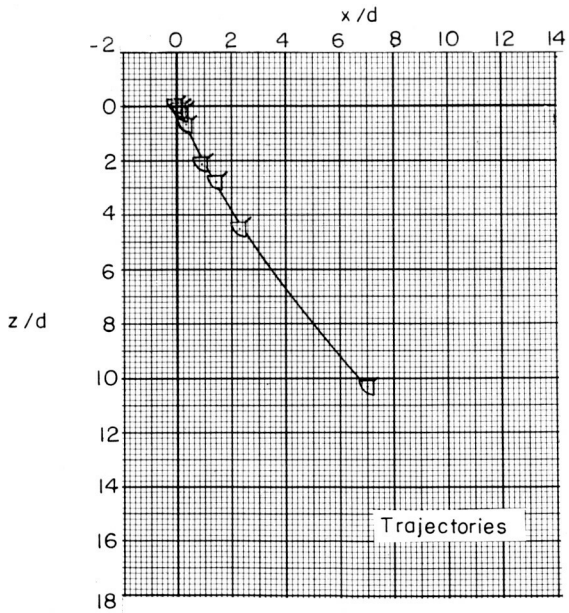

(b) Concluded.

Figure 15.- Continued.

L-915

[redacted]

DECLASSIFIED

L-915

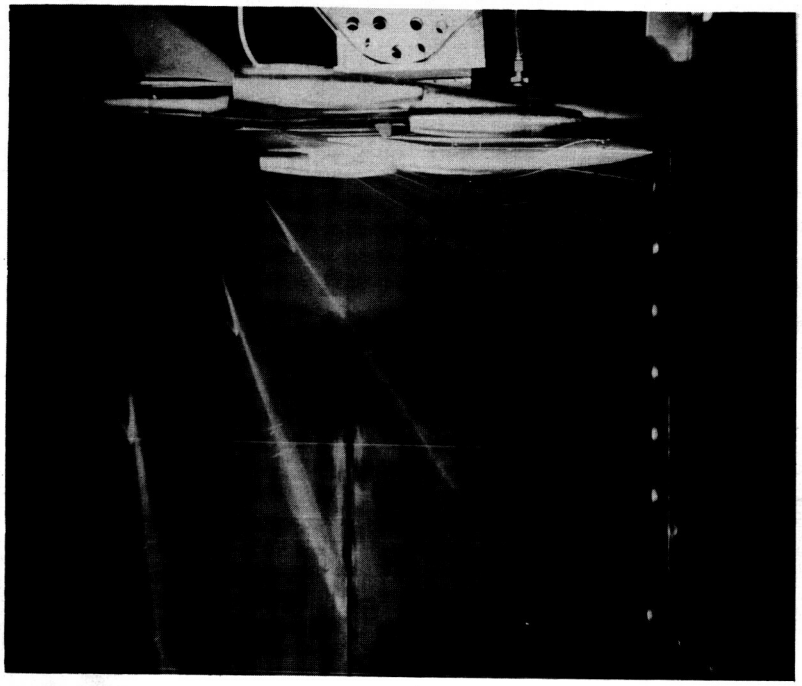

Side view

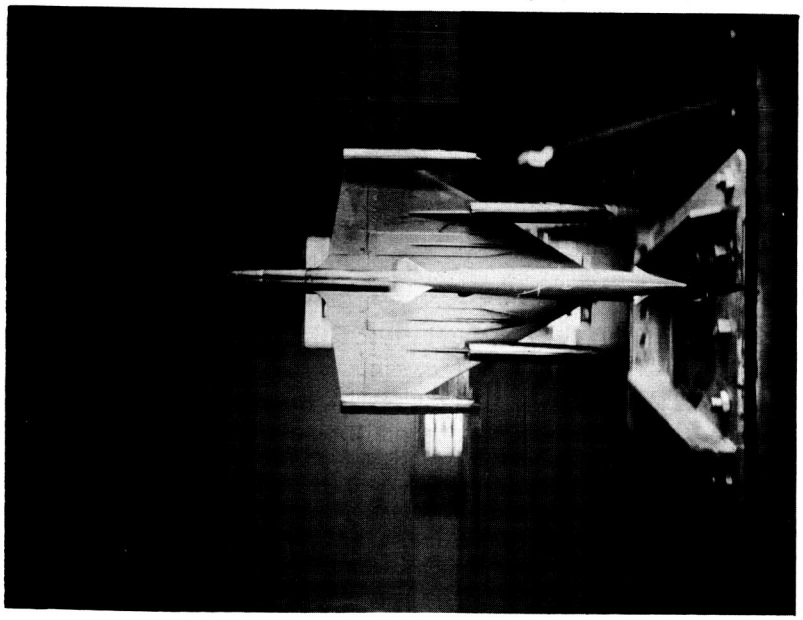

Bottom view

L-60-5510

(c) Test 37. $M = 1.39$; $h = 26{,}150$ feet; $\delta = -2^{\circ}$; $\alpha = 3^{\circ}40'$; $\beta = 0^{\circ}$.

Figure 15.- Continued.

[redacted]

[redacted]

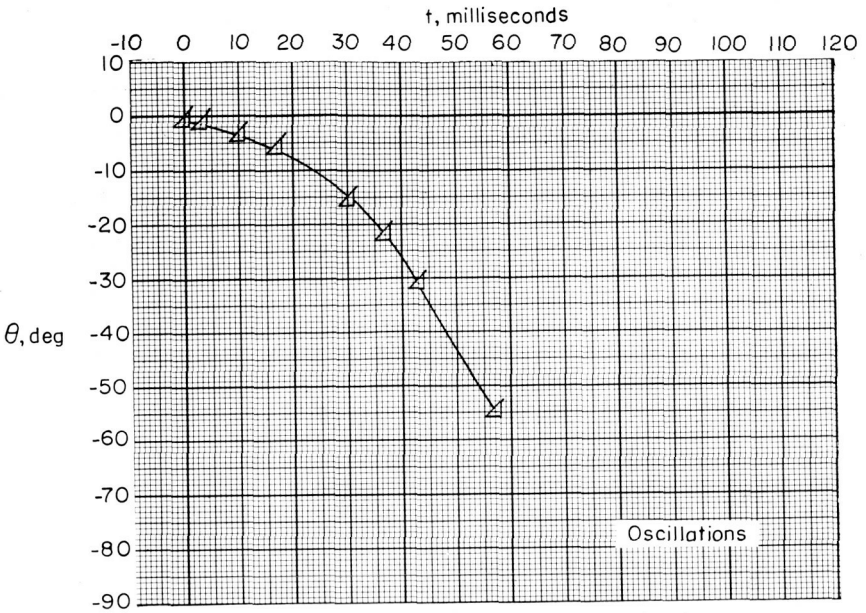

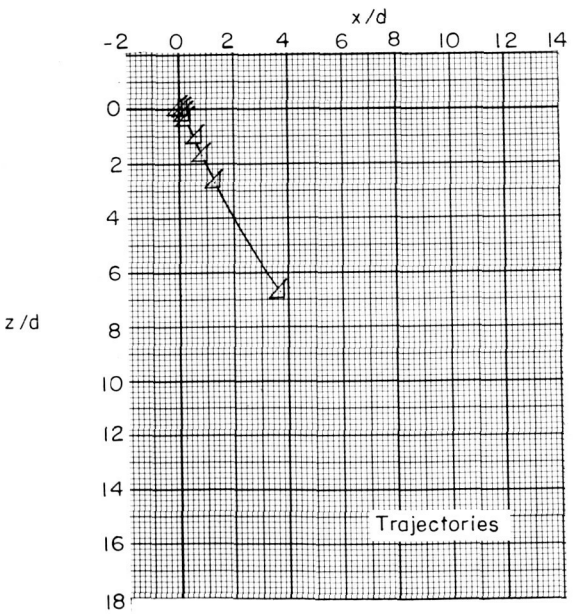

(c) Concluded.

Figure 15.- Continued.

[redacted]

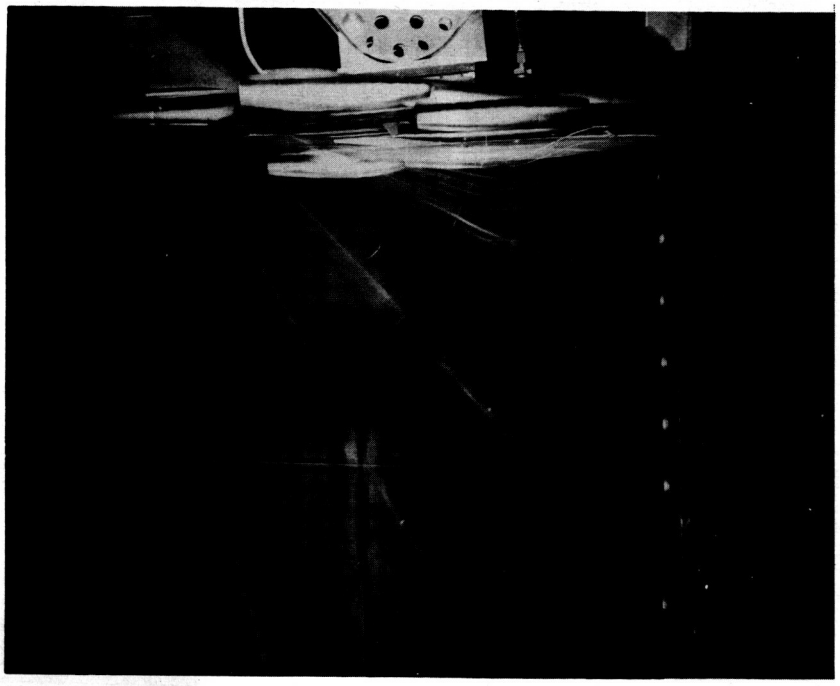

Side view

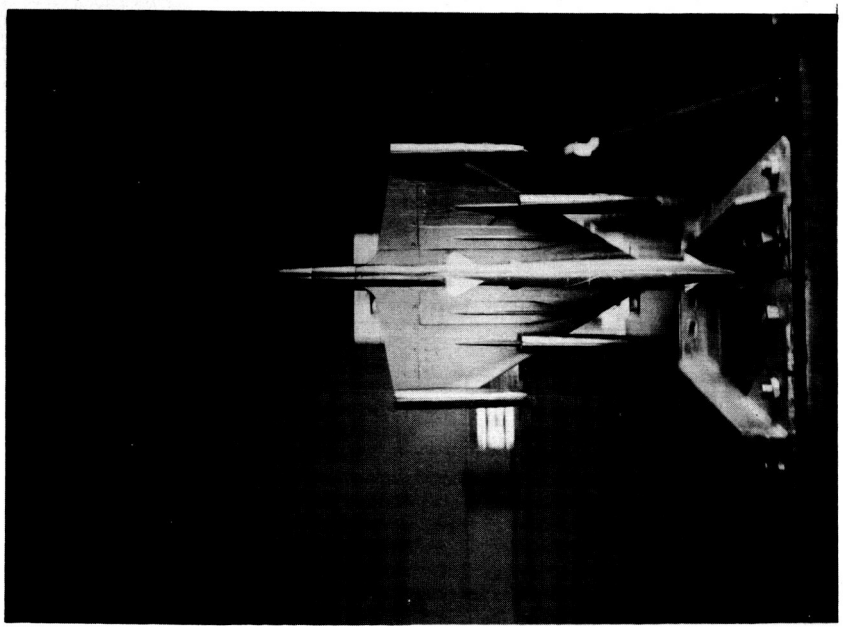

Bottom view

L-60-5511

(d) Test 38. $M = 1.39$; $h = 25{,}400$ feet; $\delta = -20^{\circ}$; $\alpha = 4^{\circ}56'$; $\beta = 0^{\circ}$.

Figure 15.- Continued.

[redacted]

[redacted]

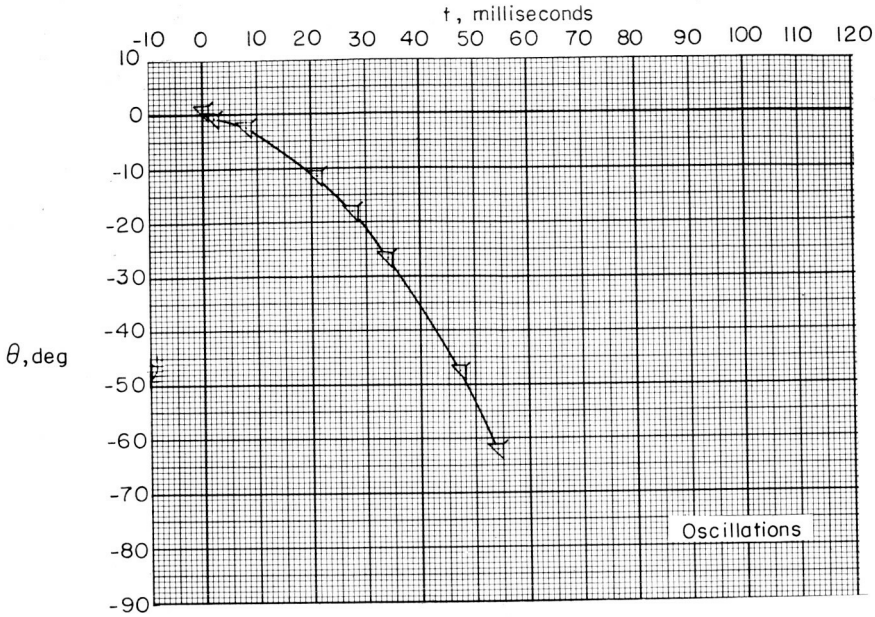

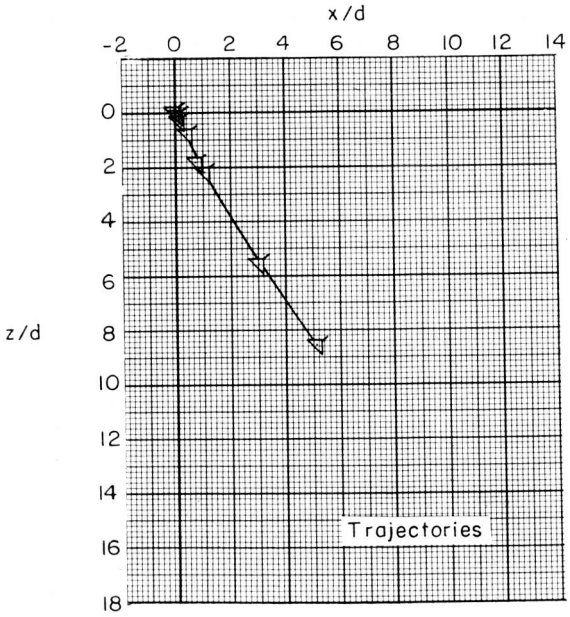

(d) Concluded.

Figure 15.- Continued.

[redacted]

L-915

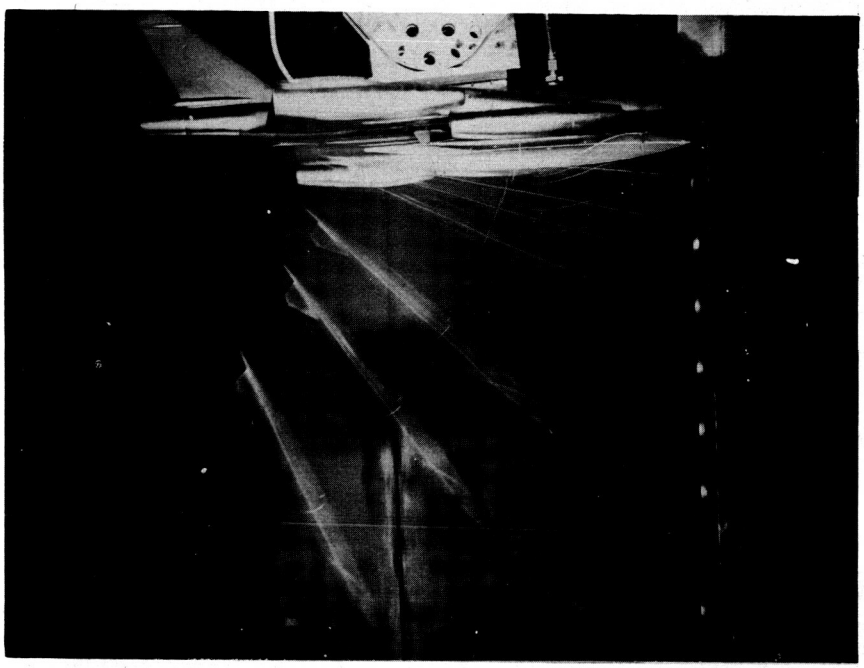

Side view

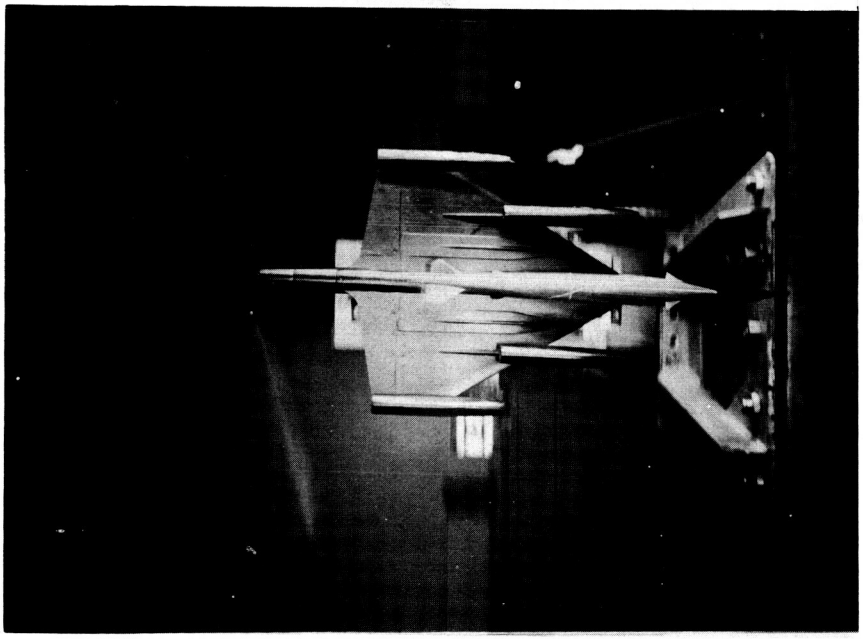

Bottom view

L-60-5512

(e) Test 39. $M = 1.39$; $h = 26{,}000$ feet; $\delta = -2^{\circ}$; $\alpha = 4^{\circ}56'$; $\beta = 1^{\circ}$.

Figure 15.- Continued.

[redacted]

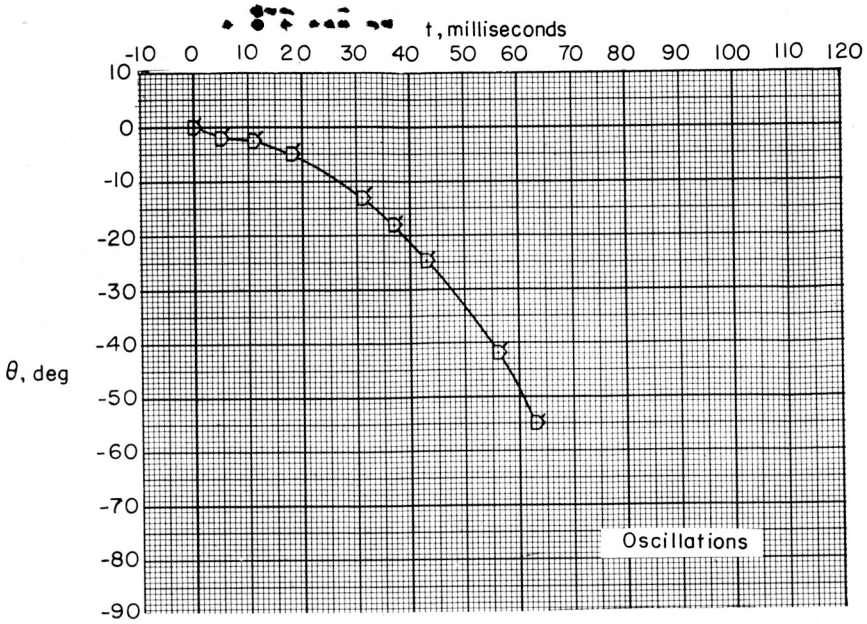

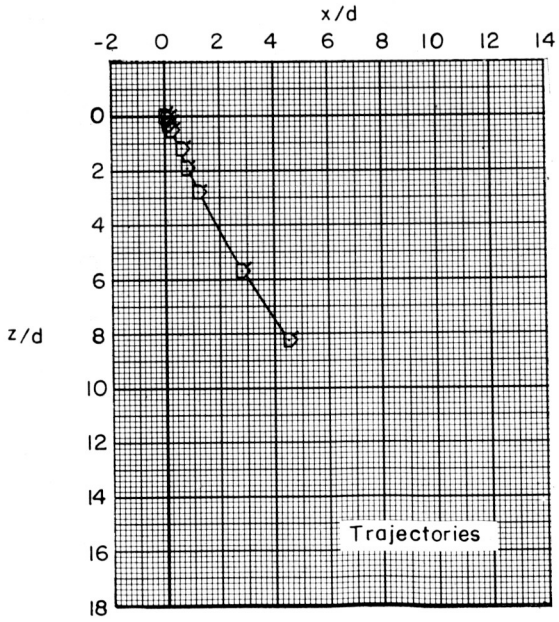

(e) Concluded.

Figure 15.- Continued.

L-915

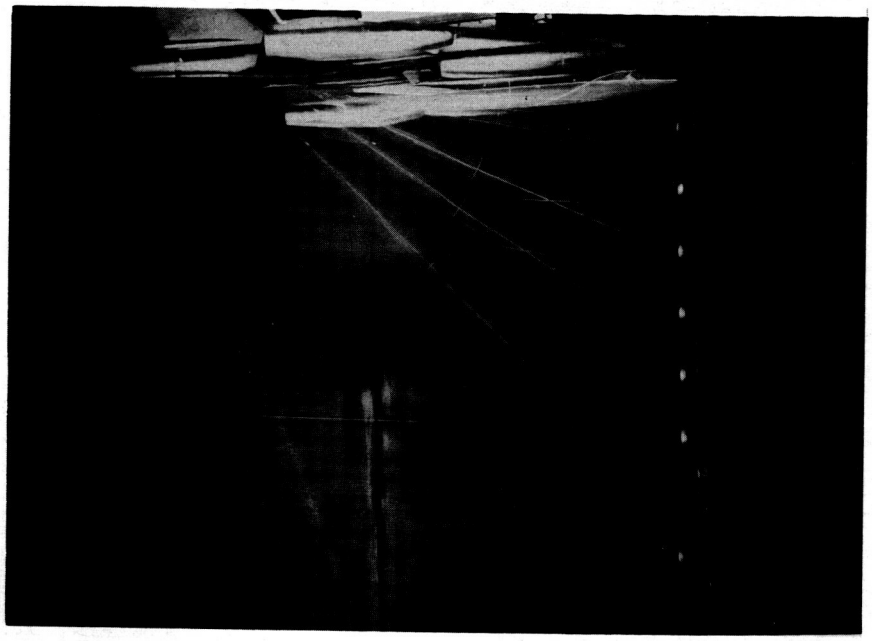

Side view

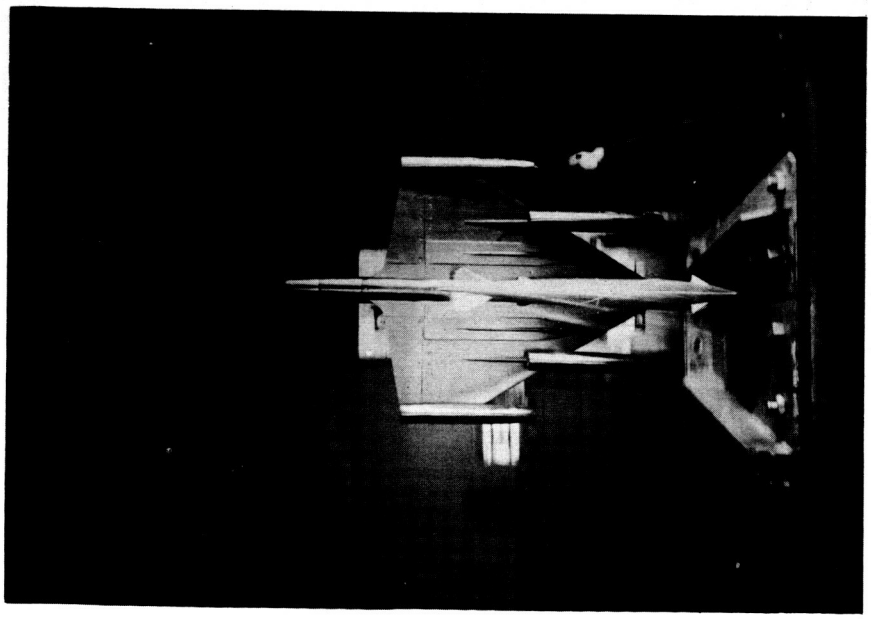

Bottom view

L-60-5513

(f) Test 40. $M = 1.39$; $h = 25{,}850$ feet; $\delta = -20^{\circ}$; $\alpha = 6^{\circ}30'$; $\beta = 1^{\circ}$.

Figure 15.- Continued.

[redacted]

[redacted]

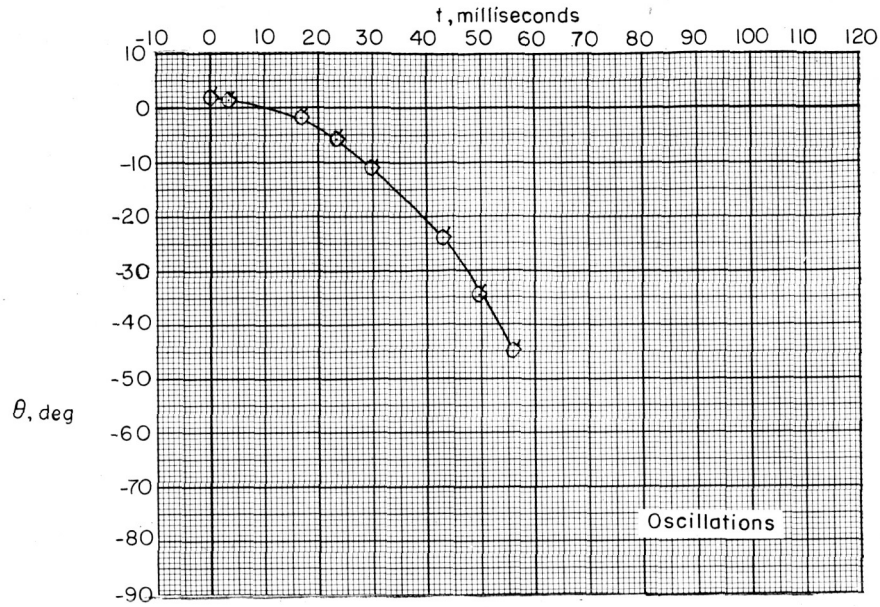

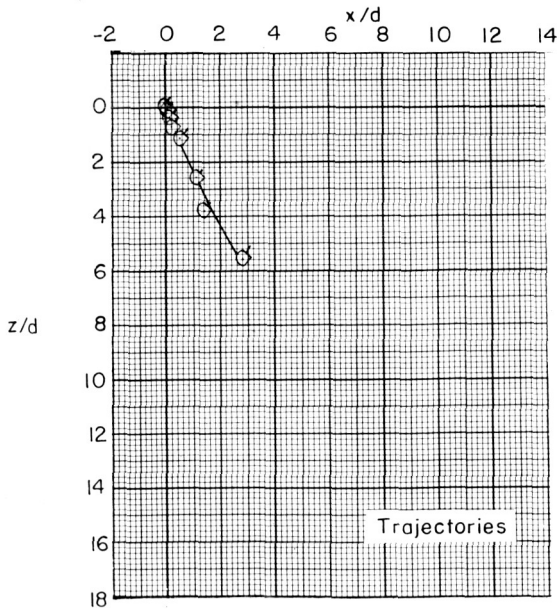

(f) Concluded.

Figure 15.- Continued.

[redacted]

L-915

L-915

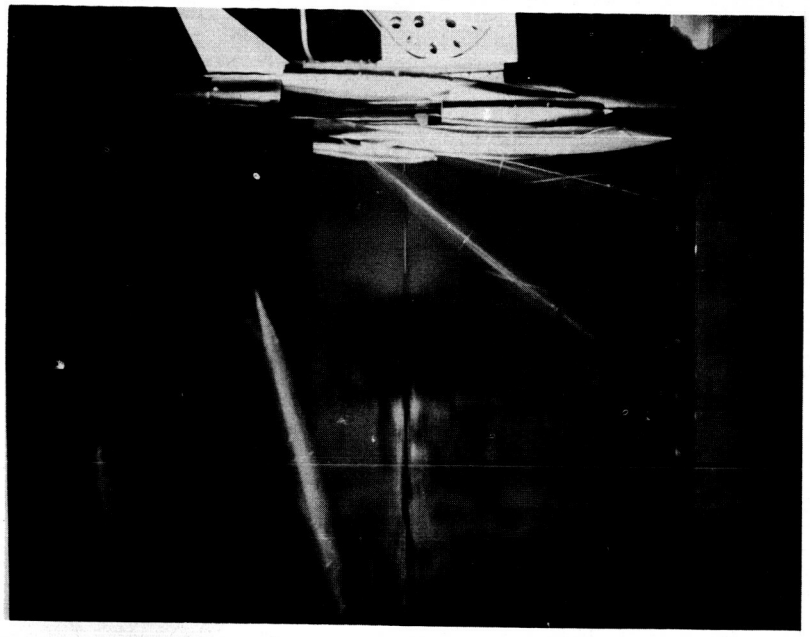

Side view

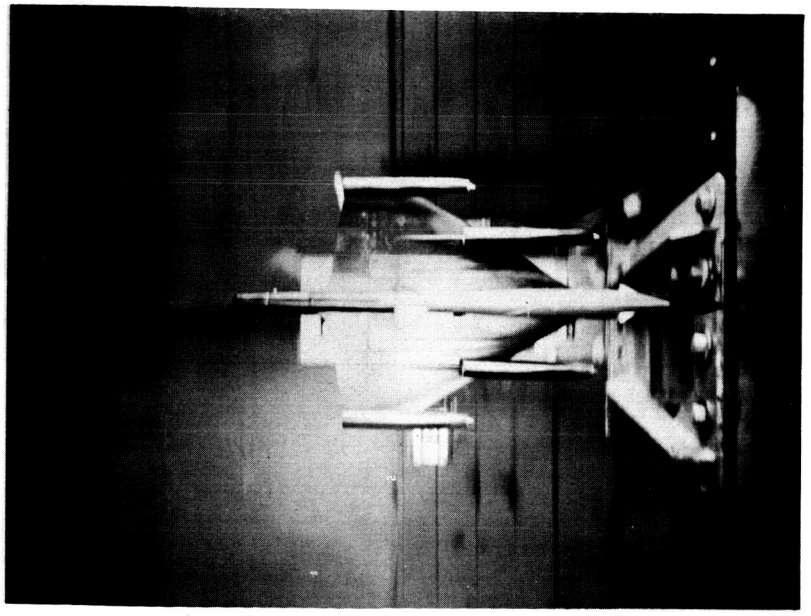

Bottom view

L-60-5514

(g) Test 41. $M = 1.59$; $h = 26{,}150$ feet; $\delta = -20^{\circ}$; $\alpha = 3^{\circ}16'$; $\beta = 0^{\circ}$; tail cone of fuel-tank model struck airplane model.

Figure 15.- Continued.

[redacted]

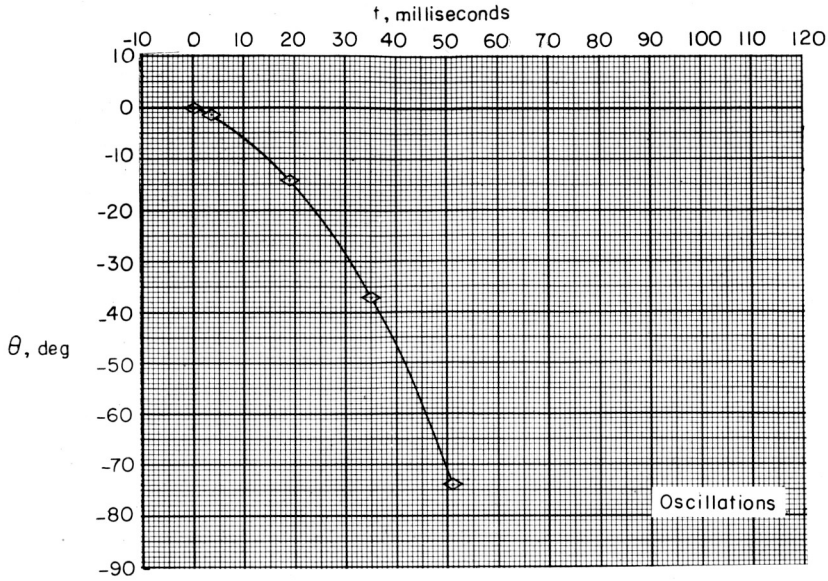

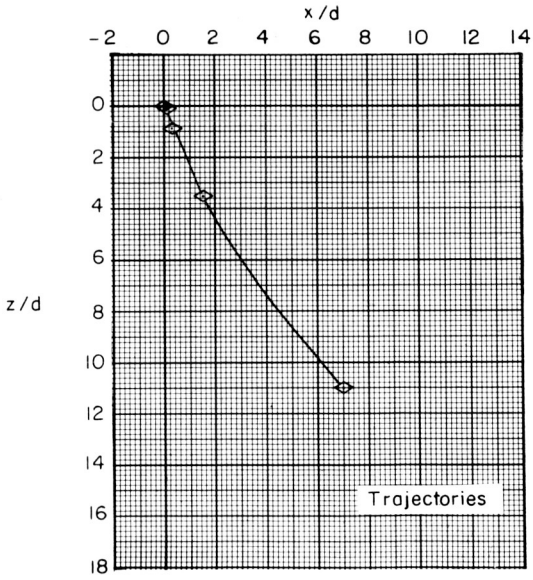

(g) Concluded.

Figure 15.- Continued.

L-915

[redacted]

DECLASSIFIED

L-915

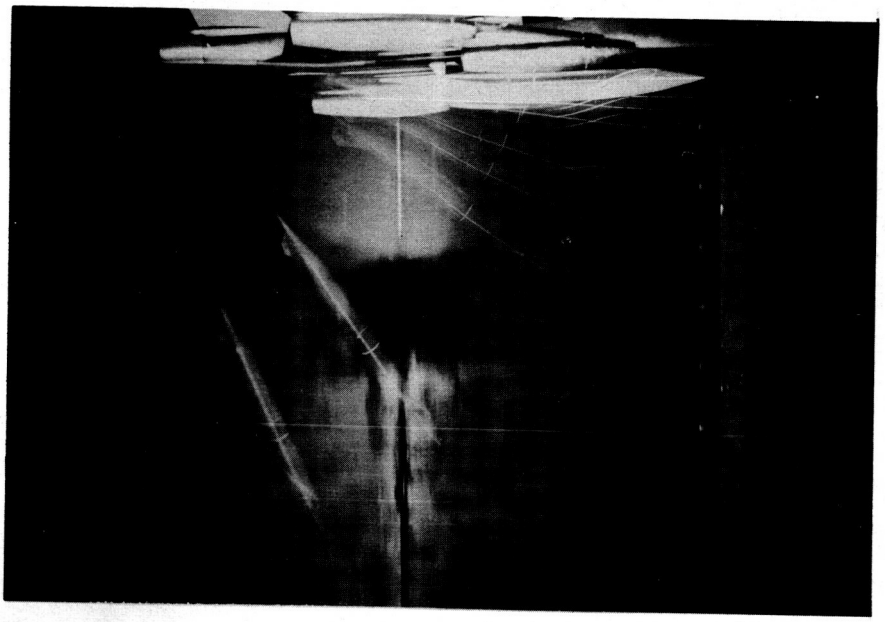

Side view

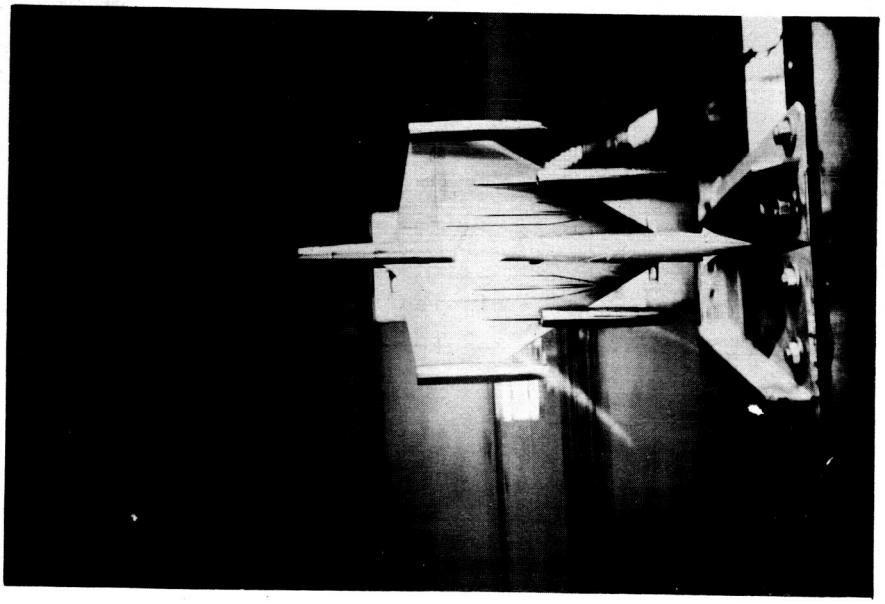

Bottom view

L-60-5515

(h) Test 42. $M = 1.59$; $h = 26{,}000$ feet; $\delta = -2^{\circ}$; $\alpha = 6^{\circ}07'$; $\beta = 1^{\circ}$.

Figure 15.- Continued.

[redacted]

[redacted]

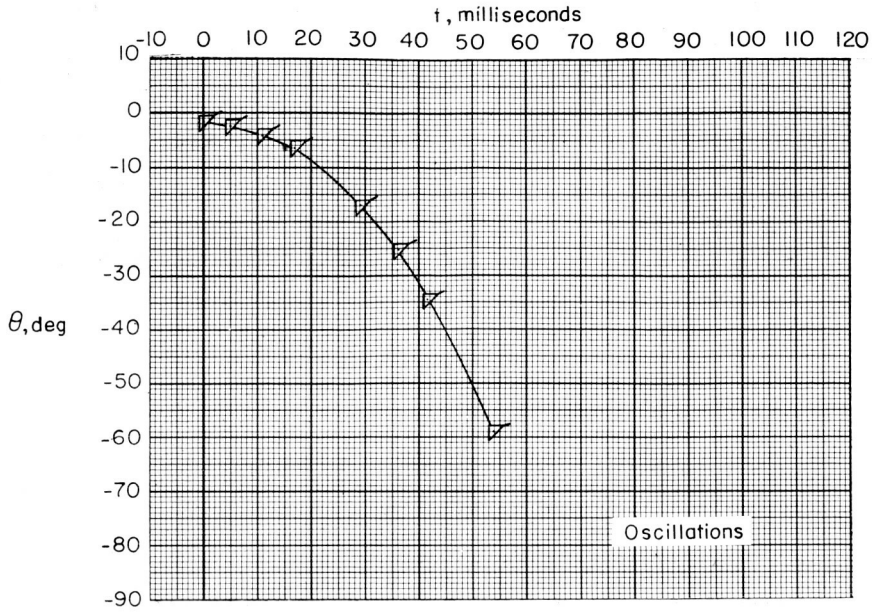

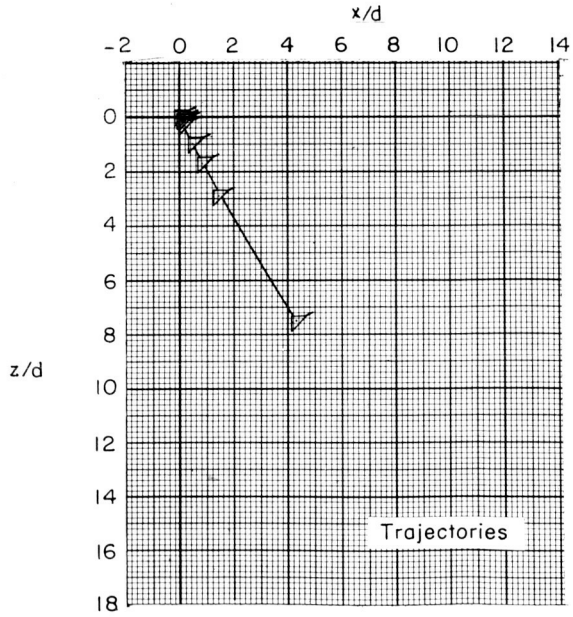

(h) Concluded.

Figure 15.- Continued.

[redacted]

L-915

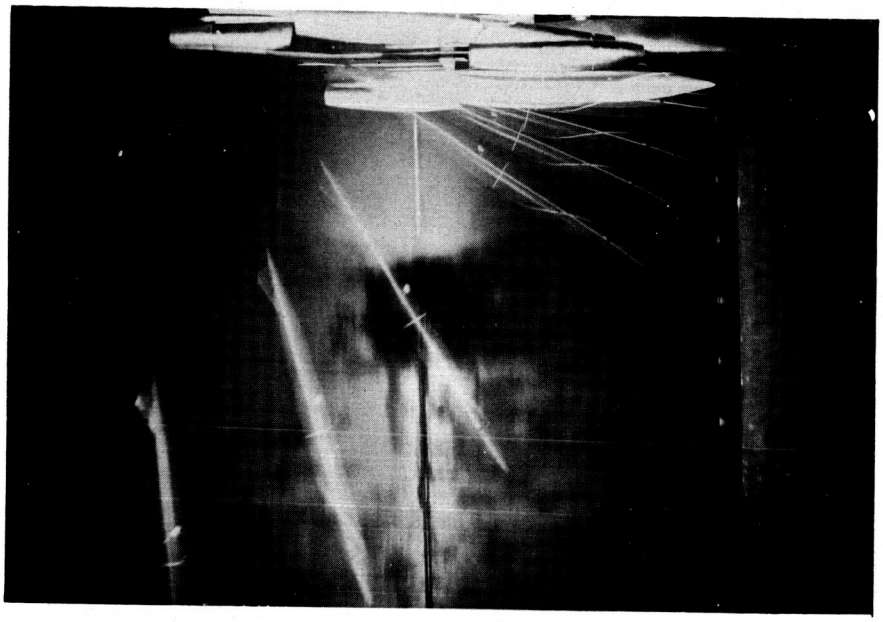

Side view

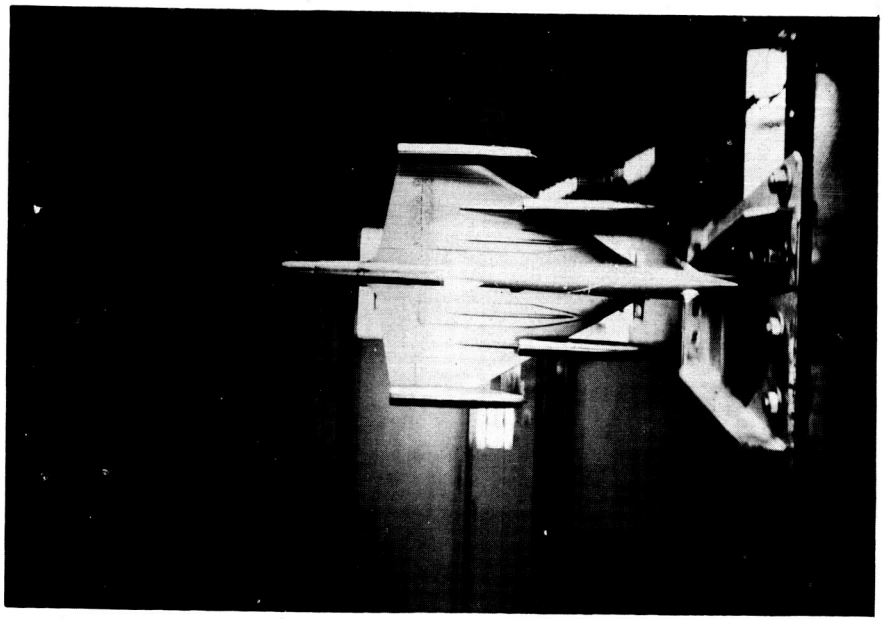

Bottom view

L-60-5516

(i) Test 43. $M = 1.59$; $h = 26{,}050$ feet; $\delta = -2^{\circ}$; $\alpha = 3^{\circ}20'$; $\beta = 0^{\circ}$; tail cone of fuel-tank model struck airplane model.

Figure 15.- Continued.

[redacted]

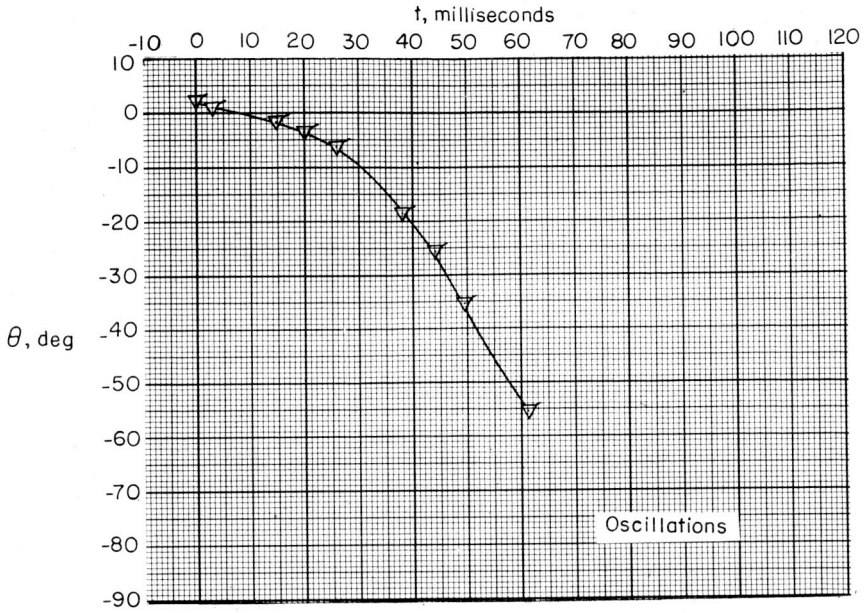

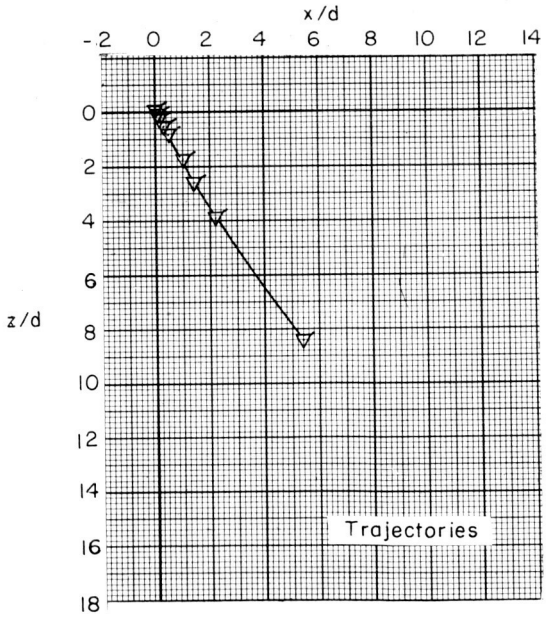

(i) Concluded.

Figure 15.- Continued.

L-915

[redacted]

Side view

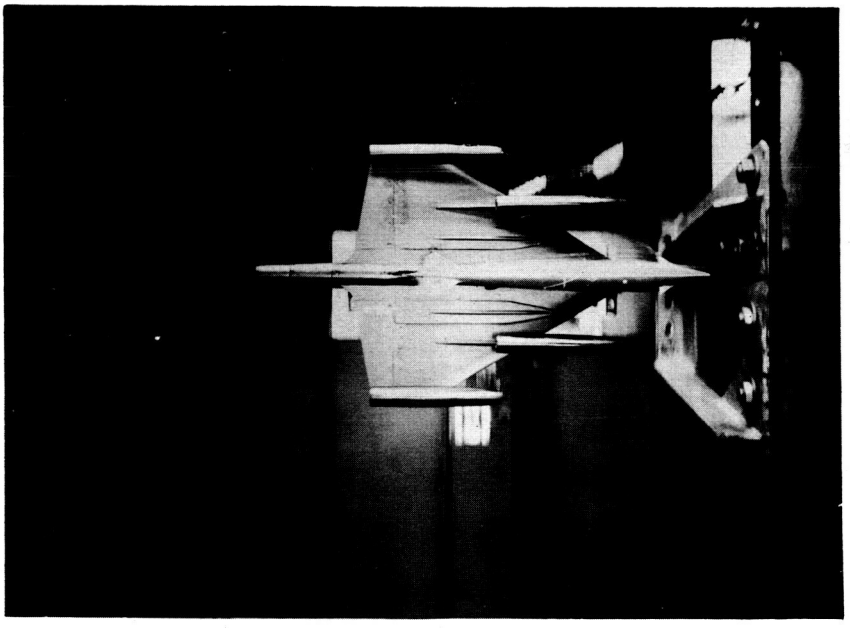

Bottom view

L-60-5517

(j) Test 44. $M = 1.59$; $h = 27{,}000$ feet; $\delta = -2^{\circ}$; $\alpha = 4^{\circ}03'$; $\beta = 0^{\circ}$.

Figure 15.- Continued.

[redacted]

[redacted]

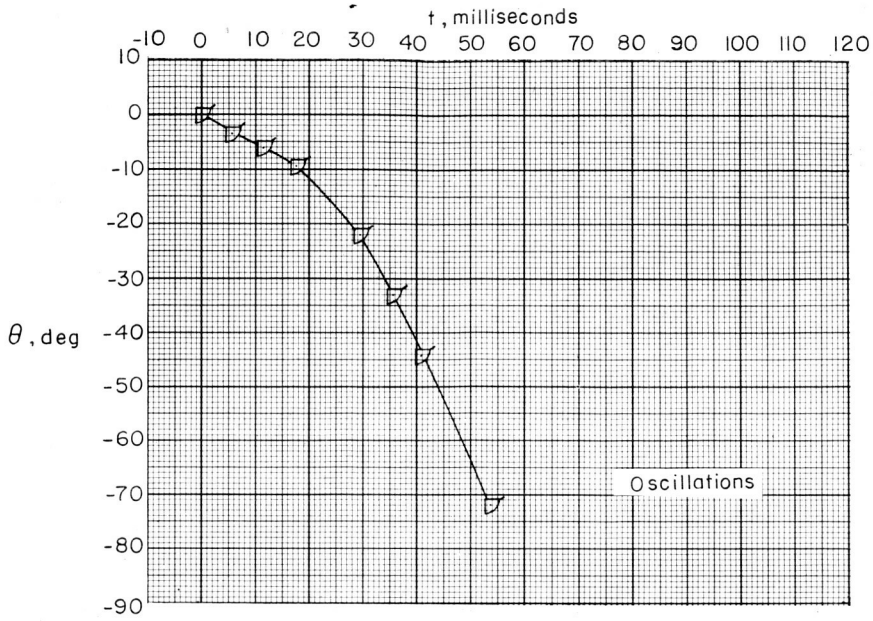

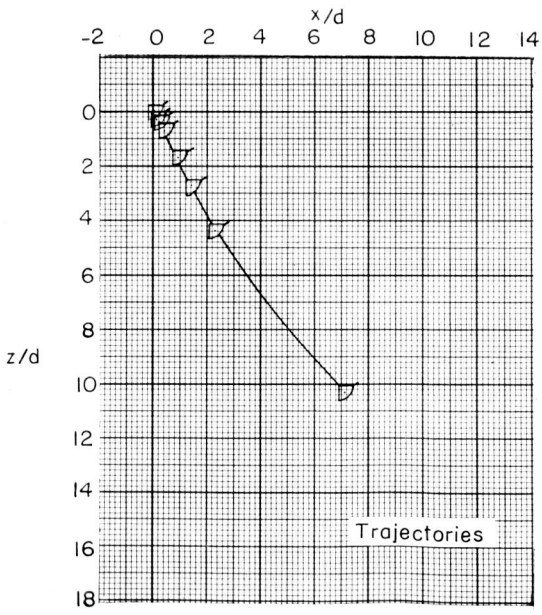

(j) Concluded.

Figure 15.- Continued.

L-915

[redacted]

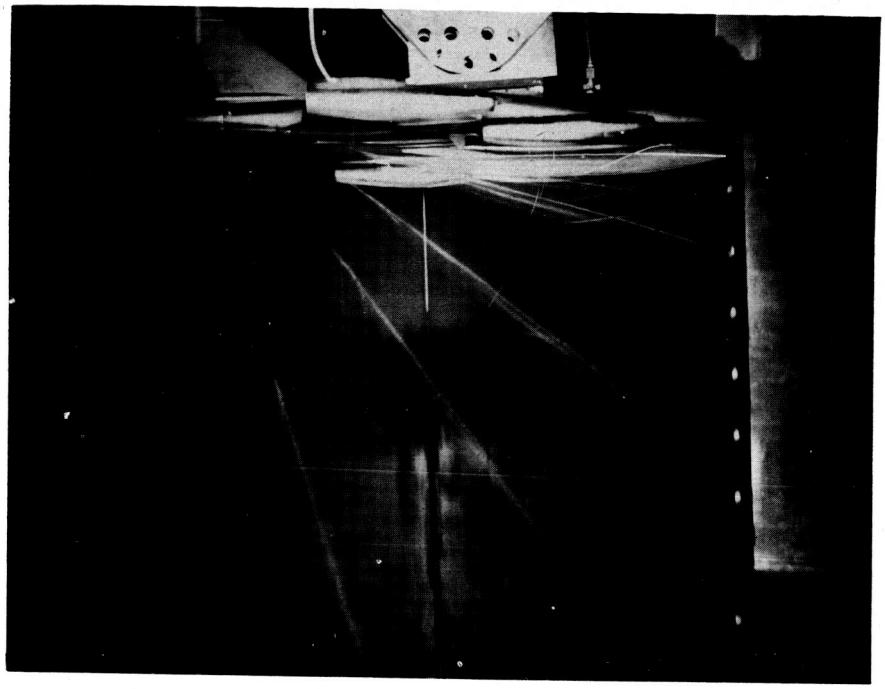

Side view

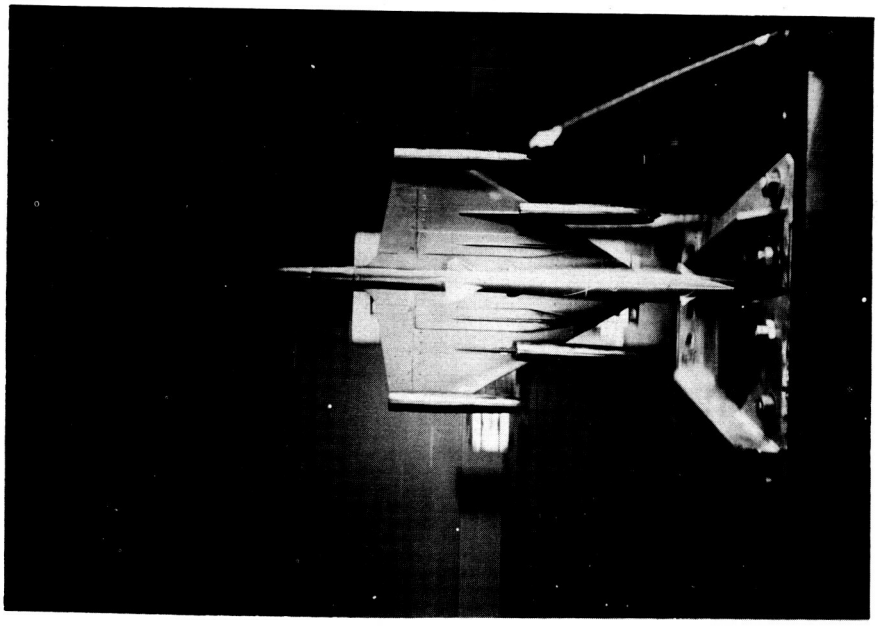

Bottom view

L-60-5518

(k) Test 45. $M = 1.80$; $h = 25{,}700$ feet; $\delta = -2^{\circ}$; $\alpha = 3^{\circ}26'$; $\beta = 0^{\circ}$.

Figure 15.- Continued.

[redacted]

[redacted]

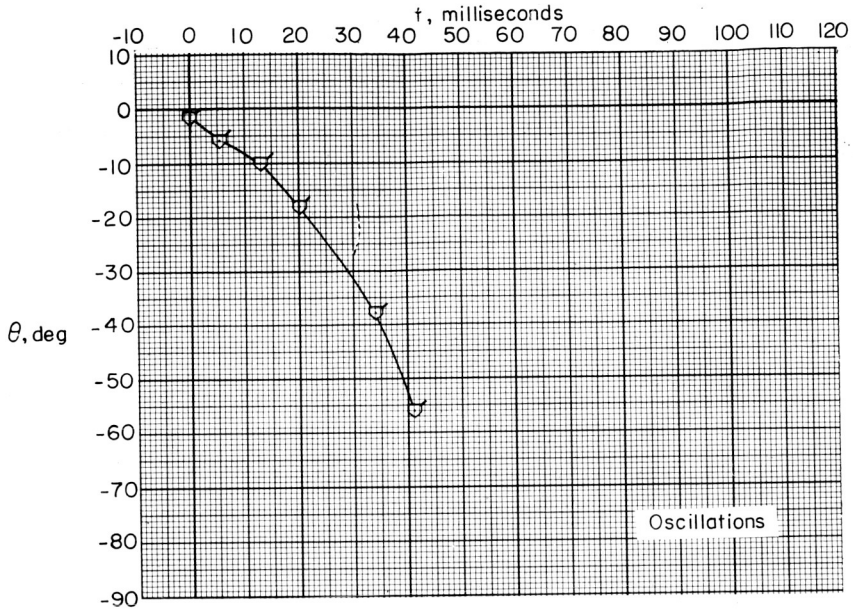

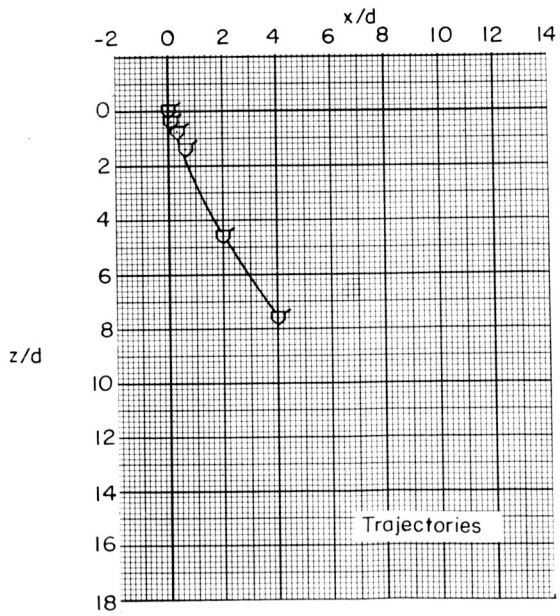

(k) Concluded.

Figure 15.- Continued.

[redacted]

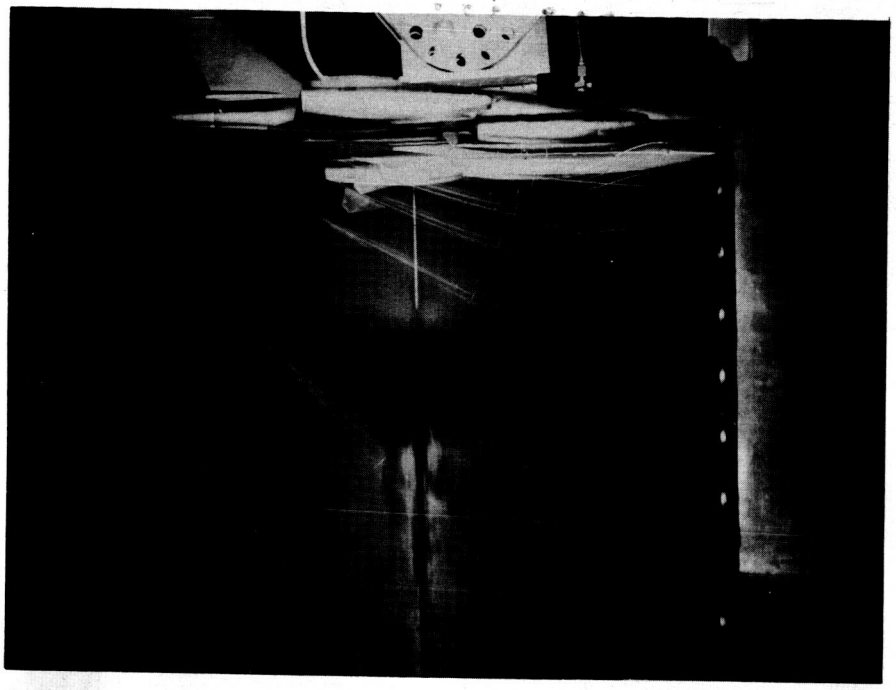

Side view

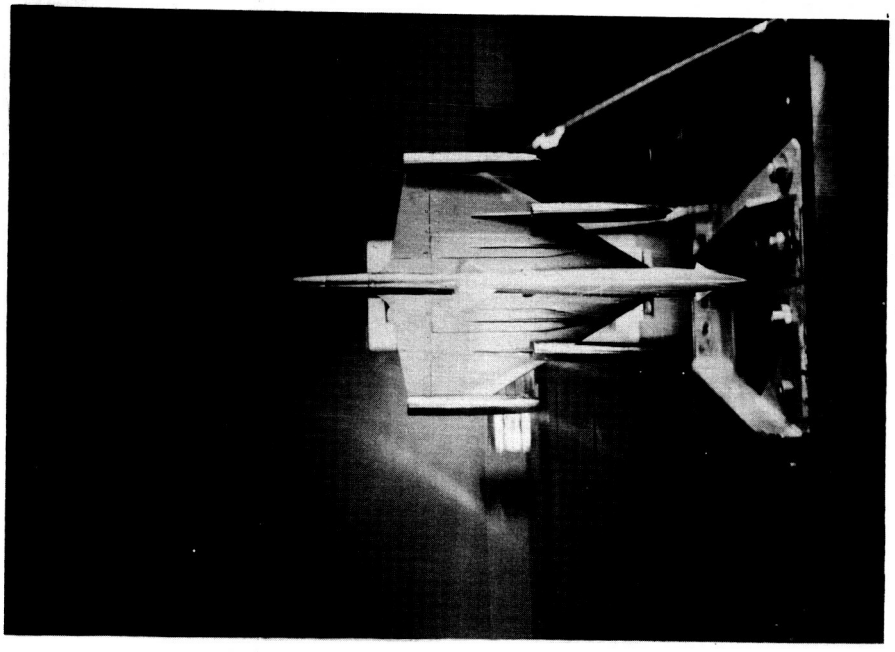

Bottom view

L-60-5519

(l) Test 46. $M = 1.80$; $h = 25,750$ feet; $\delta = -2^{\circ}$; $\alpha = 4^{\circ}09'$; $\beta = 1^{\circ}$.

Figure 15.- Continued.

[redacted]

[redacted]

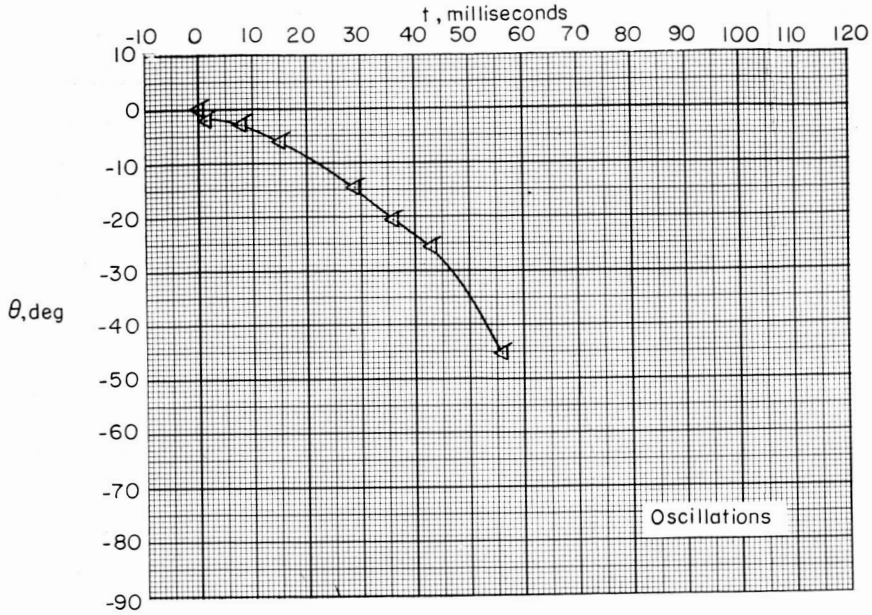

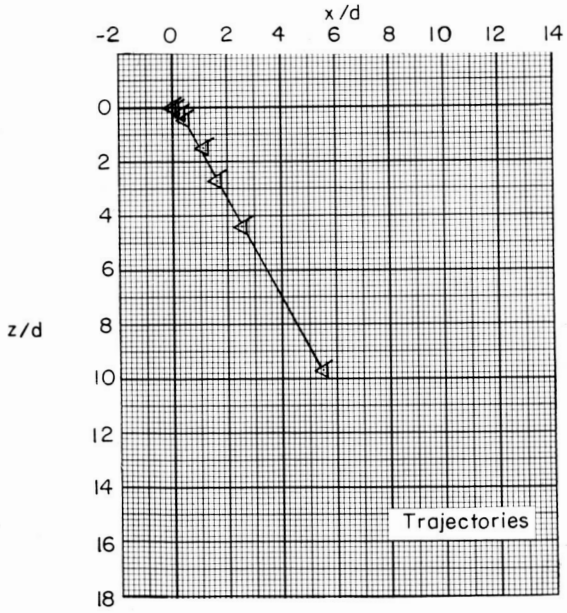

(*l*) Concluded.

Figure 15.- Continued.

[redacted]

L-915

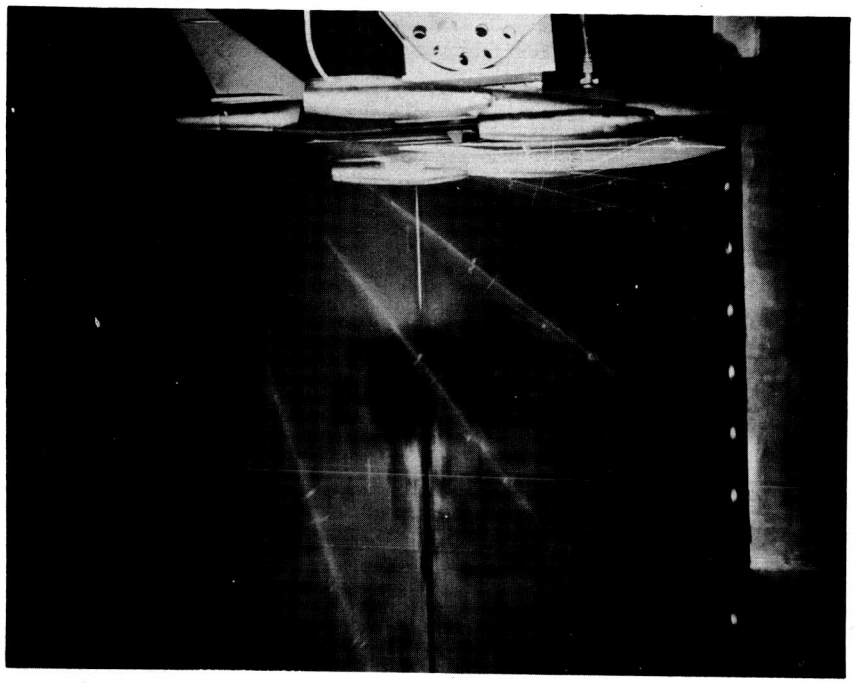

Side view

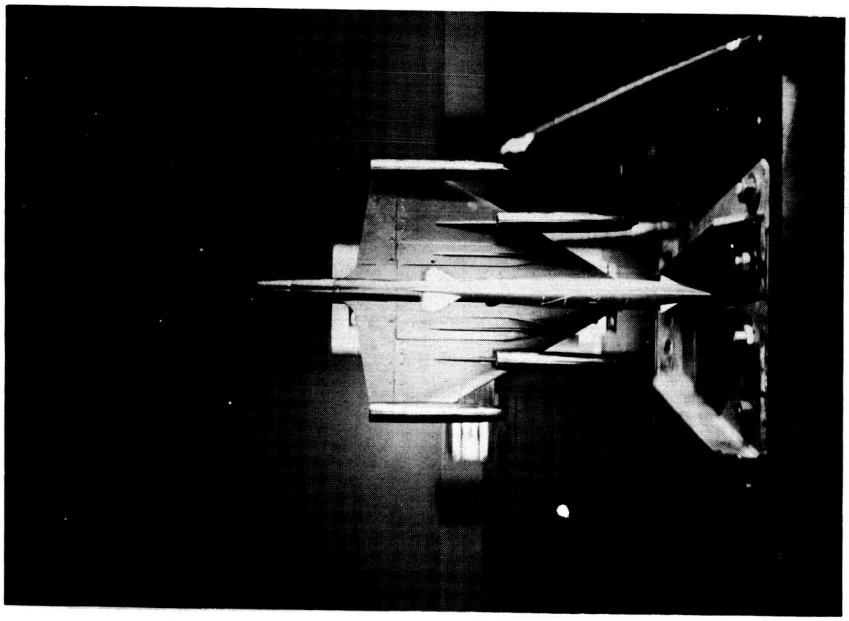

Bottom view

L-60-5520

(m) Test 47. $M = 1.80$; $h = 25{,}800$ feet; $\delta = -20^{\circ}$; $\alpha = 4^{\circ}09'$; $\beta = 0^{\circ}$.

Figure 15.- Continued.

[redacted]

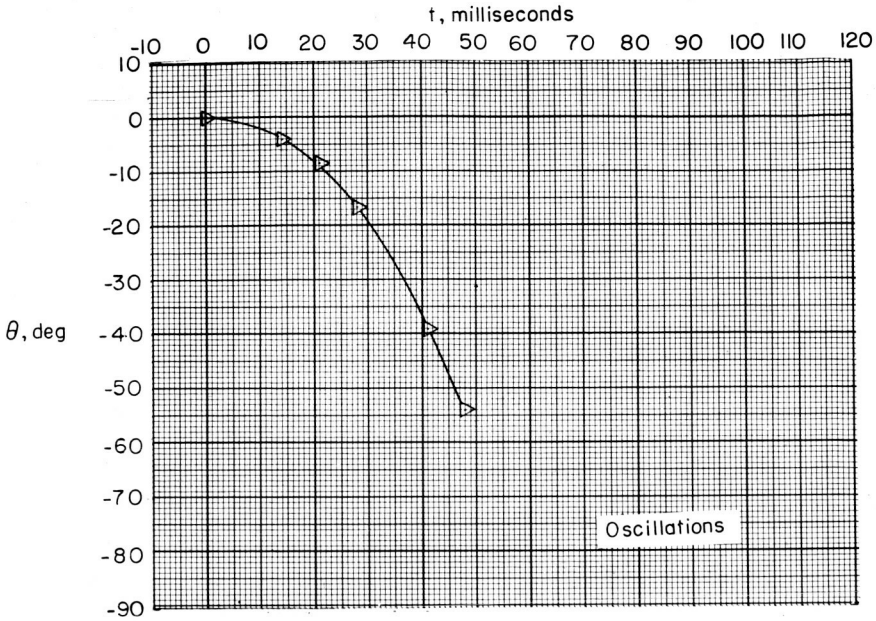

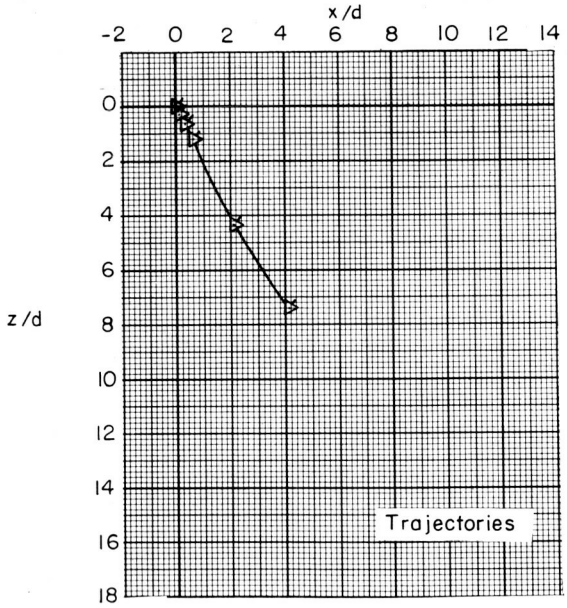

(m) Concluded.

Figure 15.- Continued.

[redacted]

L-915

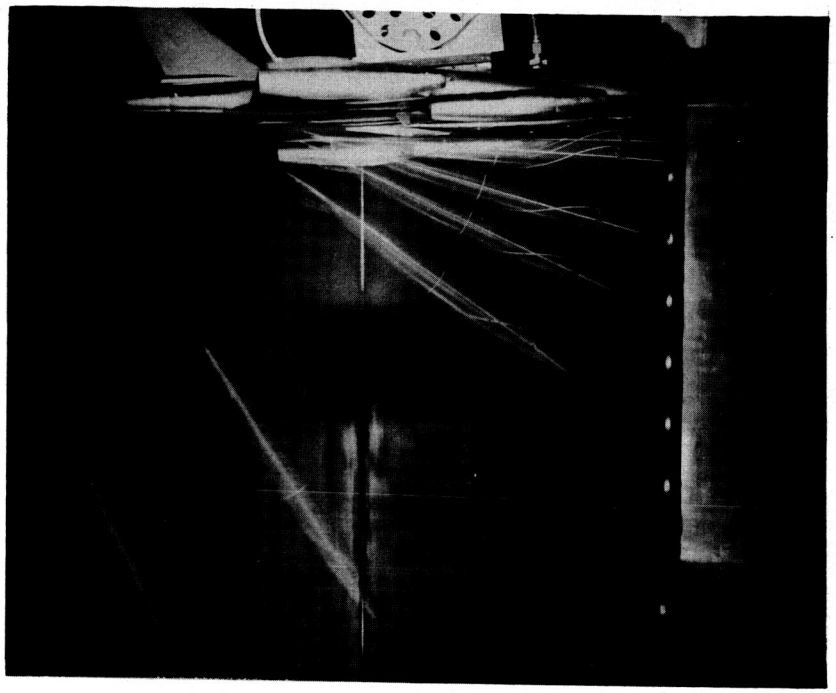

Side view

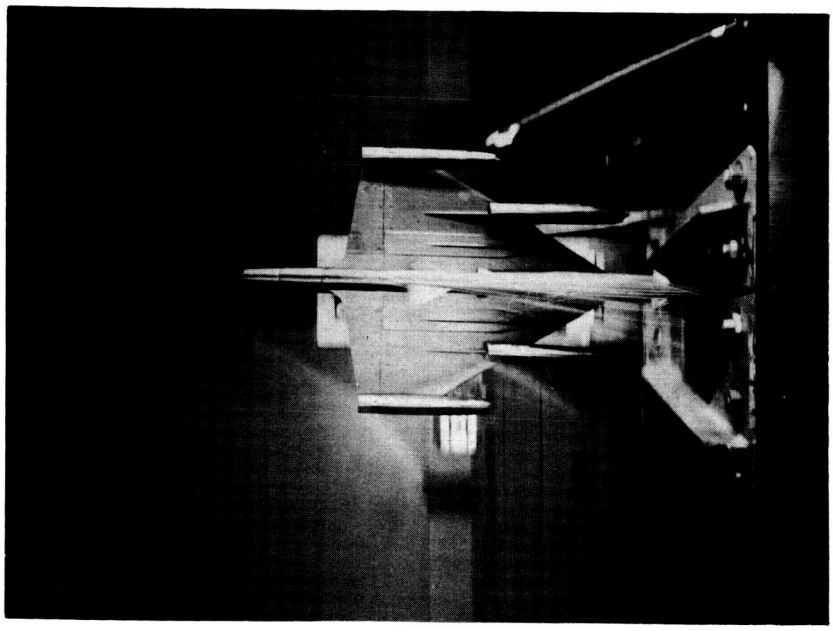

Bottom view

L-60-5521

(n) Test 48. $M = 1.80$; $h = 25{,}800$ feet; $\delta = -20^{\circ}$; $\alpha = 6^{\circ}35'$; $\beta = 1^{\circ}$.

Figure 15.- Continued.

[redacted]

[redacted]

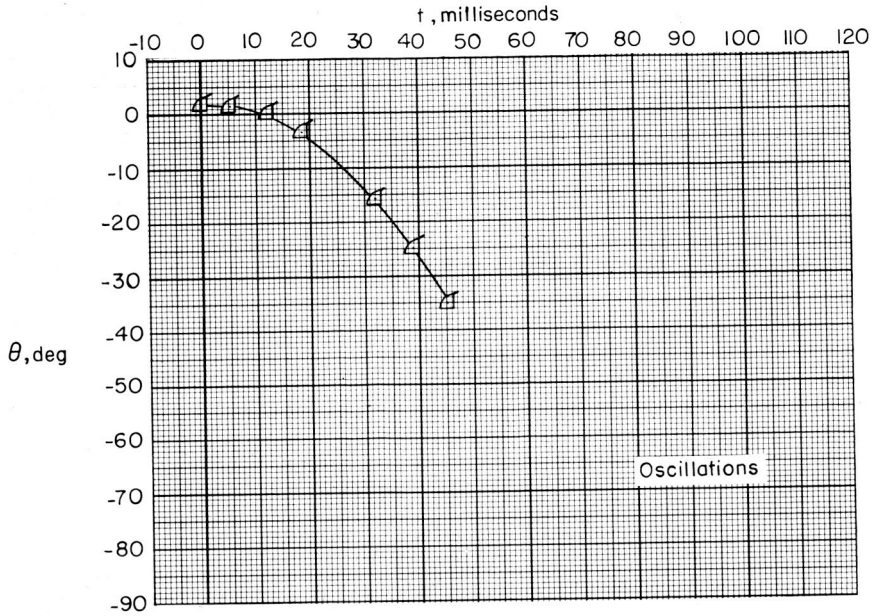

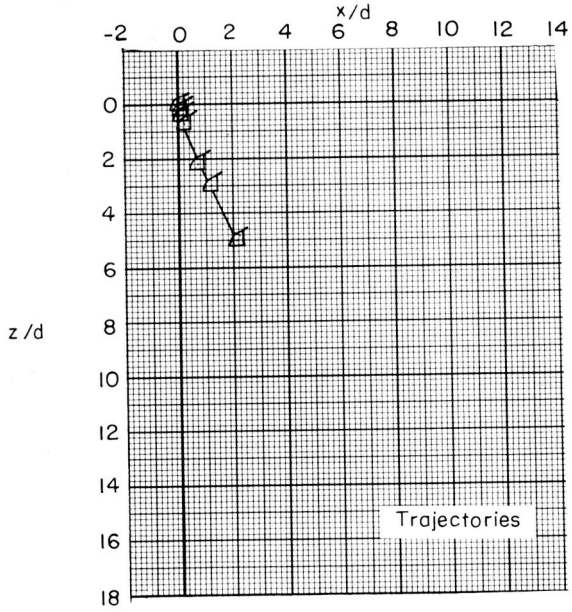

(n) Concluded.

Figure 15.- Continued.

L-915

[redacted]

DE[redacted]IFIED

L-915

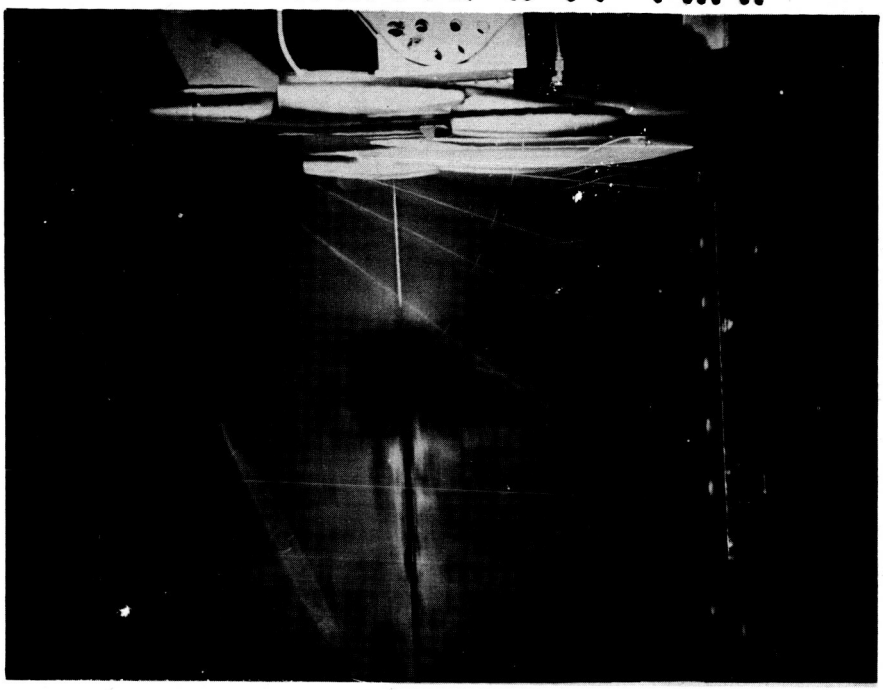

Side view

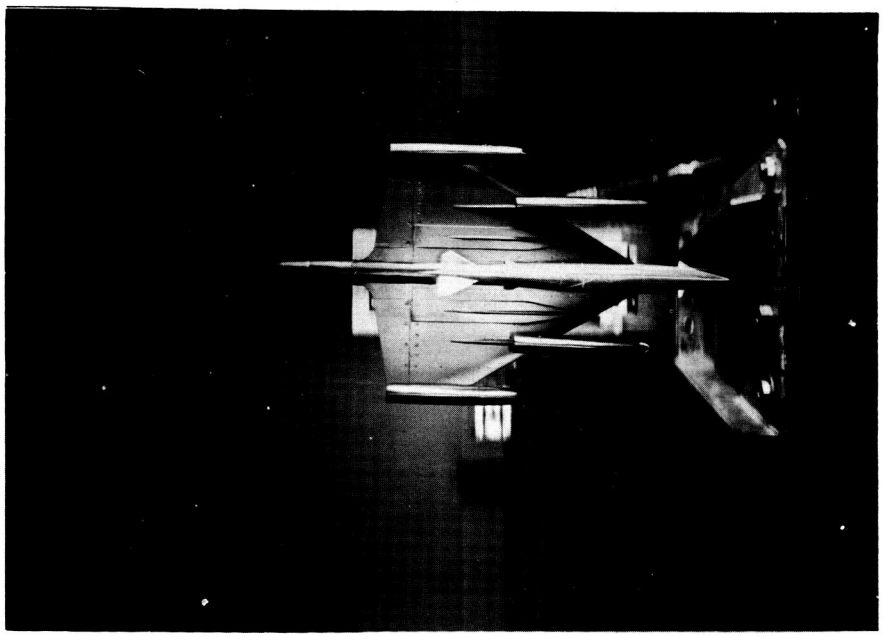

Bottom view

L-60-5522

(o) Test 49. $M = 1.98$; $h = 25{,}800$ feet; $\delta = -2^{\circ}$; $\alpha = 3^{\circ}16'$; $\beta = 1^{\circ}$.

Figure 15.- Continued.

[redacted]

[redacted]

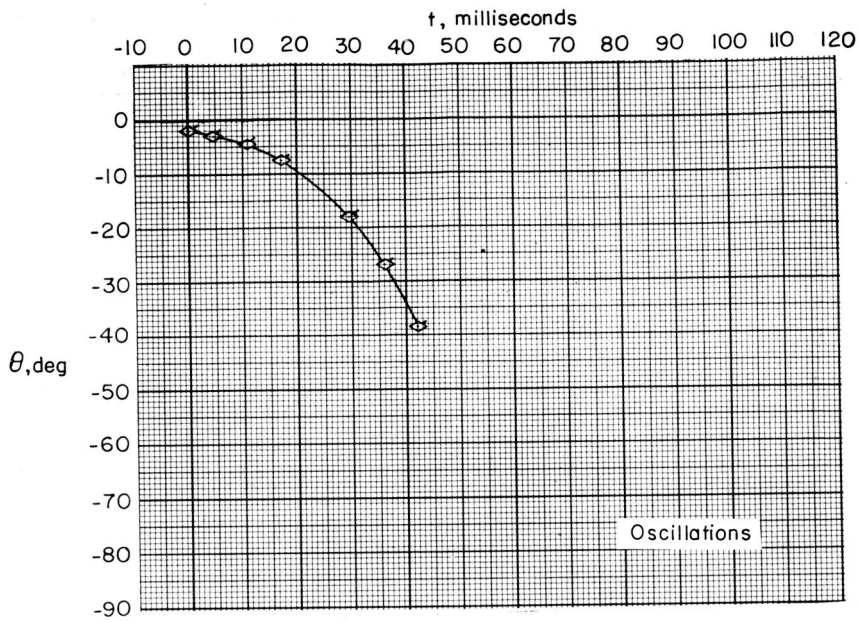

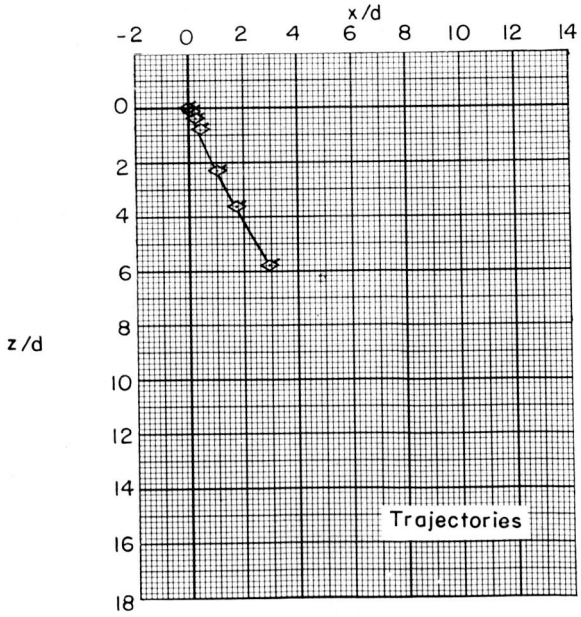

(o) Concluded.

Figure 15.- Continued.

L-915

[redacted]

DE[redacted]IFIED

L-915

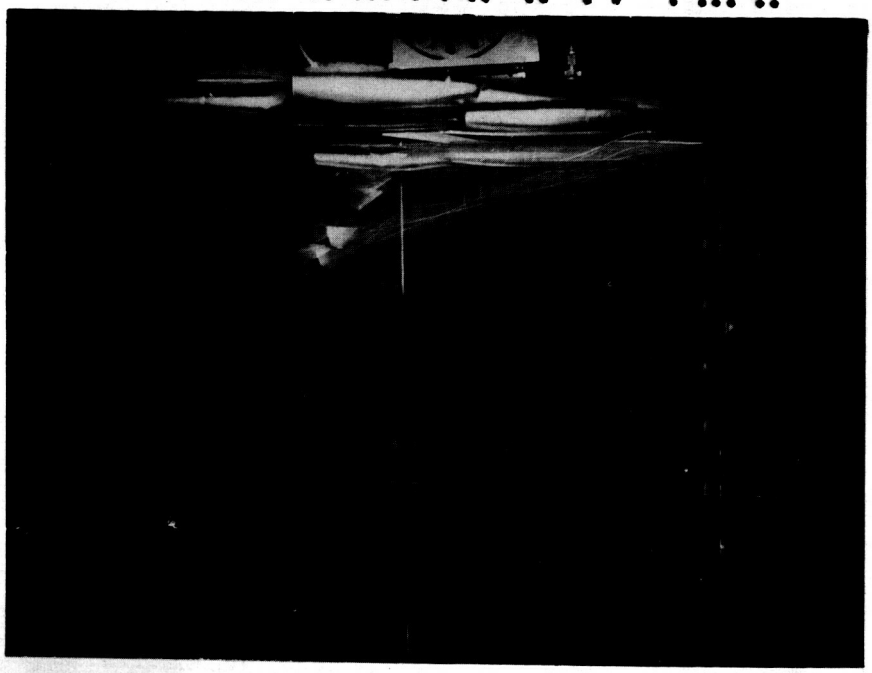

Side view

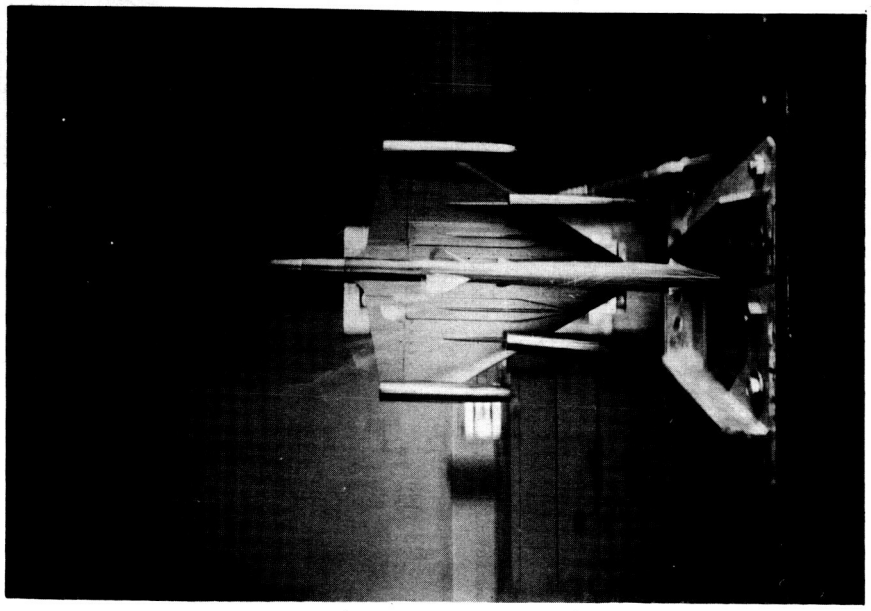

Bottom view

L-60-5523

(p) Test 50. $M = 1.98$; $h = 26{,}350$ feet; $\delta = -2^{\circ}$; $\alpha = 4^{\circ}03'$; $\beta = 1^{\circ}$; fuel-tank model experienced positive pitching moment and struck airplane model.

Figure 15.- Continued.

[redacted]

[redacted]

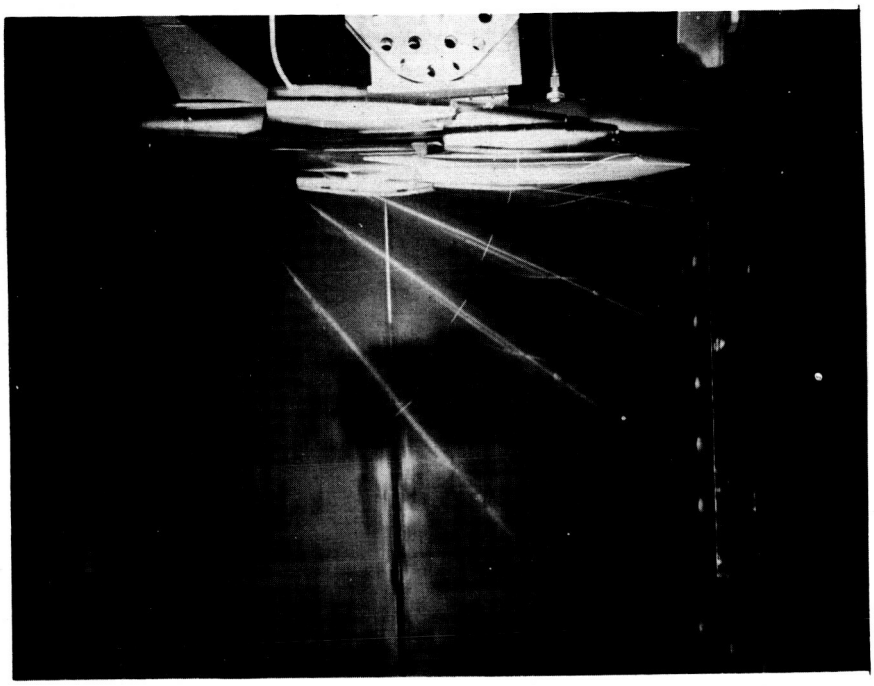

Side view

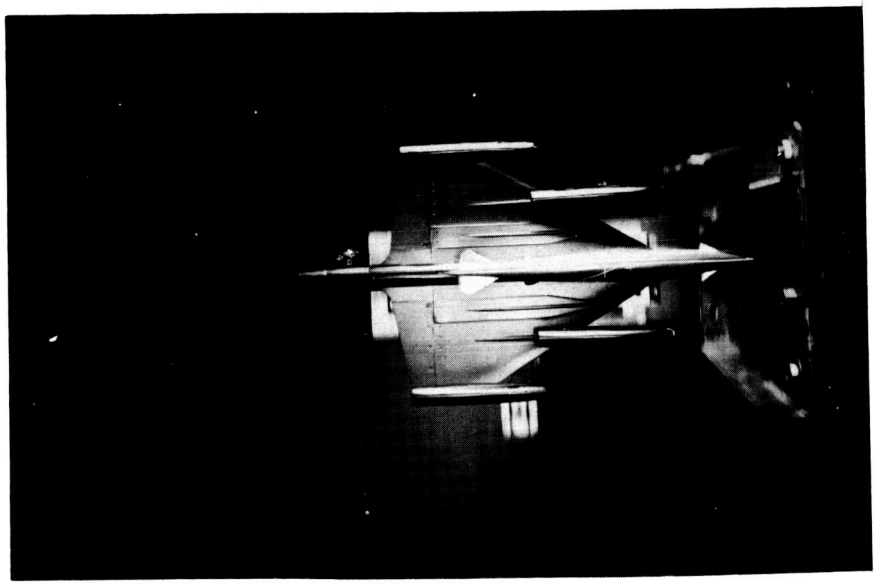

Bottom view

L-60-5524

(q) Test 51. $M = 1.98$; $h = 25{,}450$ feet; $\delta = -20^{\circ}$; $\alpha = 3^{\circ}16'$; $\beta = 0^{\circ}$.

Figure 15.- Continued.

[redacted]

L-915

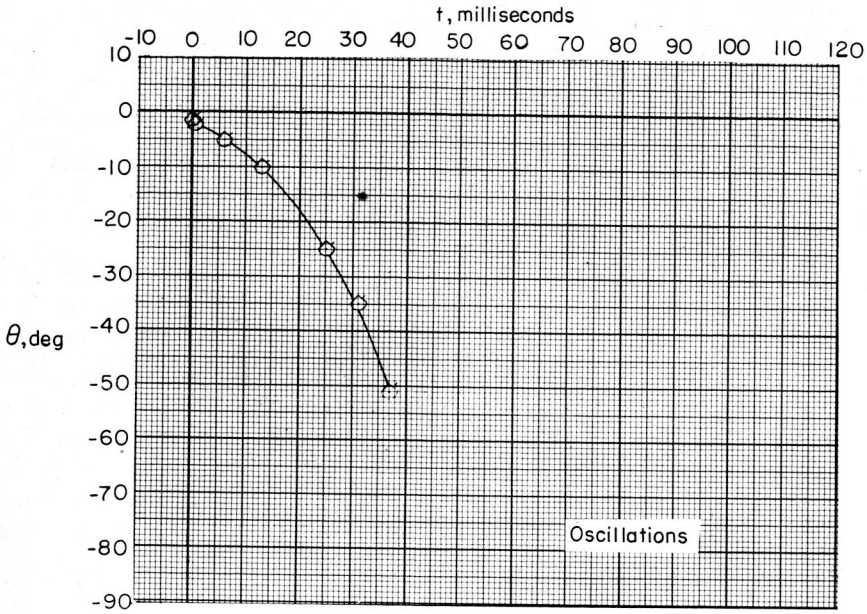

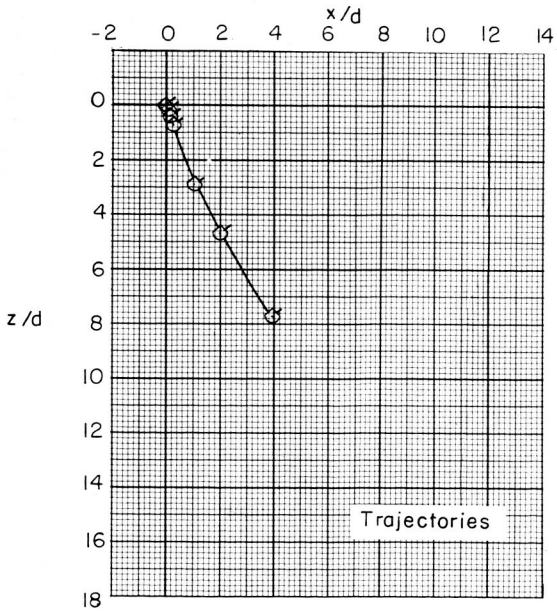

(q) Concluded.

Figure 15.- Continued.

[redacted]

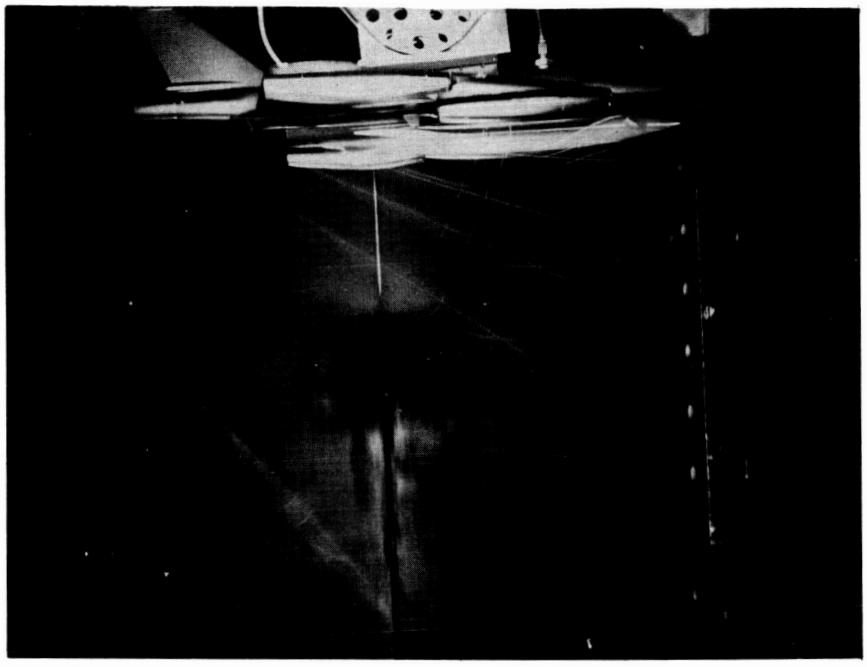

Side view

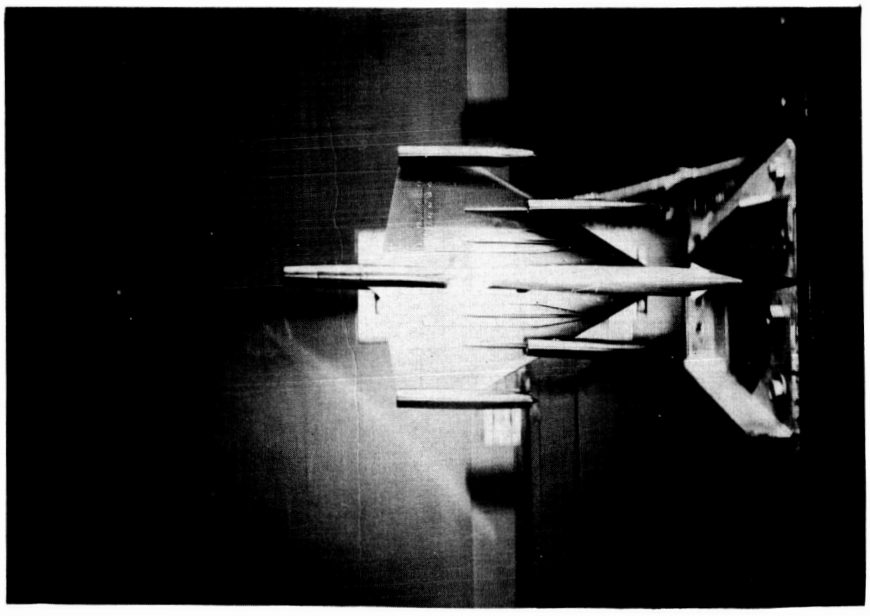

Bottom view

L-60-5525

(r) Test 52. $M = 1.98$; $h = 26{,}075$ feet; $\delta = -20^{\circ}$; $\alpha = 5^{\circ}03'$; $\beta = 1^{\circ}$.

Figure 15.- Continued.

[redacted]

L-915

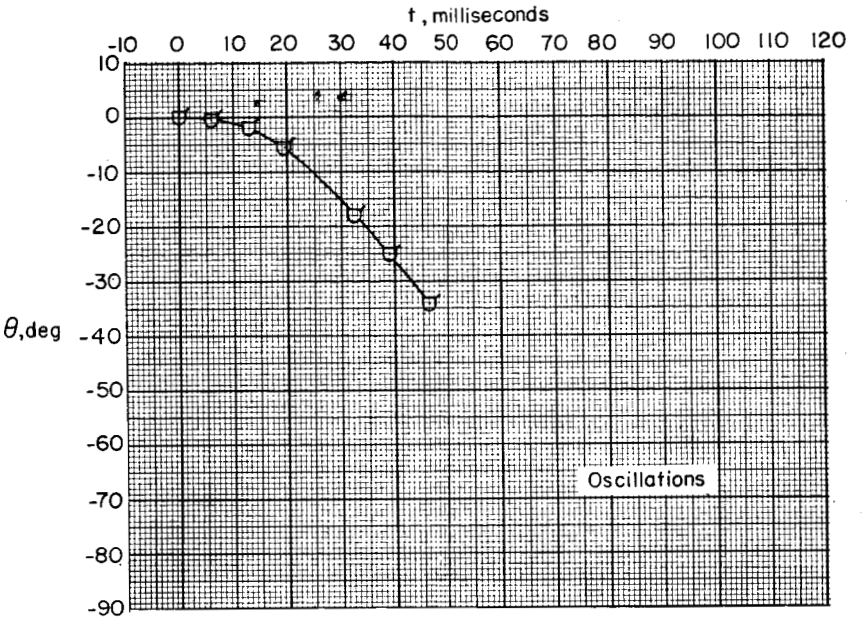

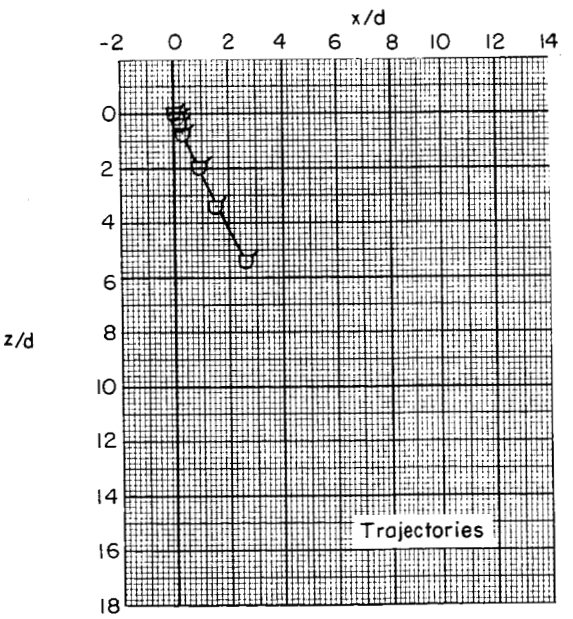

(r) Concluded.

Figure 15.- Concluded.

[redacted]

L-976

[redacted]

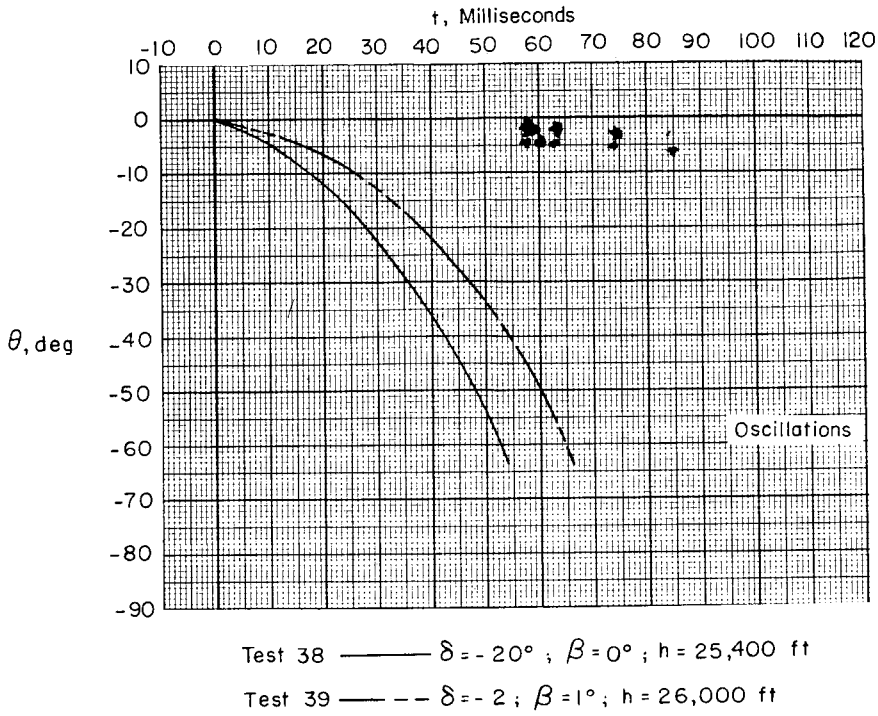

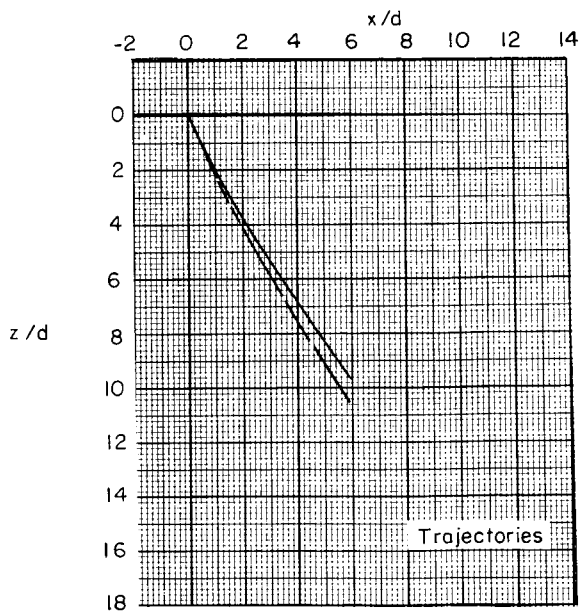

(a) Effect of change in canard-surface deflection at M = 1.39; $\alpha = 4^{\circ}56'$.

Figure 16.- Comparison plots of fuel-tank releases incorporating two tail fins.

L-915

[redacted]

L-915

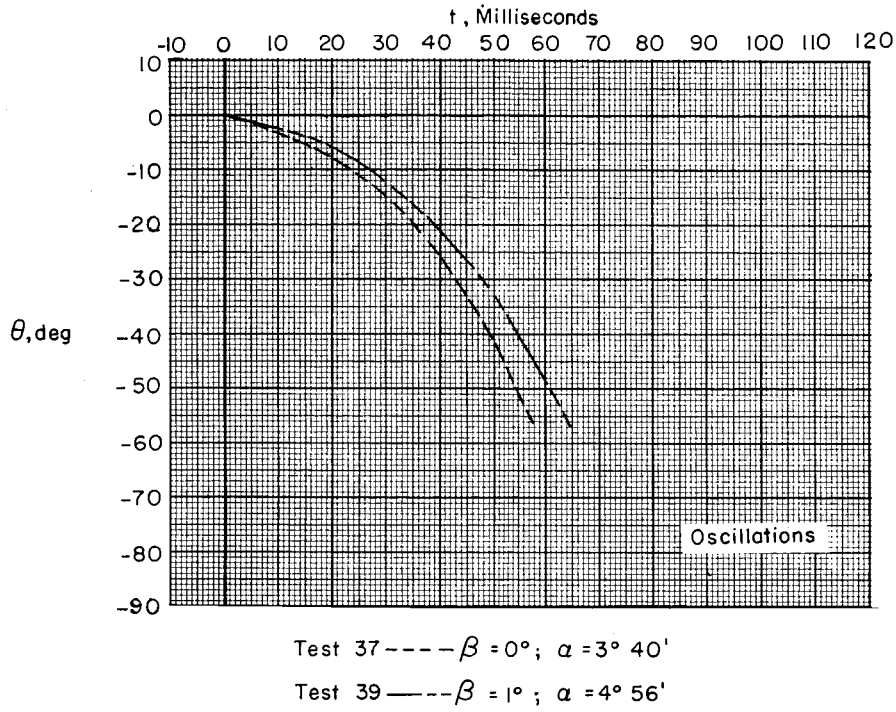

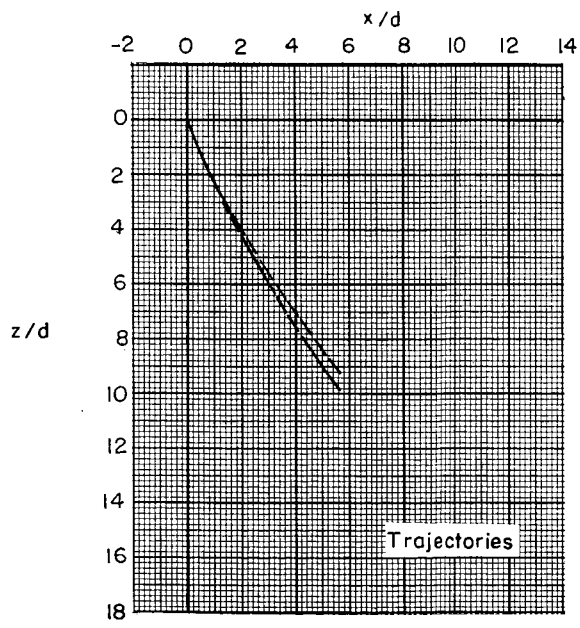

(b) Effect of change in wing angle of attack at $M = 1.39$; $\delta = -2^{\circ}$.

Figure 16.- Continued.

[redacted]

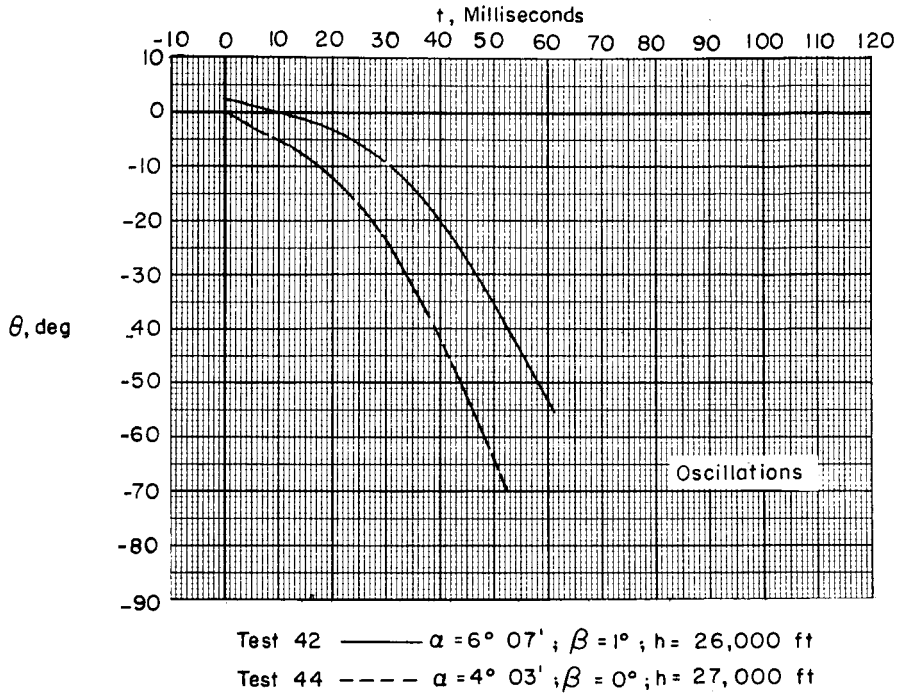

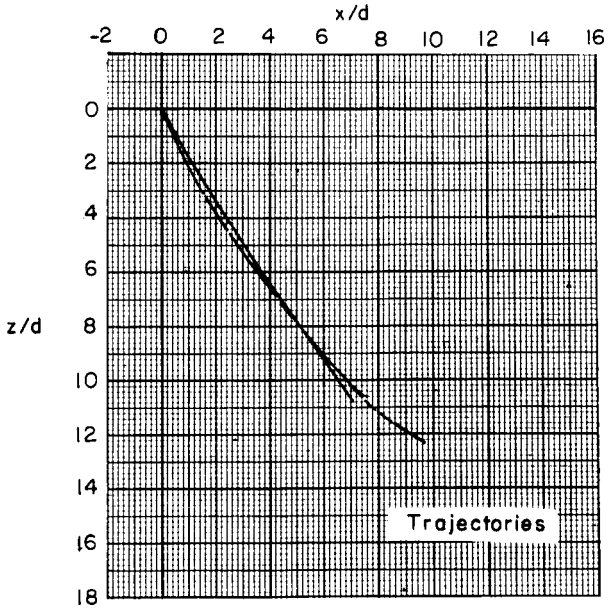

(c) Effect of change in wing angle of attack at $M = 1.59$; $\delta = -2^{\circ}$.

Figure 16.- Continued.

[redacted]

DE[redacted]FIED

L-915

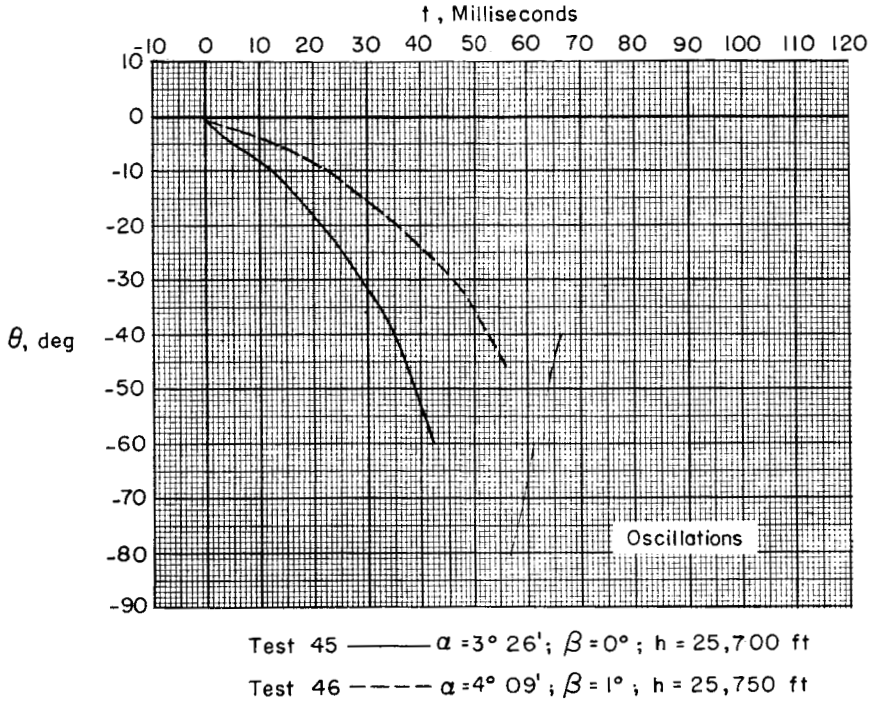

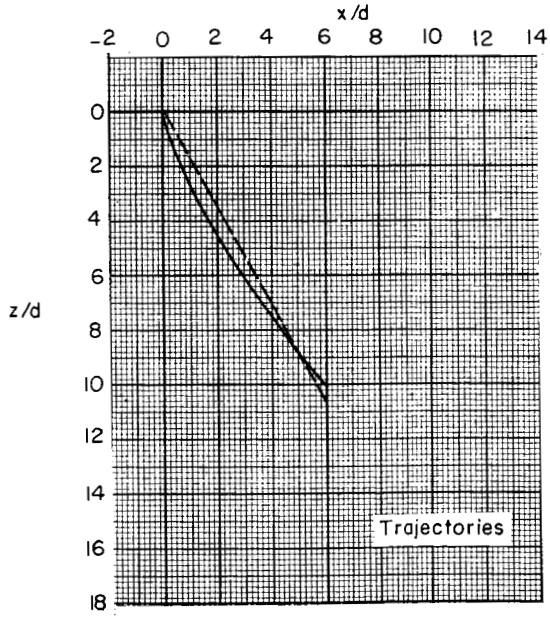

(d) Effect of change in wing angle of attack at $M = 1.80$; $\delta = -2^{\circ}$.

Figure 16.- Concluded.

A motion-picture film supplement, carrying the same classification as the report, is available on loan. Requests will be filled in the order received. You will be notified of the approximate date scheduled.

The films (two reels, each 16 mm, 15 min, B&W, silent) show the motions of the fuel tank as it traverses the airstream.

Requests for the film should be addressed to the

National Aeronautics and Space Administration
Office of Technical Information and Educational Programs
Technical Information Division (Code ETV)
Washington 25, D.C.

NOTE: The handling of requests for this classified film will be expedited if application for the loan is made by the individual to whom this copy of the report was issued. In line with established policy, classified material is sent only to previously designated individuals. Your cooperation in this regard will be appreciated.

[redacted]

CUT

Date_____

Please send, on loan, copy of film supplement to NASA Technical Memorandum X-354 (Film Nos. L-446 and L-472).

_____

Name of organization

_____

Street number

_____

City and State

Attention: *Mr._____

Title_____

(*To whom copy No. ___ of the Technical Memorandum was issued)

Place
Stamp
Here

National Aeronautics and Space Administration
Office of Technical Information and Educational Programs
Technical Information Division (Code ETV)
Washington 25, D.C.